Fall 2014

Tools for efficient design of multicomponent separation processes

Joshua Lee Huff
Purdue University

Graduate School Form 30
(Revised 08/14)

PURDUE UNIVERSITY
GRADUATE SCHOOL
Thesis/Dissertation Acceptance

This is to certify that the thesis/dissertation prepared

By Joshua Lee Huff

Entitled
Tools for Efficient Design of Multicomponent Separation Processes

For the degree of Doctor of Philosophy

Is approved by the final examining committee:

Rakesh Agrawal

Mohit Tawarmalani

Joseph Pekny

Gintaras Reklaitis

To the best of my knowledge and as understood by the student in the Thesis/Dissertation Agreement, Publication Delay, and Certification/Disclaimer (Graduate School Form 32), this thesis/dissertation adheres to the provisions of Purdue University's "Policy on Integrity in Research" and the use of copyrighted material.

Rakesh Agrawal

Approved by Major Professor(s): _____

_____

Approved by: John Morgan 09/24/2014

Head of the Department Graduate Program Date

TOOLS FOR EFFICIENT DESIGN OF MULTICOMPONENT SEPARATION PROCESSES

A Dissertation

Submitted to the Faculty

of

Purdue University

by

Joshua Lee Huff

In Partial Fulfillment of the

Requirements for the Degree

of

Doctor of Philosophy

December 2014

Purdue University

West Lafayette, Indiana

ACKNOWLEDGEMENTS

I am grateful to many people for their help while I worked on this thesis, as well as for being positive influences in many other factors in my life. I thank Professor Mohit Tawarmalani, Professor Gintaras Reklaitis, and Professor Joseph Pekny for their insightful feedback into my research as members of my PhD advisory committee. I thank the US Department of Energy and the US Department of Education for funding my research projects and my life at Purdue University.

I thank my colleagues both past and present in the Separations and Optimization groups at Purdue. I thank Rugved Pathare, Vishesh Shah, Anirudh Shenvi, Dharik Mallapragada and Easa Al-Musleh for paving the way with their work as well as for regular interesting discussions related to research, academic survival, job hunting, and life in general. I thank Nathan Nallasivam and Haibo Zhang for aiding in several of the projects in this thesis. I am very grateful to Gautham Madenoor Ramapriya and Emre Genger for always being willing to listen to my ideas and provide feedback, and wish them nothing but success as they finish their own thesis work.

Thank you to the staff in Chemical Engineering who make my job so much easier. I owe a lot to the administrative support and patience of Katherine Yater-Henke, Melissa Laguire, Deb Bowman, and Katie Field.

Thank you to the people who inspired me to pursue the paths I did. Special thanks to Mrs. Young for sparking my interest in chemistry, and Prof. Lale Yurttas and Prof. Mahmoud El-Halwagi for their enthusiasm for chemical engineering and their aid in planning my future.

I owe a lot of gratitude to my advisor, Prof. Rakesh Agrawal, for his patience and wisdom. I have learned much from his experience and even more from his example.

Thank you to all the gang at WLCC and the Wednesday night study for letting me be a part of your lives. Thanks to Nicholas, Coco, and Anshu for getting me through the first year – somehow. Thanks to Kristen, Kara, & Kathryn for making me feel like I never left every time I came home.

The biggest thanks of all goes out to my parents, Mike & Delia, for their constant loving support and encouragement. It was hard to feel alone in this process when I knew they would always be there for me. Their belief in me not just at Purdue, but in my teen years when I took a very unconventional path to reach this point, has kept me going and they have instilled in me a great love of God and family that will keep me going for many more.

TABLE OF CONTENTS

Page

Page

LIST OF TABLES

Table Page

LIST OF FIGURES

Figure Page

Figure Page

Figure Page

ABSTRACT

Huff, Joshua Lee. Ph.D., Purdue University, December 2014. Tools for Efficient Design of Multicomponent Separation Processes. Major Professor: Rakesh Agrawal.

Separations account for as much as 85% of plant operating costs in chemical production; it is therefore important that they be designed with energy efficiency in mind. This can only be achieved if two things are achieved: the complete space of design options is known, and an accurate way is developed to compare all possible design options. For both membrane separation cascades and multicomponent distillation configurations, this dissertation explores methods for designing energy efficient separations.

The operating cost of membranes used in production of nitrogen gas from air is largely driven by the compressors required to maintain a pressure differential. Optimization of the total compressor duty can reveal an ideal cascade arrangement and set of operating conditions for a given feed and recovery. With this optimization technique in hand, it is then possible to examine the effect of introducing extra stages to form intermediate stage cascades. Furthermore, the effect of varying the recovery of the nitrogen stream can be examined to discover a U-shaped relationship between recovery and energy requirement.

Conventional distillation configurations use $n - 1$ distillation columns to separate a multicomponent feed mixture into pure products. Past research has identified a way to quickly and algorithmically generate the complete ranklist of regular-column configurations using an integer programming formulation called the matrix method. Using this method, a formulation is here presented for the complete nonlinear programming problem which, for a given configuration, can ensure the globally minimum vapor duty of the configuration. Furthermore, a set of nonlinear equations designed to represent the capital and operating costs of the system are described. The need for a global optimization algorithm in the formulation of the cost product is demonstrated by comparison with a two-stage search algorithm; in addition, the cost formulation is compared to that of the vapor duty formulation and the relative effect of capital and operating cost is weighed for an example feed.

Previous methods based on Underwood's equations have no accounting for the temperature at which utilities are required. To account for this, a thermodynamic efficiency function is developed which allows the complete search space to be ranklisted in order of the exergy loss occurring within the configuration. Examining these results shows that this objective function favors configurations which move their reboiler and condenser duties to milder temperature exchangers.

A graphical interface is presented which allows interpretation of any of the above results in a quick and intuitive fashion, complete with system flow and composition data and the ability to filter the complete search space based on numerical and structural criteria. This provides a unique way to compare and contrast configurations as well as

allowing considerations like column retrofit and maximum controllability to be considered.

Using all five of these screening techniques, the traditional intuition-based methods of separations process design can be augmented with analytical and algorithmic tools which enable selection of a process design with low cost and high efficiency.

.

CHAPTER 1. INTRODUCTION TO MULTICOMPONENT SEPARATIONS

1.1 Motivation

In the course of producing almost any chemical product, it becomes necessary to separate the desired product from any number of side products, leftover reactants, or impurities. Almost every existing element and compound occurs naturally in an impure state, and almost any chemical reaction process will also yield a product in an impure state. As a result, the ability to separate and purify chemicals is one of the major foundations of a modern industrial economy. A large number of different processes have been proposed to perform separations based on a number of different physical, chemical, and mass transfer properties of substances. Common separation techniques include distillation, adsorption, stripping, filtration, crystallization, chromatography, and membrane permeation. It is estimated that between 40 and 70 percent of the average yearly energy cost to operate a chemical process in the petroleum or chemical industries will be spent on separations [1].

Separations are driven by exploiting differences in the components of a given mixture. For example, the driving force for distillation is the difference in boiling points of different compounds. Stripping is a separation technology driven by the difference between solubilities of various liquids in a given gas. Filtration separates particles or molecules of different sizes. In attempting to study any of these separation technologies,

it is critical to understand the fundamentals of the technology before attempting to design the separation process in an efficient way.

The large global scale of the separation process industry and the fact that multiple designs can achieve the same ends make chemical separations a prime target for studies in process design and optimization. By creating a detailed model representing a separation process, it is possible to study the effect of design changes on the energy efficiency and installation cost of a separation process. If these design changes are aided by a strong knowledge of mathematical optimization, process designers can aim to create a separation process which achieves its tasks within the process as a whole with high energy efficiency and low costs. Even a modest improvement in the efficiency and cost of large-scale separation processes could have a profound impact on the chemical and petrochemical industries. The focus of this research is to design computational tools which will allow selection of efficient and low-cost separation schemes when using membrane permeation and distillation as primary separation technologies.

1.2 Membrane separation fundamentals

Membrane-based gas separation is a pressure-driven separation technique. It takes advantages of differences in permeabilities between two or more gaseous components across a permselective barrier. Materials often used in membranes include ceramics, metallic compounds, gels, liquid phase membranes, or polymers. Polymeric membranes are most commonly used; the ease of forming polymer chains into hollow fiber modules allows them to be produced with a low cost and extremely high membrane area to volume ratios.

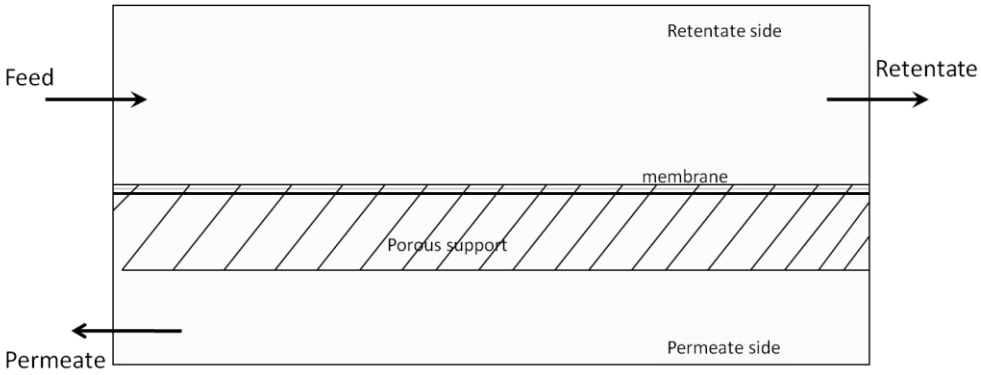

Figure 1-1: A simple representation of a single membrane stage

To operate a membrane, a pressure differential is maintained between the feed side of the membrane (also called the retentate side) and the product side (also called the permeate side). The lower pressure on the permeate side means that all of the chemicals in the feed will be driven to cross the membrane barrier. However, the membrane has different permeabilities for each component. These permeabilities depend upon the diffusion and sorption coefficients between the membrane material and each individual gas present in the feed. This means that the pressure gradient will cause more permeable compounds to be concentrated on the permeate side of the membrane, and less permeable compounds to be concentrated on the retentate side. The ratio of permeabilities between two components is called the permselectivity.

The permselectivities of commercially available membrane materials are enough to gain a significant amount of separation with a modestly sized membrane stage – however, achieving high purity and recovery is a difficult task due to the trade-off between high total permeability and high selectivity. Due to this limitation, most available commercial membranes have modest values of permselectivity in the range of 5

to 20 for applications like air separation or CO_2 removal. [2] In order to obtain products with high recovery and high purity simultaneously, it is useful and often necessary to utilize multiple membrane stages (collectively referred to as a membrane separation cascade), where low-pressure permeate streams are recompressed and inserted at suitable points on the high-pressure side of a membrane.[3-6]

The introduction of these compressors serves to introduce a number of decision variables with the membrane cascade can be controlled. When the compressor energy requirement is changed, the pressure ratio between the permeate and retentate sides change. If a constant retentate-side pressure is assumed, this means that the driving force of each individual membrane stage is controlled completely by adjusting the permeate side pressure. Thus, by adjusting the number, size, and pressure ratio of the membrane stages, it is possible to optimize a membrane separation in an attempt to lower the energy requirement of the process.

1.3 Distillation fundamentals

When a liquid mixture is heated and partially vaporized, and the resulting liquid and vapor phases are allowed to reach equilibrium, the two phases will contain different distributions of the chemicals in the mixture. The tendency of a component to gravitate towards the vapor phase rather than the liquid phase in this scenario is called its volatility. By convention throughout this dissertation, highly volatile components will tend to rise in the column, are often present as top products, and are referred to as “light”. Less volatile components tend to fall in the column, are often present as bottom products, and are referred to as “heavy”. By allowing liquids and vapors to exchange heat and mass across

a number of equilibrium stages, distillation allows mixtures to be separated using volatility differences as a driving force.

The earliest instances of distillation were batch processes, and are believed to have existed as early as 3500 BC. Continuous distillation was a more modern innovation, coming into practice about 1830 AD. Distillation is the most prevalent separation technique in the chemical and petrochemical industries, comprising an estimated 90-95% of separation processes as of 1992.[7]

Figure 1-2 shows a diagram representing a typical continuous binary distillation process. The two components in the feed are labeled “A” and “B”. Component A is taken to be the lighter component, and will be produced as a top product. Component B is the heavier component, which will be removed from the bottom. A number of equilibrium stages within the column allow the transfer of components between liquid and vapor phase. Moving upwards from the feed towards the top product, each successive stage will have a mixture which contains more of component A and less of component B. Moving downwards towards the bottom product, the mixture present around each stage is richer in B and poorer in A. At the top of the column, some (or, in some cases, all) of the rising vapor is condensed into liquid – some is extracted as the final product and some is returned to the column as reflux. At the bottom of the column, the descending liquid is captured and likewise is partially or totally vaporized, and partially refluxed into the column. The product leaving from the top is known as the distillate, and the product from the lower end of the column is the bottoms product. It is also possible to withdraw products directly from any stage in the column, which is known as a “side draw” stream.

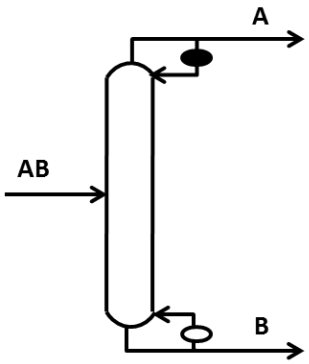

Figure 1-2: A continuous distillation column

With the column in Figure 1-2, an arbitrarily high purity of both A and B can be achieved simply by increasing the number of stages. However, while it is possible to use a single column to produce any number of product streams through side draws, the purity of a side draw stream is difficult to guarantee and thus many multicomponent distillations are achieved through the use of distillation column sequences – that is, multiple distillation columns interacting in a combined process.

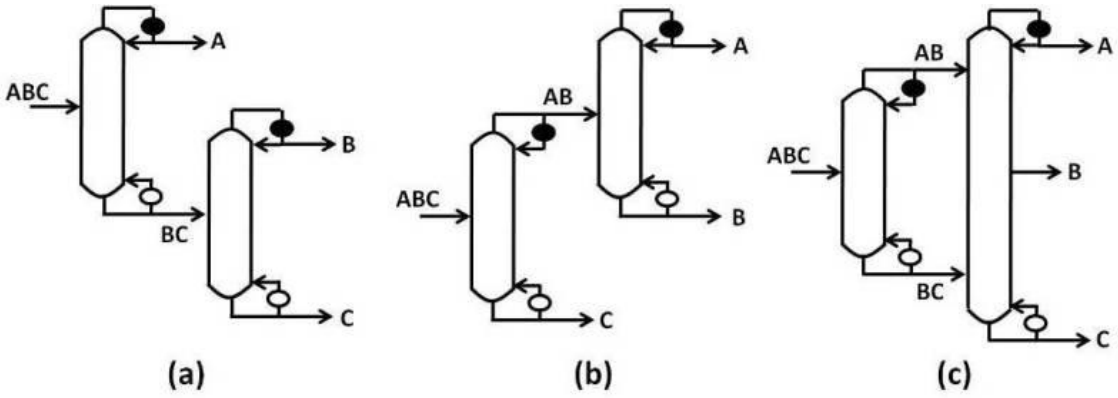

Figure 1-3: Three possible column sequences for separating mixture ABC

Figure 1-3 shows three different column sequences that achieve the task of separating ABC into its three pure components. It is possible to achieve the same purity and recovery with any of the three configurations pictured. However, each of the three configurations will have a distinct cost to install and run the column equipment. It is not immediately apparent which of the column sequences is the most energy and cost effective to perform the required separation. Thus, a large portion of this dissertation is devoted to developing tools which can identify which possible distillation alternatives are the best candidates for a given separation. This problem will be attacked on four fronts, to be further detailed in section 1.4:

- Finding the distillation column sequence with the lowest total vapor generation requirement
- Finding the distillation column sequence with the lowest total estimated capital and operating cost
- Finding the distillation column sequence with the highest thermodynamic efficiency
- Representing the possible column sequences and their desirability in the form of a graphical screening tool

1.4 Research objectives

This dissertation is organized into the following chapters:

Chapter 2: Minimum-energy design of membrane gas separation processes. This chapter centers on designing a multistage cascade which produces a given purity product

from a given feed utilizing a selected membrane material with a known permselectivity. Global optimization techniques are applied to model the governing equations of the membrane cascade and determine the proper membrane areas, recycle locations, number of stages, and pressure ratios to achieve a particular purity and recovery while using minimum compression work. The effect of utilizing intermediate stage cascades to reduce energy requirement is examined. The effect of varying recovery on the energy efficiency of a cascade is also studied.

Chapter 3: Enumeration of distillation configurations and screening using global optimization. This chapter describes methods that exist for the complete enumeration of the distillation search space for zeotropic, regular column configurations. Using one of these methods, global optimization techniques are introduced for the purpose of minimizing the vapor duty requirement of a single configuration. Afterwards, these techniques are applied across the entire search space to create an ordered ranklist of the vapor duty for all possible sequence designs. This chapter lays out a general formulation to minimize vapor duty in a single configuration. This formulation is known as the Global Minimization Algorithm for multicomponent distillation. A theoretical formulation to quicken evaluation of a search space with the use of integer constraints is described and evaluated. Finally, simple quickscreening techniques are introduced which allow search space reduction based on the user requirements for the ranklist of sequence vapor duties.

Chapter 4: Total annualized cost formulation for multicomponent distillation. In this chapter, a formulation for estimating and minimizing the total cost of a configuration is outlined. A study is made whether it is more suitable to evaluate configurations using

the Global Minimization Algorithm outlined in chapter 3, or the Two-Step Minimization Algorithm based on literature. Results from different weighted values of capital and operating costs are compared to determine which types of configurations are favored by each.

Chapter 5: Thermodynamic efficiency global maximization in distillation. In this chapter, equations are developed to estimate the thermodynamic efficiency of a distillation sequence at any set of operating conditions. The Global Minimization Algorithm is applied across the search space for regular-column distillation in conjunction with these new equations, and all configurations are ranklisted in terms of thermodynamic efficiency for several case studies. These ranklists are compared and contrasted with those generated by minimizing vapor duty, in an attempt to address temperature considerations not present in the vapor duty objective function.

Chapter 6: Novel graphical screening interface for multicomponent distillation. This chapter introduces a software tool for multicomponent distillation which will allow distillation practitioners to view instantly-generated flowsheet drawings of all sequences in a distillation search space. Any of the optimization results in the other chapters of this dissertation can by imported into the tool for comparison. The total flow and composition of any steam in the distillation configuration, the vapor flow in any column section, and the vapor duty of all heat exchangers is viewable on the flowsheets. The search space can be screened using criteria like total number of transfer streams, number of exchangers, or total vapor duty. Results diagrams can be printed, exported, and saved. This tool provides great opportunities to demonstrate the power of the methods advocated in this

dissertation to those who may not be familiar with their specifics, and is an excellent program for preliminary design of distillation configurations for a number of applications.

Chapter 7: This chapter summarizes the results presented throughout this dissertation, and remarks on possible avenues for future research in multicomponent separations.

CHAPTER 2. MINIMUM ENERGY DESIGN OF MEMBRANE GAS SEPARATION PROCESSES

2.1 Modeling of membrane gas separations

In using multi-staged membrane cascades, there are many possible cascade designs which can be utilized to arrive at the same final separation products. Often, cascades are arranged so that the permeate stream from a particular stage is recycled through a compressor and mixed with the retentate stream produced by the next stage.[8-10] Such arrangements can be termed “classical” cascades.

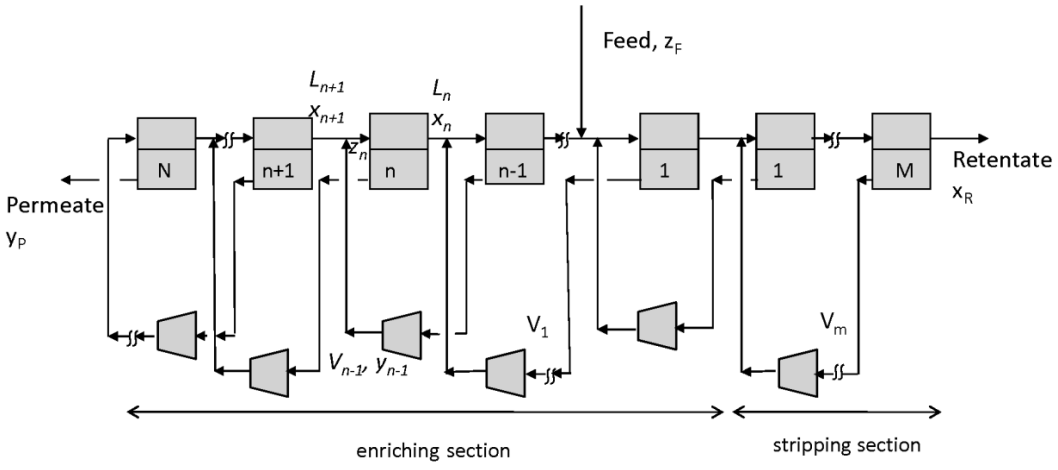

Figure 2-1: A classical membrane cascade

Figure 2-1 illustrates a classical cascade. The stages between the feed and permeate end are termed the "enriching" stages and the stages between the feed and the retentate end are termed the "stripping" stages. In this illustration, the classical cascade is shown to have N enriching stages and M stripping stages, and could be drawn for any value of N and M. By convention, both sections are numbered starting at the feed, and the stage the feed immediately enters upon introduction is counted as enriching stage 1. Other non-classical arrangements of membranes exist [8-15] – most of the cascades studied here, though, are of the classical variety.

In order to analyze the performance of an individual membrane stage in an optimization, it is necessary to choose a mathematical model to represent the stage. There are two widely used types of membrane modules: hollow fiber modules and spiral wound modules. There are also four widely used mathematical representations for flow patterns within modules: complete mixing, counter-current flow, co-current flow, and cross-flow.[16] The driving forces for separation depend on the model, each of which treats the partial pressures of the components differently. As a result, the flow pattern chosen for a stage impacts its simulated performance greatly. The mode of operation with the highest driving force and thus the largest potential for separation is the counter-current flow. Most actual membrane stages operate in a fashion that is between that modeled by counter-current flow and that modeled by cross-flow.

A model for the quick estimate of the performance of a hollow-fiber, cross flow binary membrane stage was developed by Pathare.[17] In this model, a local separation factor is introduced relating the molar fraction of the most permeable component in the local permeate (y') and retentate (x').

$$S_{local} = \frac{y'}{1-y'}\left(\frac{1-x'}{x'}\right) \tag{2-1}$$

The local separation factor varies within a membrane stage. However, the variation of S_{local} is small enough that a reasonable model can still be constructed while assuming it constant through the stage.[17] Indeed, assuming a constant local separation factor is an extremely strong assumption in cases where pressure ratio is relatively high.

The head and tail separation factors of a membrane stage can be defined by

$$h = \frac{\frac{y_p}{1-y_p}}{\frac{z_f}{1-z_f}}, t = \frac{\frac{z_f}{1-z_f}}{\frac{x_r}{1-x_r}} \tag{2-2}$$

where y_p is the permeate composition in the more permeable component, x_r is the retentate composition, and z_f is the feed composition. When local separation factor is assumed constant throughout the stage, it is related to the head and tail separation factors by the following equation:

$$t = \left(\frac{t(1-h)}{1-ht}\right)^{1-S_{local}} \tag{2-3}$$

Using the cross-flow method outlined above, it is possible to calculate the compositions obtained at any pressure ratio within the membrane for a given feed. Armed with these equations, there are several possibilities for an energy-efficient way to operate the system.

2.2 Constant Separation Factor Method versus Variable Separation Factor method

The constant separation factor method for binary separations was published in 1951.[8] This method assumes that no mixing loss occurs in the cascade due to mixing of dissimilar streams. It also assumes that all separation stages in the membrane cascade have identical stage separation factor, tail separation factor, and head separation factor. From this point this method will be referred to as CSF. The second assumption in CSF is that

$$h = t = (S_{stg})^{0.5} \tag{2-4}$$

Thus, in this method, the only independent variable is the stage separation factor. If this is specified, the values of h and t can be immediately calculated. Pathare and Agrawal [18] used local optimization to determine the optimal value of the stage separation factor for a given feed in a CSF system.

It is also possible to constrain stage separation factors to being the same for each membrane stage while relaxing the requirement that head and tail separation factors be identical. This is referred to as the variable head-tail method (VHT).[17,19-21] This leads to an equation similar to CSF – however, the relation of the head to tail separation factors is no longer fixed, leading to this equation:

$$h = \left(S_{stg}\right)^{p}, t = \left(S_{stg}\right)^{1-p}, p \in (0,1) \tag{2-5}$$

Finally, the Variable Separation Factor (VSF) method is a method of operating a membrane cascade in which each stage within the cascade is allowed to individually assume a unique value of stage separation factor, and the head and tail separation factors may differ. The VSF method can be implemented with the assumption that streams of

dissimilar composition can never be mixed, or it can be implemented with this constraint relaxed. Examples of cascades designed with the VSF method to avoid mixing loss are present in the literature.[22-24]

Pathare and Agrawal [18] compared the CSF method to the VSF method with and without mixing loss. The VHT method was not studied, but was assumed to lie somewhere between the two sets of results. They found the following:

- When the number of enriching and stripping stages were allowed to vary, each of the three methods yielded the same membrane configuration as the optimal solution.
- The CSF method had a lower efficiency for the optimal configuration than either VSF method.
- In a VSF system, the inclusion of the mixing loss constraint had no effect at global optimality; that is, at global optimality an unconstrained system will tend to minimize mixing loss.
- When the number of stages is decreased from that identified as optimal, however, disallowing mixing loss leads to a less efficient configuration. This is because a trade-off exists between the inefficiency resulting from mixing losses and the inefficiency within the membrane stage – a trade-off that is optimized for when mixing loss is allowed, but is fixed when mixing loss is disallowed.[18]

In the remainder of this chapter, the VSF method will be used as the basis of further studies contained in the next sections.

2.3 Intermediate Stage Cascades

Alternative membrane cascade structures have been suggested which may alleviate inefficiencies in the classical cascade design.[11-15] Among these is a form known as the intermediate stage cascade (ISC). This arrangement uses additional stages at intermediate locations not present in the classical cascade. Recycle streams in a cascade with intermediate stages have the same composition as the streams they are mixed with, completely avoiding mixing losses. As in the previous section, this lack of mixing losses can be enforced without additional stages; however, it often leads to inefficiencies within the membrane since it must be enforced specifically at the feed composition of each stage. An example of this arrangement is shown in Figure 2-2.

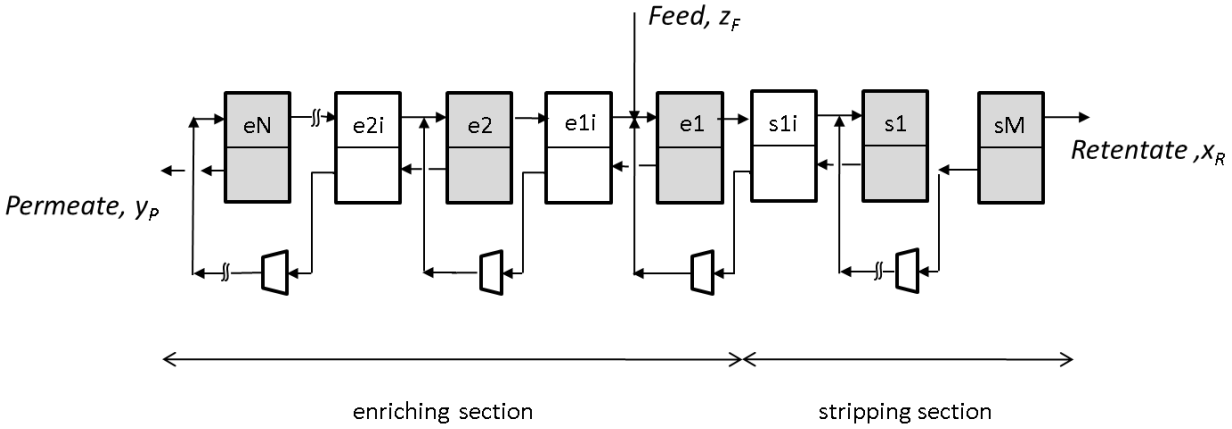

Figure 2-2: Illustration of the intermediate stage cascade design [17]

In this figure, the light stages represent intermediate stages that are present in this process; these are not present in the classical cascade structure (which has only the shaded stages).[17] Figure 2-2 represents a panoptic structure in which many cascade

configurations are embedded. Individual ISC configurations similar to Figure 2-2 may or may not employ all of the additional stages possible. If none of the intermediate stages from the panoptic structure of Figure 2-2 are present, all that remains is the classical cascade arrangement. Although in general, the pressure ratio in any additional stage may be chosen to be different from that in the succeeding stage, in this study these two pressure ratios are constrained to be the same. This eliminates the need for additional compressors to be introduced with additional stages.

In previous works, the suitability of ISC cascades for general separations was studied; it was demonstrated that single-compressor ISC configurations have lower energy requirements compared to single-compressor classical cascades; this is because mixing losses due to mixing of dissimilar streams can be minimized or eliminated for the ISC cascade.[11-12] It was also demonstrated that increasing the number of recycle compressors from one to two increases the energy efficiency of the ISC cascade.[13] For a classical cascade, increasing the number of compressors aids the energy efficiency, until a certain number of stages are present, after which adding additional stages or compressors makes no impact. However, none of these past works address whether the ISC structure is still significantly more energy-efficient than the classical cascade at a higher number of recycle compressors or whether the ISC is lower in energy consumption only when a low number of recycle compressors is used. The past works also remain silent on whether all of the possible intermediate stages are necessary in order to realize the savings in specific energy requirement.

To address this question, Pathare [17] suggested a methodology: the ISC arrangement is compared with the classical cascade arrangement for different number of

stages and compressors for an example of a binary gas separation problem (in this case nitrogen synthesis from an air source). The example is such that the separation targets to be achieved are pre-specified along with the permselectivity and permeability of the membrane to be used. It is demonstrated that the energy consumption advantage of the ISC compared to the classical structure diminishes with increasing number of recycle compressors, in accordance with the findings of Pathare. [17] Hence, a practitioner must include ISC structures as possible design candidates in order to improve energy efficiency when only one or two recycle compressors are used; however, if additional recycle compressors are permissible the classical cascade will likely be all that is needed.

2.3.1 Method

A case study is considered in which 100 kmol/hr of 99.9% pure nitrogen at 10 bar pressure needs to be produced from air. Air is assumed to be a binary mixture with 20.95% oxygen and 79.05% nitrogen. The feed is pre-compressed to 10 bar pressure before feeding it into a cascade. The oxygen-enriched permeate product is rejected back to the atmosphere. The oxygen permeability constant (Q/l) is 3.2 x 105 Barrer/cm and the permselectivity of the membrane with respect to nitrogen (α) is 6.00. These values of permeability and permselectivity are consistent with commercially available polyimide membranes for this application[3,25-26]. The same membrane properties are used for each stage in the membrane cascade. A set nitrogen recovery of 58.5% is used, in accordance with Pathare.[17] This value is chosen to facilitate convenient comparison with the results reported for the classical cascades. The product purity for nitrogen is

99.9%; the purity of oxygen is 38.94% (calculable directly from the recovery value). This purity and recovery is impossible with a single stage, requiring a membrane cascade.

The first case studied in Pathare [17] considers ISC cascades that may have any number of stages in the stripping section, but only one stage in the enriching section. It should be noted that for economic reasons, using three or more compressors may not be attractive in practice. However, the goal is to understand the energy behavior of ISC cascades as number of recycle compressors are varied. Furthermore, for the classical cascade arrangement overall minimum in energy demand for the same feed and recovery was observed with four recycle compressors. Hence, the first case is restricted to examining those cascades with four compressors or less.

Any cascade with an ISC structure is named using the form '$n.e_j.s_k(a_{1i}, a_{mi}, \ldots).c_p$'. *n* represents the total number of stages; *j* represents the total number of stages in the enriching section and *k* represents the total number of stages in the stripping section. The terms within parentheses identify which stages are split relative to the classical cascade. The intermediate stage derived from splitting stage a_k is referred to as 'stage a_{ki}' (where '*i*' stands for 'intermediate'), and p is the total number of recycle compressors in the cascade (where '*c*' stands for 'compressor').

The configuration in Figure 2-3a has 5 total stages, with 4 stages in the enriching section and 1 stage in the stripping section. When looking at the classical cascade from which this configuration is derived, the added stage in this configuration is stage e_{1i} of the enriching section. According to the introduced form above, this configuration is identified as $5.e_4.s_1.(e_{1i}).c_3$. In the same way, Figure 2-3b is identified as $6.e_2.s_4(e_{1i},s_{2i}).c_3$. Furthermore, for purposes of comparison, the classical cascade structures will be handled

with the same nomenclature. For example, a cascade with two enriching stages and two stripping stages would require three compressors, and would thus be labeled *4.e_2.s_2.c_3.*[17]

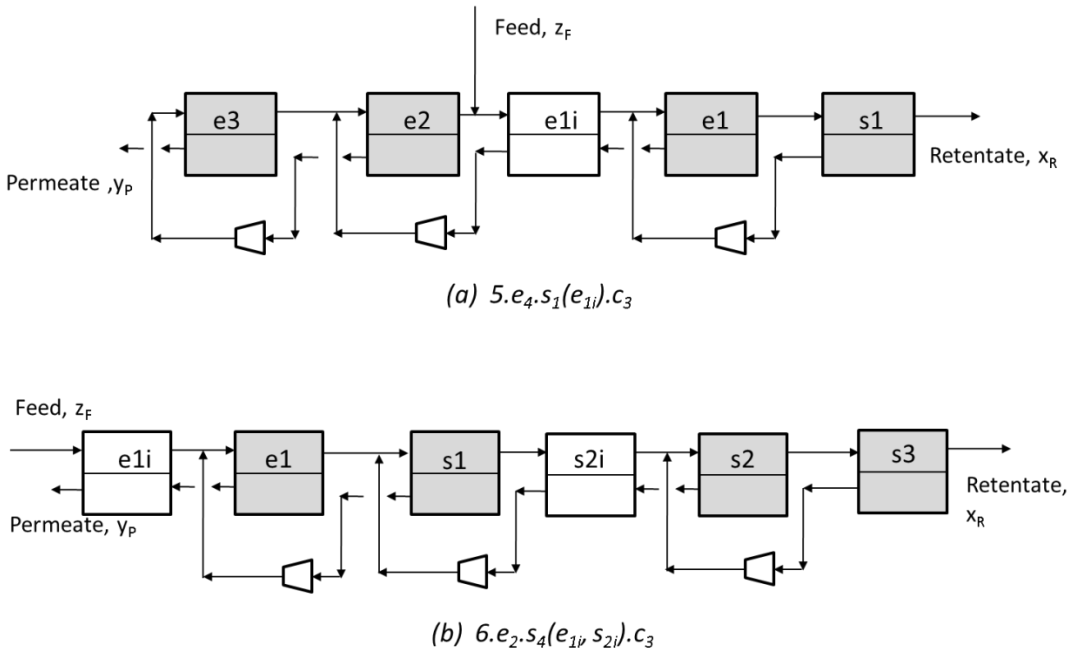

Figure 2-3: Three-compressor ISC cascades with less than three intermediate stages [17]

2.3.2 Modeling and optimization

For each candidate cascade with a fixed number of recycle compressors and membrane stages, only the feed and product stream compositions and flow-rates are fixed. All intermediate stream flowrates and molar fractions may take any values that satisfy mass balances, as may the operating pressure ratios for each membrane stage in the cascade; all this together can be combined to calculate a unique power demand. The objective of an optimization of such a cascade is to find the optimal set of intermediate

stream flow-rates and compositions which give the minimum specific energy consumption. The specific energy consumption is defined as the energy requirement for the separation of one mole of the nitrogen product.

The optimization method used here also takes advantage of the panoptic nature of the ISC cascade structure. In general, it is observed that the ISC cascade with p intermediate stages and p recycle compressors also embeds all other ISC cascades with less than p intermediate stages and p recycle compressors. For instance, configuration $7.e_1.s_6\ (e_{1i},\ s_{2i},\ s_{4i}).c_3$ embeds all possible ISC cascades having exactly three recycle compressors and three or fewer intermediate stages, including the classical configuration $4.e_1.s_3.c_3$ which contains no intermediate stages. Thus, configuration $7.e_1.s_6\ (e_{1i},\ s_{2i},\ s_{4i}).c_3$ could be considered a master-structure for all other cascades with three recycle compressors. Taking advantage of this property, a generalized set of equations modeling a p-compressor master-structure using the membrane stage model of Naylor and Backer is developed.[16] The model included nonlinear constraints ensuring that all streams that are mixed must be the same composition. In addition, all intermediate stages are such that pressure ratios maintained in these stages equal the pressure ratios in the corresponding succeeding stages and that component and overall mass balances around each stage are met. Head and tail separation factor values of each stage within the cascade are also calculated and related to the area and pressure ratio of a stage by constraints. Separation factors are useful to characterize the performance of a stage; definitions of stage, head, and tail separation factors can be found in numerous papers and textbooks, including the work by Pathare and Agrawal. [9-10,18]

It is easy to examine any of the daughter configurations within each master-structure using constraints on separation factor values. For example if one wanted to consider a candidate ISC cascade with one or more of the p intermediate stages absent, then the corresponding tail separation factor could be set to 1.00 (since a tail separation factor of unity indicates that no separation occurs on that membrane stage). Conversely, if at the optimal specific energy requirement of a p-compressor master-structure, some of the intermediate stages show tail separation factor values in the vicinity of 1.00 and permeate flow rates of near zero, it indicates that those intermediate stages were not required.

The equations described above were implemented as a set of nonlinear equations in the General Algebraic Modeling System (GAMS). In order for a specific energy value to be considered feasible, all constraints must be met. The feasible solution with the lowest value of specific energy required is the optimum. The solver chosen for the problem was the Branch and Reduce Optimization Navigator (BARON). BARON uses branch-and-reduce algorithms including convex underestimation and relaxation of the problem to solve non-convex problems to global optimality. It improves on traditional Branch and Bound method solvers by using range reduction techniques based on optimality and feasibility. It can solve linear and nonlinear continuous problems as well as integer and mixed-integer problems. BARON treats all system variables as decision variables, but the values they can take are restricted by the constraints representing feasibility. Providing the solver with conditions for cascade feasibility, it will return the feasible solution with the minimum specific energy consumption. With proper constraints and bounds on the variables, the solutions are guaranteed to be globally optimal. Thus,

for each individual cascade configuration, the solution with globally minimal specific energy consumption is found that satisfies a set of constraints unique to that configuration.[27-28]

2.3.3 Results of implementing ISC arrangements

Since the introduction of intermediate stage cascade is designed to reduce mixing losses, it is apparent that as the number of recycle compressors in a cascade increases, the number of intermediate stages required to avoid mixing losses also increases. For a cascade with *p* recycle compressors, it is possible to include up to *p* intermediate stages in the cascade to avoid mixing due to recycle streams. One may expect to see improved energy-efficiency by the use of all three intermediate stages, since mixing losses due to recycling could be completely avoided. Yet, when an ISC cascade is optimized to minimize specific energy requirement, some of the intermediate stages are absent under the optimal operating conditions.

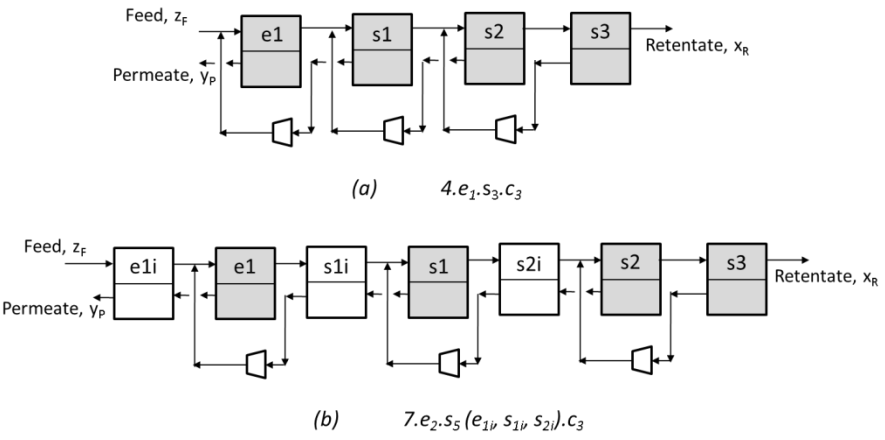

Figure 2-4: Classical and ISC master configurations with p = 3 [17]

In the nitrogen production example, for the case where exactly three recycle compressors are to be used (p = 3), the results are presented in Tables 2-1 and 2-2 and compared with those for the p = 3 classical cascade designed by the method of variable separation factors with no external mixing loss.

Table 2-1: Results for configuration 4.e1.s3.c2

Configuration: $4.e_1.s_3.c_3$ *(NO MIX)* *Normalized Specific Energy Requirement: 0.9791* Normalized Area Requirement: 0.9952										
Stages	**Optimal values of Separation factors**			**Composition**			**Flow-rate** kmol/hr		**Pr. Ratio**	**Normal. Area**
	h	***t***	S_{local}	***x***	***y***	***z***	***L***	***V***	***Pr***	***Area***
e1	2.40	2.90	3.78	0.0838	0.3893	0.2095	115.99	115.99	5.38	0.355
s1	2.90	3.52	4.93	0.0253	0.2095	0.0838	65.81	40.91	17.42	0.1983
s2	3.52	2.05	4.88	0.0125	0.0838	0.0253	41.58	155.25	19.84	0.1376
s3	2.05	12.66	5.03	0.0010	0.0253	0.0125	89.99	115.99	24.61	0.3043
Configuration: $4.e_1.s_3.c_3$ *(MIX)* *Normalized Specific Energy Requirement: 0.9654* Normalized Area Requirement: 0.9211										
Stages	**Optimal values of Separation factors**			**Composition**			**Flow-rate** kmol/hr		**Pr. Ratio**	**Normal. Area**
	h	***t***	S_{local}	***x***	***y***	***z***	***L***	***V***	***Pr***	***Area***
e1	2.57	3.59	4.38	0.0646	0.3893	0.1985	165.24	115.99	8.12	0.3226
s1	2.92	3.28	4.84	0.0198	0.1622	0.0623	153.36	65.16	16.78	0.2054
s2	3.08	2.91	4.89	0.0065	0.0550	0.0186	161.28	53.64	20.53	0.1813
s3	2.40	6.50	4.96	0.0010	0.0154	0.0065	100.08	61.20	23.36	0.2117

The no-mixing case of the classical cascade $4.e_1.s_3.c_3$ (Figure 2-4a) has a normalized specific energy requirement (NSER) of 0.9791 and a normalized area requirement (NAR) of 0.9952 (Table 2-1), while the intermediate stage cascade $7.e_2.s_5(e_{1i},s_{1i},s_{2i}).c_3$ (Figure 2-4b) has an NSER of 0.9674 and an NAR of 0.9406 (Table 2-2).

Table 2-2: Results for configuration 7.e2.s5(e1i,s1i,s2i).c3

Configuration: $7.e_2.s_5\ (e_{1i},s_{1i},s_{2i}).c_3$ *Normalized Specific Energy Requirement: 0.9674* Normalized Area Requirement: 0.9406										
Stages	**Optimal values of Separation factors**			**Composition**			**Flow-rate** kmol/hr		**Pr. ratio**	**Normal. Area**
	h	***t***	S_{local}	***x***	***y***	***z***	***L***	***V***	***Pr***	***Area***
e1i	3.97	1.17	4.28	0.1851	0.3892	0.2095	199.94	16.08	7.37	0.0361
e1	2.58	3.18	4.21	0.0666	0.3693	0.1851	155.36	99.95	7.37	0.2889
s1i	4.80	1.00	4.80	0.0666	0.1851	0.0666	155.36	0.01	15.92	0.0000
s1	3.18	2.53	4.80	0.0274	0.1851	0.0666	167.47	55.36	15.92	0.1709
s2i	3.75	1.78	4.90	0.0156	0.0666	0.0274	142.64	24.83	20.12	0.0812
s2	3.31	2.37	4.86	0.0066	0.0497	0.0156	163.10	42.64	20.12	0.1451
s3	2.37	6.67	4.93	0.0010	0.0156	0.0066	100.00	63.10	22.34	0.2185

It is observed that both stage s_{1i} and stage e_{1i} of this configuration were found to have low values of the tail separation factor (1.00 and 1.17 respectively). Thus, these two intermediate stages do not perform appreciable separation and hence may not be required.

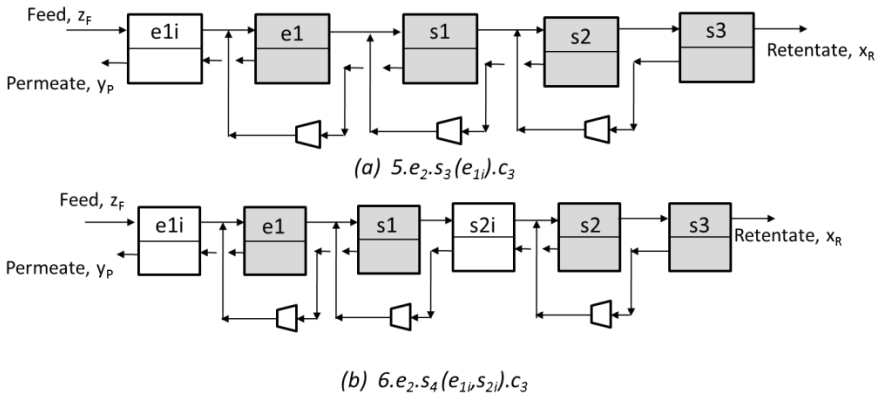

Figure 2-5: Optimal ISC-type cascades with three recycle compressors[17]

The ISC process with three compressors and exactly one intermediate stage that had the lowest NSER is configuration $5.e_2.s_3(e_{1i}).c_3$, which has an NSER of 0.9723 and an NAR of 0.9083 (Figure 2-5a and Table 2-3).

Table 2-3: Results for configuration 5.e2.s3(e1i).c3

Configuration: $5.e_2.s_3\ (e_1).c_3$						*Normalized Specific Energy Requirement: 0.9723* Normalized Area Requirement: 0.9083				
Stages	**Optimal values of Separation factors**			**Composition**			**Flow-rate** kmol/hr		**Pr. Ratio**	**Normal. Area**
	h	***t***	S_{local}	***x***	***y***	***z***	***L***	***V***	***Pr***	***Area***
e1i	3.86	1.36	4.48	0.1627	0.3892	0.2095	186.52	29.50	8.52	0.0660
e1	2.77	2.85	4.35	0.0637	0.3495	0.1627	163.43	86.53	8.52	0.2466
s1i	2.85	3.43	4.81	0.0194	0.1626	0.0637	141.66	63.38	16.29	0.2003
s1	3.44	2.21	4.91	0.0089	0.0637	0.0194	174.55	41.62	21.01	0.1396
s2	2.21	8.93	4.99	0.0010	0.0194	0.0089	100.00	74.55	23.79	0.2556

Similarly, the most energy-efficient three compressor ISC-type cascade using two intermediate stages is $6.e_2.s_4(e_{1i},s_{2i}).c_3$ (Figure 2-5b, Table 2-4).This configuration has an NSER of 0.9677, and an NAR of 0.9410. Comparison of the results for $6.e_2.s_4(e_{1i},s_{2i}).c_3$ and $5.e_2.s_3(e_{1i}).c_3$ suggests that using only one intermediate stage can still capture most of the benefits of using an ISC configuration with three recycle compressors. Additionally, the tables show that the location of the intermediate stages is also important in minimizing the specific energy requirement and must be optimized accordingly. In this case, if only one intermediate stage is to be used, then using the e_{1i} stage rather than the s_{2i} stage has greater benefit.

Table 2-4: Results for configuration 6.e2.s4(e1i,s2i).c3

Configuration: $6.e_2.s_4\ (e_1,s_2).c_3$ *Normalized Specific Energy Requirement: 0.9677* Normalized Area Requirement: 0.9410										
Stages	**Optimal values of Separation factors**			**Composition**			**Flow-rate** kmol/hr		**Pr. Ratio**	**Normal. Area**
	h	***t***	S_{local}	***x***	***y***	***z***	***L***	***V***	***Pr***	***Area***
e1i	3.97	1.17	4.28	0.1851	0.3892	0.2095	199.94	16.08	7.36	0.0361
e1	2.58	3.18	4.21	0.0667	0.3694	0.1851	155.46	99.94	7.36	0.2890
s1	3.18	2.53	4.80	0.0274	0.1851	0.0666	167.30	55.41	15.91	0.1710
s2i	3.75	1.78	4.90	0.0156	0.0666	0.0274	142.66	24.64	20.10	0.0806
s2	3.31	2.36	4.86	0.0067	0.0499	0.0156	163.36	42.66	20.10	0.1451
s3	2.36	6.70	4.93	0.0010	0.0156	0.0067	100.00	63.36	22.34	0.2191

The same analysis is performed for cascades with two and four recycle compressors. When two compressors are used, it is found that the energy-optimal cascade has two intermediate stages (configuration $5.e_2.s_3(e_{1i},s_{1i}).c_2$). The NSER of this configuration is 0.9965, and the NAR is 0.9018. The optimal cascade with one intermediate stage is $4.e_1.s_3(s_{2i}).c_2$, which has an NSER of 1.0205 and an NAR of 1.0516. These results again show that most of the benefit of the ISC configuration can be obtained with only one intermediate stage.

In the case when four compressors are used, it was found that all four intermediate stages have a tail separation factor approaching 1.00, indicating that the classical configuration $5.e_1.s_4.c_4$ does not have any significant disadvantage with respect to specific energy requirement as compared to any of the intermediate stage configurations and intermediate stages may not be required. The result that none of the intermediate stages are needed for the four compressor case also indicates that it is not necessary to investigate the space for five- or six-compressor systems. Thus, for this example, the optimal number of recycle compressors for the ISC cascade is $p_{opt} = 4$. Thus the p_{opt} value is the same regardless of whether the ISC method, the VSF method is

used. Furthermore, the optimal parameters of each stage as well as the NSER are identical for the two methods.

From the results in this section, it can be confirmed that that not all feasible intermediate stages are always needed for an efficient cascade. Indeed, it can also be observed that in cases such as the two-compressor case where the globally optimal configuration has equal number of compressors and intermediate stages, most of the possible energy savings can be realized with just one intermediate stage; in this case, the addition of a second intermediate stage creates only 2.4% energy savings. This is consistent with the work of Pathare.[17]

It can be hypothesized that the addition of intermediate stages is beneficial because it increases the freedom of the optimization framework to assume additional values of flowrates and pressure ratios without violating the constraint of no mixing loss due to recycle streams. In the case of optimally designed classical cascades by the method of variable separation factors with external mixing loss allowed, it has been shown that the overall mixing loss due to recycle streams decreases as the number of compressors increases.[17] For the nitrogen production example, at the global optimum of four compressors, even when mixing losses are allowed, the classical cascade solution is such that the streams that mix have similar compositions, and there is negligible mixing loss. It stands to reason that in the case of intermediate stage cascades, as the global optimum in specific energy requirement is approached, the benefit of adding intermediate stages will decrease. This hypothesis is consistent with the result described in the previous section that not all of the p possible intermediate stages are required for a p-compressor system to achieve minimum specific energy consumption, also formulated

in Pathare.[17] Further, it can be inferred that at the globally optimum solution having p_{opt}-compressors (p_{opt} =4 for the nitrogen production case), since mixing losses due to recycle streams are inherently minimized, any intermediate stages should also provide negligible improvement from the classical cascade in a p_{opt}-compressor system. This is consistent with the observation that the values of $p_{opt,}$ as well as optimal parameters of all stages, are nearly identical regardless of whether cascades are designed by the intermediate stage method, or by the method of variable separation factors.

Table 2-5: Summary of the optimal solutions with different numbers of compressors

Number of Recycle Compressors	Classical Cascade Optimal Configuration	(No Mixing Allowed) Normalized Specific Energy Requirement	(Mixing Allowed) Normalized Specific Energy Requirement	ISC Optimal Configuration	ISC Normalized Specific Energy Requirement	Estimated Relative Savings %
1	$2.e_1.s_1.c_1$	1.238	1.140	$3.e_2.s_1(e_{1i}).c_1$	1.092	11.80
2	$3.e_1.s_2.c_2$	1.033	1.010	$5.e_2.s_3(e_{1i},s_{1i}).c_2$	0.997	3.53
3	$4.e_1.s_3.c_3$	0.979	0.965	$6.e_2.s_4(e_{1i},s_{2i}).c_3$	0.968	1.19
4	$5.e_1.s_4.c_4$	0.956	0.953	$5.e_1.s_4.c_4$	0.956	0

Table 2-5 shows the trend in the results as the number of compressors is increased. In agreement with the work of Agrawal & Xu[14] and Pathare[17], for a one-compressor system the intermediate stage can provide a significant 11.8% decrease in specific energy requirement from the ideal (no-mixing) cascade. The benefit of intermediate stages decreases in a two compressor system, but the ISC configuration still provides a 3.5% decrease in specific energy requirement from the no-mixing cascade. As the number of compressors is increased up to four, there are no energy savings of significance; all

intermediate stages effectively disappear (total normalized area of 0.0137) and the configuration is the same as the classical cascade.

The energy advantages of ISC configurations are not as pronounced when compared to an optimal cascade which allows mixing of dissimilar streams (also termed non-ideal cascades). Table 2-5 notes that for a single compressor system, the ISC cascade has an optimal NSER of 1.092 compared to the classical cascade with external mixing losses allowed with an optimal NSER of 1.140. The table shows that the relative advantage of the ISC cascade also decreases relative to the classical cascade with external mixing losses allowed as the number of compressors increases. At the global optimum of four compressors, the ISC configuration is practically identical to the classical configuration with external mixing loss disallowed and thus can at best match the classical configuration with external mixing loss allowed.

2.3.4 Validation of ISC findings with a second case

In order to further support the findings of section 2.3.3 in regards to the efficiency of ISC arrangements, it is desirable to see if the same trends apply for a different separation example. Therefore, a second case is taken in which the initial feed is a mix of 50% oxygen and 50% nitrogen, and it is desired to simultaneously enrich the oxygen to 90% and the nitrogen to 95%. The optimal solution by the method of CSF for this separation is $5.e_3.s_2.c_4$, which has a specific energy consumption of 10.6647x RT per kmole of N_2 and an area requirement of 1607 m^2/(kmol/hr). The solutions for *p*-compressor classical cascades by the VSF method and solutions for *p*-compressor ISC

cascades for between one and four recycle compressors are shown in Table 2-6, from a similar trend in energy-efficiencies to that discussed in section 2.3.3 is observed.

Table 2-6: Summary of the optimal colustions - Case 2

Number of Recycle Compressors	Classical Cascade Optimal Configuration	(No Mixing Allowed) Normalized Specific Energy Requirement	(Mixing Allowed) Normalized Specific Energy Requirement	ISC Optimal Configuration	ISC Normalized Specific Energy Requirement	Estimated Relative Savings %
1	$2.e_2.s_0.c_1$	1.784	1.143	$3.e_3.s_0(e_{1i}).c_1$	1.164	62
2	$3.e_2.s_1.c_2$	0.993	0.974	$4.e_3.s_1(e_{1i}).c_2$	0.974	1.9
3	$4.e_3.s_1.c_3$	0.952	0.941	$6.e_5.s_1(e_{1i}).c_3$	0.951	0.1
4	$5.e_3.s_2.c_4$	0.93	0.93	$5.e_3.s_2.c_4$	0.93	0

Again, for this example p_{opt} = 4 regardless of the design method employed, as expected based on the work of Pathare[17]. When only one recycle compressor is used, the ISC arrangement is again able to deliver high savings in specific energy requirements compared to the (ideal) classical configuration by VSF method with no external mixing losses. When the number of compressors is more than one but less than p_{opt} , one or more intermediate stages reduce the NSER of the cascade, but not all possible intermediate stages are required to obtain this benefit. For the classical configuration having p_{opt}-compressors by the VSF method, the intermediate stages are unnecessary since mixing losses are already negligible. Again, in this case, the ISC configurations prove to have no advantage over the classical configurations designed by VSF method with external mixing losses allowed. This is in agreement with the conclusions of Pathare.[17]

Table 2-7: Comparison of normalized areas - Cases 1 and 2

	Case 1			Case 2		
Number of Recycle Compressors	(No Mixing Allowed) Classical Cascade Area	(Mixing Allowed) Classical Cascade Area	ISC Cascade Area	(No Mixing Allowed) Classical Cascade Area	(Mixing Allowed) Classical Cascade Area	ISC Cascade Area
1	1.2528	0.9282	0.8628	0.1872	0.4749	0.4108
2	0.9411	0.8836	0.9018	0.3724	0.4035	0.4188
3	0.9952	0.9211	0.9406	0.6134	0.5661	0.6134
4	1.0094	0.9628	0.9925	0.5964	0.5862	0.5964

In general, the required membrane area does not appear to follow a set trend for either case study, as seen in Table 2-7. However, the table does show that the energy optimal ISC configurations can be achieved with similar membrane area as the VSF optimal in all cases.

2.3.5 Conclusions about ISC membrane arrangements

For producing pure nitrogen from air, varying number of recycle compressors was used to study the effects of intermediate stages inserted into classical cascades. This was performed with and without mixing losses. Conclusions drawn were in agreement with the work done by Pathare.[17]

- In an optimized ISC cascade all of the possible intermediate stages may not be present. For the nitrogen production example problem, with ISC configurations using three recycle compressors, a cascade with two intermediate stages could obtain the full energy benefit possible; almost all energy benefit could be obtained by introducing a single intermediate stage. When a reduced number of intermediate stages are used, their location does influence the amount of energy savings realized.

- ISC-type cascades have a significant advantage over the ideal classical cascade only when the losses due to the mixing of recycle streams in the classical cascade are significant. Since losses due to the mixing of recycle streams are decreased as the number of recycle streams and associated compressors and stages are increased, the advantage in energy efficiency seen for ISC cascades with low numbers of compressors decreases as the number of membrane stages and recycle compressors increase towards energy optimal values.

Intermediate stage cascades are most useful when applied to systems with only one recycle compressor. This is because mixing losses due to mismatched recycle stream compositions tend to be large for such classical cascades.

2.4 Effect of varying recovery on single-compressor membrane cascades

In air separation applications such as that studied in section 2.3, nitrogen is typically required to be produced at a high purity (~99.9%), but there need not be a strict specification on the recovery of nitrogen, as air is a free raw material. As a result, it is important to compare all the candidate configurations to produce a high purity of the nitrogen product for a wide range of recoveries. Where in section 2.3 a single, fixed recovery was examined for multiple cascade arrangements, this section will examine what happens to energy and area requirements upon varying recovery. The following questions are of interest: Is any one membrane cascade system always the best, regardless of the desired recovery? If not, can general guidelines be set for selection of a good

configuration at a given recovery? Does the optimal solution always avoid mixing losses? Do conditions exist for which multiple configurations have the same energy requirement?

It is required to produce 100 kmol/hr of 99.9% pure nitrogen at 10 atm pressure from air. Air is taken to be a binary mixture of 20.95% oxygen and 79.05% nitrogen. An oxygen-selective polymeric membrane with a permselectivity value of 6 is available. The oxygen permeability constant (Q/l) is 3.2×10^5 Barrer/cm and the permselectivity of the membrane with respect to nitrogen (α) is six. These values of permeability and permselectivity are consistent with commercially available polyimide membranes for this application.[3,25-26] It is assumed that any value of the nitrogen recovery is acceptable within the wide range of 20% to 95%. The lower bound of 20% is chosen for practical reasons: at such low recoveries, the feed through-put needed is so high that a large amount of energy is required just to compress the feed, making such a system economically not viable. Only the retentate nitrogen-enriched product is of interest, and the oxygen-enriched permeate product is discarded back into the atmosphere. The energy consumption of any membrane scheme achieving this separation is calculated under the assumption of 100% efficient isothermal compressors and expanders. The energy consumption also takes into account the energy needed to compress the feed, energy needed in the recycle compressor and pressure energy recoverable from the oxygen-enriched permeate product before it is discarded into the atmosphere. In order to facilitate comparison of the energy consumption of all of the possible schemes across all feasible recovery specifications, the energy consumption is reported on a basis of per mole of content nitrogen in the retentate product. All the considered candidate schemes having a

single recycle compressor are illustrated in Figure 2-6. In addition to these cascades, a single stage scheme with no recycle is also considered.

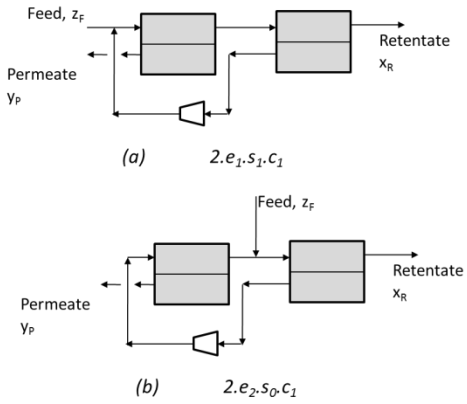

Figure 2-6: Single-recycle classical cascades [17]

The method given by Pathare & Agrawal [18] is used to find the optimal energy requirement and associated pressure ratios and membrane areas for all these candidate configurations. In these calculations, the following assumptions are made:

1. A cross-flow pattern is assumed to exist in all the membrane stages.
2. Effects due to pressure drops within each membrane stage are neglected.
3. Permselectivity value of the membrane is assumed to remain constant.

The goal of such a study, identified by Pathare [17], is as follows: “Find the cascade configuration with the maximum energy-efficiency. One way of finding the most energy-efficient configuration out of all of the possible candidates is to optimize each one individually and rank-list them according to their specific energy requirement. In each such configuration, only the feed and product stream compositions and flow-rates are

known. All of the intermediate stream flow-rates and compositions may take any feasible values. For a specified feasible set of all the intermediate stream flow-rates and compositions, there is a unique set of operating pressure ratios for each stage on the cascade, and thus a unique energy demand that can be calculated. The objective of the optimization procedure is to find the optimal set of all of the intermediate stream flow-rates and compositions such that the energy consumption is minimized." The constraints governing the feasibility of the cascade arise from the properties of the cascade structure. The entire system is subject to the no mixing loss constraint except for those candidate configurations specifically noted otherwise; all streams that are mixed must be the same composition. Because of this, the compositions of the recycle streams match the compositions of the feeds of the stage they are mixed with. In addition, for ISC configurations the extra stages have the same pressure ratio as the stages that succeed them. In addition to the above constraints, overall and component mass balances around each stage and each point of mixing must be met. The feasibility constraints which set the dependence of compositions and flows on these assumptions, can be expressed as a series of linear and nonlinear equations. As described in section 2.3.2, the equations were implemented in GAMS using the Branch and Reduce Optimization Navigator (BARON) solver to guarantee global optimality. Providing the solver with the conditions for cascade feasibility will yield a feasible solution with minimum compressor energy consumption.

2.4.1 Single stage scheme

For a single membrane stage, results are given in Table 2-8. It is clear that obtaining high purity and high recovery in a single stage is impossible. In this case, the maximum recovery to produce the desired purity with one stage is 32.7%. This result is consistent with the expectation that for a membrane with a finite permselectivity, a finite degree of separation is possible even with infinite driving force. As a result, an upper limit on recovery is seen when a fixed purity is specified.

Table 2-8: Results for single-stage membrane [17]

Single-Stage System				
% Nitrogen Recovery	**Feed flow-rate**	**Pressure ratio**	**Specific Energy Requirement**	**Normalized Area**
	kmol/hr			
15	842.50	5.92	15.52	4.262
16	789.85	6.31	15.03	3.821
17	743.39	6.75	14.60	3.442
18	702.09	7.24	14.24	3.114
19	665.14	7.80	13.92	2.828
20	631.88	8.44	13.66	2.576
21	601.79	9.18	13.44	2.354
22	574.44	10.05	13.26	2.157
23	549.46	11.09	13.13	0.949
24	526.57	12.37	13.04	1.824
25	505.50	13.97	13.01	1.683
26	486.06	16.00	13.02	1.555
27	468.06	18.80	13.11	1.440
28	451.34	22.72	13.29	1.335
29	435.78	28.71	13.59	1.240
30	421.25	39.02	14.09	1.153
31	407.66	60.96	14.96	1.073
32	394.92	140.10	16.90	1.000
32.7	386.47	infinity	N/A	0.952

The energy requirement curve is U-shaped, with a minimum energy point existing. At recoveries near the maximum recovery, a high pressure ratio is required to achieve the high recovery and purity. This leads to a high energy requirement. At lower values of recovery, a rapid decrease in required pressure ratio is seen without dramatically increasing the throughput. This leads to a minimum energy consumption which in this

case is seen at a recovery of about 25%. Past this point, decreasing recovery causes a larger throughput. This leads to an increase in energy requirement, leading to a U-shaped data trend with a clear minimum at 25%. This is in agreement with the results of Pathare.[17]

2.4.2 Single-recycle classical configuration with no mixing loss due to recycle streams

In this section, single-recycle classical cascades with no mixing loss are compared for the same sample case as in previous sections. The results obtained for configuration $2.e_1.s_1.c_1$ with no mixing loss are illustrated in Table 2-9a; the results for the configuration $2.e_2.s_0.c_1$ with no mixing loss are shown in Table 2-9b. Both configurations are illustrated in Figure 2-6. All results in this and following sections are reported in terms of specific energy requirement normalized by that of a single-stage system, consistent with the method of Pathare.[17] From Table 2-8 the single-stage system has a minimum energy requirement of 13.01 x RT per kmole of nitrogen. All subsequent energy requirement values are normalized based on this value, so that convenient comparison may be made to the single-stage system. In Table 2-9a, at 60% recovery, it is found that the specific energy requirement is 0.9978. The total energy of the cascade is thus 0.9978 x 13.01 RT per kilomole of N_2.

Using a two-stage system allows much higher possible recoveries to be reached than a single-stage cascade. Also of interest is that, when there is no mixing loss in the cascade, both designs still have an upper bound on the recovery achievable at the desired purity and it is not possible to go to arbitrarily high values of purity with only two membrane stages.[17]

Table 2-9: Results for single-recycle classical cascades with no mixing losses allowed

	(a) *2.e1.s1.c1*						(b) *2.e2.s0.c1*					
Recovery %	**Normalized Specific Energy Requirement**	**Pressure ratio Stage e1**	**Pressure ratio Stage s1**	**Norm. Area Stage e1**	**Norm. Area Stage s1**	**Total Norm. Area**	**Normalized Specific Energy Requirement**	**Pressure ratio Stage e2**	**Pressure ratio Stage e1**	**Norm. Area Stage e2**	**Norm. Area Stage e1**	**Total Norm. Area**
86.4	-	-	-	-	-	-	N/A	infinite	178.25	-	-	-
86	-	-	-	-	-	-	1.2525	254.84	30.76	0.1135	1.2169	1.3304
84	-	-	-	-	-	-	1.1147	18.98	15.44	0.1362	1.5872	1.7234
83	N/A	infinite	3.09	-	-	-	1.1022	12.65	15.10	0.1492	1.6070	1.7562
82	1.4476	504.29	5.64	0.1445	4.5412	4.6858	1.0943	9.63	14.94	0.1629	1.6166	1.7795
80	1.0871	62.08	14.16	0.1640	1.5570	1.7210	1.0848	6.70	14.80	0.1928	1.6256	1.8184
78	1.0376	19.82	17.23	0.1895	1.3856	1.5752	1.0791	5.25	14.73	0.2261	1.6297	1.8558
76	1.0205	11.82	17.88	0.2182	1.3594	1.5776	1.0752	4.39	14.70	0.2633	1.6319	1.8952
74	1.0116	8.59	18.13	0.2497	1.3497	1.5995	1.0726	3.80	14.68	0.3049	1.6330	1.9379
72	1.0062	6.85	18.26	0.2844	1.3449	1.6293	1.0705	3.38	14.67	0.3514	1.6336	1.9850
70	1.0028	5.75	18.26	0.3226	1.3422	1.6648	1.0690	3.05	14.67	0.4037	1.6338	2.0375
68	1.0005	4.99	18.38	0.3645	1.3406	1.7052	1.0677	2.79	14.67	0.4624	1.6337	2.0962
66	0.9991	4.43	18.40	0.4108	1.3397	1.7505	1.0667	2.58	14.68	0.5288	1.6334	2.1622
64	0.9983	4.00	18.42	0.4620	1.3392	1.8012	1.0657	2.41	14.68	0.6038	1.6330	2.2367
62	0.9979	3.66	18.42	0.5186	1.3390	1.8576	1.0649	2.26	14.69	0.6890	1.6323	2.3213
60	0.9978	3.37	18.42	0.5813	1.3380	1.9194	1.0642	2.13	14.71	0.7861	1.6315	2.4176
58	0.9981	3.14	18.42	0.6511	1.3382	1.9893	1.0634	2.02	14.72	0.8973	1.6306	2.5279
56	0.9986	2.94	18.42	0.7288	1.3401	2.0690	1.0627	1.92	14.74	1.0253	1.6294	2.6547
54	0.9992	2.77	18.39	0.8157	1.3408	2.1565	1.0619	1.83	14.76	1.1732	1.6282	2.8014
52	1.0001	2.61	18.37	0.9130	1.3408	2.2538	1.0612	1.74	14.78	1.3455	1.6267	2.9722
50	1.0011	2.48	18.37	1.0224	1.3408	2.3632	1.0603	1.67	14.81	1.5473	1.6251	3.1724
48	1.0023	2.36	18.37	1.1457	1.3408	2.4865	1.0593	1.60	14.84	1.7857	1.6232	3.4089
46	1.0037	2.26	18.37	1.2855	1.3408	2.6263	1.0583	1.54	14.87	2.0697	1.6210	3.6907
44	1.0052	2.16	18.37	1.4444	1.3408	2.7852	1.0571	1.49	14.91	2.4119	1.6185	4.0303
42	1.0069	2.07	18.15	1.6264	1.3408	2.9672	1.0556	1.43	14.96	2.8290	1.6155	4.4445
40	1.0088	1.99	18.15	1.8350	1.3408	3.1758	1.0540	1.38	15.02	3.3455	1.6120	4.9574
38	1.0108	1.92	18.15	2.0757	1.3492	3.4249	1.0521	1.34	15.09	3.9969	1.6077	5.6046
36	1.0131	1.85	18.10	2.3557	1.3510	3.7067	1.0498	1.29	15.18	4.8393	1.6023	6.4416
34	1.0156	1.79	18.10	2.6830	1.3510	4.0340	1.0470	1.25	15.30	5.9660	1.5952	7.5612
32	1.0184	1.73	17.98	3.0696	1.3555	4.4251	1.0435	1.21	15.47	7.5521	1.5852	9.1373
30	1.0214	1.67	17.98	3.5285	1.3555	4.8840	1.0388	1.17	15.77	10.0029	1.5689	11.5718
28	1.0249	1.62	17.71	4.0825	1.3659	5.4484	1.0319	1.12	16.60	14.9926	1.5274	16.5199
26	1.0288	1.57	17.71	4.7523	1.3659	6.1182	-	-	-	-	-	-
24	1.0332	1.52	17.71	5.5760	1.3659	6.9419	-	-	-	-	-	-
22	1.0382	1.48	17.71	6.6044	1.3659	7.9703	-	-	-	-	-	-
20	1.0450	1.44	17.38	7.9212	1.3792	9.3004	-	-	-	-	-	-

In order to further study this result, consider the configuration $2.e_1.s_1.c_1$. At any recovery, with no mixing loss in the system recycle stream composition always matches the feed stream composition. In this case, this composition is that of the feed, 79.05% N2. Thus the feed entering stage e1 is always precisely 79.05% N_2 to avoid mixing losses. When mixing losses are allowed, producing high purity nitrogen, it is necessary to have a permeate from e1 very high in oxygen concentration. However, even when driving force is near infinity, nitrogen still has some tendency to permeate due to the modest permselectivity of the selected material of the membrane. Therefore, a relatively high-oxygen feed is required to stage e1 to produce such a permeate. With a feed high in

oxygen, relatively little driving force exists for nitrogen permeation. When little nitrogen passes through the membrane, higher recovery of both products can be achieved. However, when no mixing loss due to the recycle stream is permissible, the recycle composition cannot be adjusted on the feed stage and thus a nitrogen-lean stream may not be produced as a permeate from stage e1. Consequently, a high purity product has a strict upper bound on the possible recovery. For the configuration $2.e_1.s_1.c_1$.the upper bound occurs at 83% recovery.

In the same way, the feed stream to enriching stage e2 for configuration $2.e_2.s_0.c_1$ is heavily limited; as a result if there is a no mixing loss constraint there is an upper bound on recovery for configuration $2.e_2.s_0.c_1$ as well, occurring at 86.4% recovery. At values near this bound, large pressure ratios are needed on each stage for both configurations as seen in Table 2-8a and Table 2-8b. At lower values of recovery, the throughput increases but the pressure ratios drop rapidly resulting in a drop in the specific energy requirement, similar to the single-stage case.

For $2.e_1.s_1.c_1$ the energy requirement is minimized at 60% recovery. At lower values of recovery, the effect of the increased throughputs outweighs the effect of falling pressure ratios, increasing the specific energy requirement. This results in another trend with a U-shape. For this feed, solutions with a lower energy requirement are typically obtained for configuration $2.e_1.s_1.c_1$ compared to configuration $2.e_2.s_0.c_1$, except when recovery is very high. This is because the feed is already rich in the less permeable component; if a lower recovery is needed, then having a single stage in the stripping section is superior to having an additional stage in the enriching section. This leads to the preference of configuration $2.e_1.s_1.c_1$. However, if a high purity retentate product is

desired at a similarly high recovery, it then becomes useful to have stages in the enriching section, thus configuration $2.e_2.s_0.c_1$ is preferred over configuration $2.e_1.s_1.c_1$ when purity and recovery must be simultaneously high.

As recovery decreases, the specific energy requirement for configuration $2.e_2.s_0.c_1$ continues to decrease due to a decrease in the pressure ratio of stage e2. This continues until the pressure ratio reaches a value of approximately 1.0; then the stage e2 performs no separation due to a lack of driving force. Due to the 'no-mixing loss allowed' constraint no solution exists at a recovery lower than this. This is consistent with results obtained by Pathare.[17]

The single-stage scheme is not a relaxation of either the configuration $2.e_2.s_0.c_1$ or the configuration $2.e_1.s_1.c_1$ due to the constraint requiring no mixing loss. There is thus no guarantee that the latter two configurations will outperform a single-stage process. In this case for low recoveries, the single-stage scheme can provide more energy-efficient solutions than the configuration $2.e_1.s_1.c_1$ as long as the mixing loss constraint is in place.

The required membrane areas for these separations are also shown in Table 2-8. The total area required is low at high recoveries, but becomes very high in order to obtain low recoveries. High throughputs are needed at low recovery; a high surface area of membrane is thus required. The intermediate stage cascades, despite having high number of stages, has a similar total area compared to classical cascades. The area required when using configuration $2.e_1.s_1.c_1$ is lower at any available recovery than that required by configuration $2.e_2.s_0.c_1$, By comparison, the value of the membrane area required for single-stage separation was estimated to be 29070 m^2.

2.4.3 Single-recycle classical configurations with mixing losses allowed

Consistent with the results of Pathare[17], the previous sections demonstrated an upper limit exists in recovery for a single-recycle configuration. Since composition matching restrictions create this limit, it seems likely that allowing mixing of any compositions will remove this upper limit. To confirm this, optimization is performed on both possible configurations with this restriction absent. Table 2-10 demonstrates results for configuration $2.e_1.s_1.c_1$ and Table 2-11 shows results for configuration $2.e_2.s_0.c_1$.

Table 2-10: Results for configuration $2.e_1.s_1.c_1$ with mixing losses allowed

$2.e_1.s_1.c_1$							
Recovery %	Normalized Specific Energy Requirement	Recycle Composition	Pressure ratio stage e1	Pressure ratio stage s1	Norm. Area Stage e1	Norm. Area Stage s1	Total Norm. Area
95	1.7540	0.5190	59.03	8.63	0.0531	3.2219	3.2751
93	1.4847	0.4406	45.10	10.03	0.0662	2.5981	2.6644
91	1.3333	0.3839	37.16	11.30	0.0800	2.2333	2.3133
89	1.2350	0.3406	31.94	12.44	0.0944	1.9914	2.0859
87	1.1654	0.3064	28.18	13.48	0.1097	1.8174	1.9271
85	1.1131	0.2786	25.16	14.42	0.1259	1.6856	1.8114
83	1.0723	0.2552	23.04	15.31	0.1429	1.5793	1.7221
81	1.0395	0.2355	21.09	16.13	0.1609	1.4929	1.6539
79	1.0124	0.2185	19.50	16.89	0.1801	1.4198	1.5999
78	1.0006	0.2108	18.80	17.27	0.1902	1.3869	1.5772
77	0.9898	0.2036	18.13	17.62	0.2005	1.3568	1.5573
75	0.9707	0.1904	16.95	18.32	0.2222	1.3014	1.5236
73	0.9542	0.1786	15.90	18.99	0.2453	1.2520	1.4972
71	0.9402	0.1680	14.97	19.63	0.2700	1.2074	1.4773
69	0.9279	0.1583	14.13	20.28	0.2964	1.1660	1.4624
67	0.9174	0.1494	13.38	20.88	0.3247	1.1285	1.4532
65	0.9082	0.1412	12.68	21.48	0.3552	1.0936	1.4489
63	0.9002	0.1335	12.08	22.12	0.3880	1.0593	1.4473
61	0.8933	0.1263	11.51	22.74	0.4234	1.0275	1.4509
59	0.8875	0.1196	10.98	23.37	0.4617	0.9967	1.4584
57	0.8826	0.1131	10.50	24.02	0.5033	0.9669	1.4701
55	0.8785	0.1069	10.08	24.67	0.5483	0.9376	1.4859
53	0.8753	0.1010	9.65	25.36	0.5978	0.9093	1.5071
51	0.8730	0.0929	9.79	26.60	0.6468	0.8664	1.5132
49	0.8713	0.0897	8.92	26.82	0.7111	0.8525	1.5636
47	0.8704	0.0842	8.60	27.61	0.7763	0.8238	1.6001
45	0.8705	0.0789	8.29	28.44	0.8487	0.7951	1.6438
43	0.8712	0.0734	8.03	29.38	0.9286	0.7646	1.6932
41	0.8734	0.0733	7.07	29.00	1.0366	0.7676	1.8041
39	0.8757	0.0621	7.62	31.55	1.1158	0.6980	1.8139
37	0.8798	0.0621	6.74	31.16	1.2520	0.7005	1.9525
35	0.8845	0.0516	7.17	33.99	1.3564	0.6290	1.9854
33	0.8910	0.0450	7.13	35.69	1.4940	0.5820	2.0760
31	0.8994	0.0448	6.34	35.11	1.6954	0.5835	2.2789
29	0.9095	0.0337	6.86	38.95	1.8398	0.4886	2.3284
27	0.9227	0.0336	6.09	38.51	2.1145	0.4898	2.6043
25	0.9412	0.0416	4.87	35.44	2.5336	0.5610	3.0946
23	0.9623	0.0416	4.45	35.41	2.9504	0.5612	3.5116
21	0.9878	0.0416	4.07	35.49	3.4680	0.5608	4.0289

Recoveries from 21% up to 95% are used. 95% was chosen as an arbitrarily high value however even higher values can be reached. The optimization proved the previous statement: upon relaxing the constraint of 'no mixing losses due to the recycle stream allowed', any recovery can be obtained for either single-recycle configuration and there is no upper limit. Relaxing this requirement in both cases decreases the total energy consumption. This observation is consistent with the results obtained reported by Pathare and Agrawal[18] and by Pathare[17].

Table 2-11: Results for configuration 2.e2.s0.c1 with mixing losses allowed

$2.e_2.s_0.c_1$							
Recovery %	Normalized Specific Energy Requirement	Recycle Composition	Pressure ratio stage e2	Pressure ratio stage e1	Norm. Area Stage e1	Norm. Area Stage s1	Total Norm. Area
95	1.6122	0.4835	49.57	10.34	2.6581	0.0533	2.7115
93	1.3861	0.4086	37.12	11.79	2.2237	0.0666	2.2902
91	1.2616	0.3576	29.88	12.94	1.9759	0.0805	2.0565
89	1.1828	0.3210	24.98	13.84	1.8173	0.0954	1.9127
87	1.1290	0.2938	21.33	14.54	1.7085	0.1112	1.8197
85	1.0902	0.2730	18.48	15.07	1.6306	0.1281	1.7587
83	1.0616	0.2570	16.15	15.47	1.5734	0.1462	1.7196
81	1.0400	0.2444	14.20	15.76	1.5307	0.1658	1.6965
79	1.0235	0.2345	12.55	15.97	1.4988	0.1870	1.6857
77	1.0110	0.2266	11.14	16.11	1.4750	0.2100	1.6851
75	1.0016	0.2206	9.91	16.20	1.4577	0.2353	1.6930
73	0.9946	0.2159	8.84	16.24	1.4457	0.2630	1.7087
71	0.9896	0.2124	7.91	16.24	1.4378	0.2937	1.7316
69	0.9863	0.2099	7.09	16.22	1.4335	0.3279	1.7614
67	0.9844	0.2083	6.37	16.18	1.4322	0.3661	1.7983
65	0.9836	0.2075	5.73	16.12	1.4334	0.4091	1.8425
63	0.9837	0.2074	5.16	16.05	1.4370	0.4578	1.8948
61	0.9848	0.2080	4.66	15.96	1.4425	0.5134	1.9559
59	0.9864	0.2092	4.20	15.87	1.4499	0.5772	2.0271
57	0.9864	0.2092	4.20	15.87	1.4499	0.5772	2.0271
55	0.9887	0.2109	3.80	15.77	1.4589	0.6512	2.1101
53	0.9914	0.2132	3.44	15.67	1.4694	0.7377	2.2071
51	0.9945	0.2160	3.11	15.57	1.4814	0.8399	2.3213
49	0.9978	0.2194	2.82	15.47	1.4946	0.9623	2.4569
47	1.0013	0.2233	2.55	15.37	1.5089	1.1112	2.6201
45	1.0047	0.2278	2.30	15.27	1.5243	1.2958	2.8201
43	1.0079	0.2329	2.08	15.18	1.5404	1.5309	3.0713
41	1.0107	0.2386	1.88	15.11	1.5569	1.8413	3.3981
39	1.0128	0.2449	1.69	15.06	1.5732	2.2735	3.8466
37	1.0135	0.2597	1.35	15.12	1.6004	4.0721	5.6725
35	1.0106	0.2683	1.20	15.31	1.6063	6.7661	8.3723
33	1.0038	0.2778	1.05	15.77	1.5984	24.6818	26.2802
31	-	-	-	-	-	-	-
29	-	-	-	-	-	-	-
27	-	-	-	-	-	-	-
25	-	-	-	-	-	-	-

This result is explained in this way: Consider configuration *2.e1.s1.c1*. The recycle stream has a high oxygen content when recovery is high. When more oxygen is present in the recycle than the feed, less driving force is present for nitrogen permeation. With less nitrogen permeating, overall recovery is higher. The permeate product is also high in oxygen purity. However, high requirements in energy are required to reach this purity due to mixing loss and high pressure ratios. As the desired recovery level is lowered, some losses of nitrogen from the permeate stream are permissible. As a result, the recycle stream faces less stringent requirements for being very rich in oxygen and may be closer to the feed air composition. Since a high O_2 purity is not required, the pressure ratios are lower, and mixing losses are also lessened. This yields a low energy requirement. As the recovery level is further reduced, the specific energy requirement is reduced as well. The reduction continues until the recovery level leads to a recycle composition exactly matching the feed composition and mixing losses are zero. For the nitrogen production example, this happens at recovery = 70%. Comparing Table 2-10 and Table 2-9a demonstrates that energy consumption for *2.e1.s1.c1* is identical at this point whether or mixing losses are constrained.

At low recoveries, much higher permeation of nitrogen is tolerated. It becomes advantageous to have recycle streams with less oxygen than the feed. This decreases the separation burden on the stripping stage, requiring a lower pressure ratio and leading to a lower overall energy use. This continues until a certain minimum energy point, at which the effect of dropping pressure ratio is again offset and surpassed by the high throughput in the compressor. Any further reduction in recovery from this point increases the energy requirement. Well below 78% recovery, the amount of mismatch between the recycle and

the feed compositions was high and mixing losses became increasingly dominant in determining the energy efficiency.

The same type of explanation applies to configuration $2.e_2.s_0.c_1$. At high recovery, configuration $2.e_2.s_0.c_1$ has a low specific energy consumption compared to $2.e_1.s_1.c_1$ even when the mixing losses are allowed. As noted by Pathare [17], when mixing losses were forced to be absent the presence of the enriching stage is advantageous for making the product in high recovery.

As recovery is reduced, the pressure ratio in enriching stage e2 approaches 1.0. At this point enriching stage e2 performs no appreciable separation, reducing the configuration to a single-stage system. Thus, below a particular recovery, the configuration $2.e_2.s_0.c_1$ cannot produce the required purity, confirming previous work.[17]

Once again, the $2.e_1.s_1.c_1$ configuration is observed to have lower membrane area requirements to perform the desired separation than does the $2.e_2.s_0.c_1$. configuration. Furthermore, compared to the case with mixing loss disallowed, these configurations have slightly lower areas in most cases. The exception comes when comparing the configurations with only one enriching stage at high recoveries; at these points, the case with no mixing loss has a slightly lower area required. In general, the areas required in each of the two cases are very close to one another, save at recoveries less than 30%.

2.4.4 Single-recycle cascades with intermediate stages

The ISC type configuration $3.e_1.s_2(e_{1i}).c_1$ adds one intermediate stage to the configuration $2.e_1.s_1.c_1$ in order to avoid mixing losses. Both cascades are seen in Figure

2-7. For the configuration $3.e_1.s_2(e_{1i}).c_1$, stages e1 and s1 have the same pressure ratio. The system thus needs only one recycle compressor.

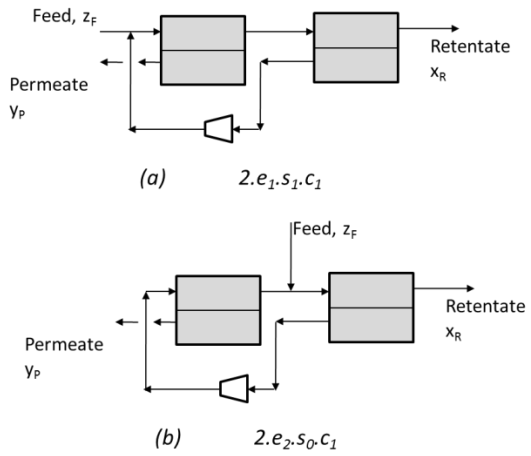

Figure 2-7: Single-recycle cascade options [17]

The results for configuration $3.e_1.s_2(e_{1i}).c_1$ at various recoveries appear in Table 2-12. For low recovery, energy required for configuration $3.e_1.s_2(e_{1i}).c_1$ is lower than that for configuration $2.e_1.s_1.c_1$ with mixing losses allowed. This confirms the observations of Pathare et al.[17,18] However, the potential savings created by the ISC configuration $3.e_1.s_2(e_{1i}).c_1$ compared to the classical configuration $2.e_1.s_1.c_1$ are not the same at all recoveries. For configuration $3.e_1.s_2(e_{1i}).c_1$, the minimum specific energy requirement occurs at a value of recovery = 43% . This recovery yields a recycle composition of 4.10% oxygen. Though these results are numerically different than literature [17], the general trend is the same.

Table 2-12: Results for ISC configuration

$3.e_1.s_2\,(e_{1i})\,.c_1$								
Recovery %	Normalized Specific Energy Requirement	Recycle Composition	Pressure ratio stage e1/s1	Pressure ratio stage s2	Norm. Area Stage e1	Norm. Area Stage s1	Norm. Area Stage s2	Total Norm. Area
81	-	-	-	-	-	-	-	-
79	-	-	-	-	-	-	-	-
78	-	-	-	-	-	-	-	-
77.6	1.0330	0.2095	18.24	17.37	0.0016	0.1928	1.3771	1.5715
77	1.0264	0.2032	18.43	17.61	0.0080	0.1921	1.3563	1.5565
75	1.0053	0.1872	18.64	18.27	0.0295	0.1909	1.2957	1.5161
73	0.9856	0.1721	18.64	18.92	0.0515	0.1904	1.2388	1.4806
71	0.9673	0.1578	18.49	19.55	0.0743	0.1906	1.1851	1.4500
69	0.9503	0.1444	18.23	20.15	0.0980	0.1914	1.1345	1.4239
67	0.9345	0.1319	17.88	20.72	0.1229	0.1928	1.0865	1.4022
65	0.9198	0.1203	17.46	21.24	0.1492	0.1947	1.0408	1.3847
63	0.9063	0.1094	17.00	21.72	0.1770	0.1972	0.9973	1.3715
61	0.8940	0.0993	16.47	22.14	0.2067	0.2003	0.9557	1.3626
59	0.8827	0.0901	15.92	22.51	0.2384	0.2039	0.9158	1.3581
57	0.8726	0.0817	15.34	22.82	0.2724	0.2082	0.8774	1.3581
55	0.8636	0.0739	14.72	23.05	0.3092	0.2132	0.8408	1.3631
53	0.8557	0.0669	14.11	23.25	0.3492	0.2186	0.8045	1.3722
51	0.8490	0.0605	13.47	23.37	0.3926	0.2252	0.7701	1.3880
49	0.8436	0.0548	12.81	23.43	0.4403	0.2325	0.7371	1.4099
47	0.8395	0.0496	12.16	23.44	0.4929	0.2408	0.7052	1.4389
45	0.8368	0.0451	11.47	23.39	0.5512	0.2503	0.6745	1.4760
43	0.8356	0.0410	10.83	23.29	0.6163	0.2610	0.6452	1.5225
41	0.8362	0.0375	10.16	23.15	0.6894	0.2736	0.6184	1.5813
39	0.8382	0.0345	9.48	22.99	0.7722	0.2876	0.5926	1.6525
37	0.8424	0.0319	8.84	22.79	0.8670	0.3042	0.5701	1.7413
35	0.8487	0.0297	8.20	22.57	0.9765	0.3235	0.5505	1.8505
33	0.8574	0.0280	7.57	22.38	1.1039	0.3453	0.5329	1.9821
31	0.8687	0.0269	6.93	22.16	1.2550	0.3721	0.5214	2.1485
29	0.8831	0.0263	6.32	22.00	1.4360	0.4045	0.5151	2.3555
27	0.9006	0.0262	5.73	21.93	1.6563	0.4443	0.5155	2.6161

The recycle is mixed with the retentate stream of stage e1, a stream with identical composition. As the recovery is increased, the required recycle composition also increases. Because of this, the mismatch between feed and recycle streams lessens. The retentate stream of stage e1 is therefore not required to be significantly lower than the feed in oxygen content. As the retentate composition of stage e1 approaches its feed composition, the stage performs no appreciable separation. When recovery = 77.6%, the recycle composition must approach the feed composition, stage e1 disappears and configuration $3.e_1.s_2(e_{1i}).c_1$ is equivalent to configuration $2.e_1.s_1.c_1$.

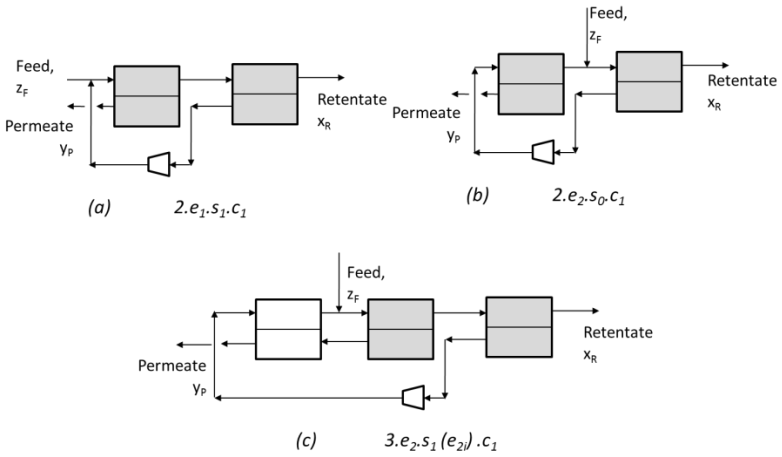

Figure 2-8: Configuration 3.e2.s1(e2i).c1 [17]

When recovery further increases, the recycle stream has more nitrogen than the feed. Therefore, the ISC cascade $3.e_1.s_2(e_{1i}).c_1$ is no longer valid for use because the recycle stream is leaner than the feed thanks to the location of the additional stage in the stripping section. Instead, an additional stage is required in the enriching section. This suggests that an alternate ISC- cascade must be used with an extra stage in the enriching section rather than placing one in the stripping section. This need can be filled by the configuration $3.e_2.s_1(e_{2i}).c_1$. Figure 2-8 illustrates the configuration, showing also $2.e_1.s_1.c_1$ and $2.e_2.s_0.c_1$ to allow comparison.

Table 2-13: Results for configuration $3.e_2.s_1(e_{2i}).c_1$

$3.e_2.s_1(e_{2i}).c_1$								
Recovery %	Normalized Specific Energy Requirement	Recycle Composition	Pressure ratio stage e2	Pressure ratio stage e1/s1	Norm. Area Stage e2	Norm. Area Stage e1	Norm. Area Stage s1	Total Norm. Area
89	-	-	-	-	-	-	-	-
87	-	-	-	-	-	-	-	-
85	-	-	-	-	-	-	-	-
83.7	1.1102	0.2626	16.48	15.30	0.1399	0.0001	1.5950	1.7350
83	1.1011	0.2565	16.62	15.49	0.1234	0.0222	1.5712	1.7168
81	1.0752	0.2372	18.46	16.22	0.0707	0.0912	1.4917	1.6536
79	1.0499	0.2188	19.29	16.91	0.0235	0.1565	1.4199	1.5998
77.6	1.0331	0.2095	17.39	17.45	0.0000	0.1950	1.3759	1.5709
77	-	-	-	-	-	-	-	-

The results obtained for $3.e_2.s_1(e_{2i}).c_1$ at various recoveries are summarized in Table 2-13. As the recovery is increased starting from recovery of 77.6%, the oxygen content is high in the feed stream compared to the feed stream. This leads to increased mixing mismatch. In order to reduce losses due to mismatch, more separation must be performed in enriching stage e2, making it increasingly important. The transition between $3.e_1.s_2(e_{1i}).c_1$ and $3.e_2.s_1(e_{2i}).c_1$ appears to be smooth in energy requirement, a phenomenon also observed by Pathare.[17]

When the recovery level is further increased, the recycle stream increases in oxygen concentration. However, for $3.e_2.s_1(e_{2i}).c_1$ this is the permeate stream of stage s1. Being a stripping stage, its feed stream is always lower in oxygen content than the cascade's feed. However at high recovery, the permeate composition of this stage is expected to be higher than the feed in oxygen content. It is obvious then that producing high recoveries would be easier and less energy intensive if producing the recycle stream from an enriching stage rather than a stripping stage. Indeed, at 83.7% nitrogen recovery, configuration $3.e_2.s_1(e_{2i}).c_1$ contains an enriching stage e1 with nearly no area, making stage s1 essentially act as an enriching stage. This is seen because the feed to the stripping stage s1 has nearly the composition of the overall feed. At this point $3.e_2.s_1(e_{2i}).c_1$ is equivalent to the configuration $2.e_2.s_0.c_1$. The ISC configuration $3.e_2.s_1(e_{2i}).c_1$ has a normalized specific energy requirement of 1.1102 at this value of recovery. The classical cascade $2.e_2.s_0.c_1$ with no mixing loss allowed has an identical energy requirement of 1.1102. The classical cascade $2.e_2.s_0.c_1$ with mixing losses allowed has a normalized energy requirement of 1.0716.

This confirms the work of Pathare[17], stating that $3.e_2.s_1(e_{2i}).c_1$ is not useful for achieving arbitrarily high recovery of nitrogen at the targeted purity. Higher recoveries entail a high-oxygen recycle stream, so an additional stripping stage is required. The ISC-type configuration $3.e_3.s_0(e_{2i}).c_1$ fulfils this need.

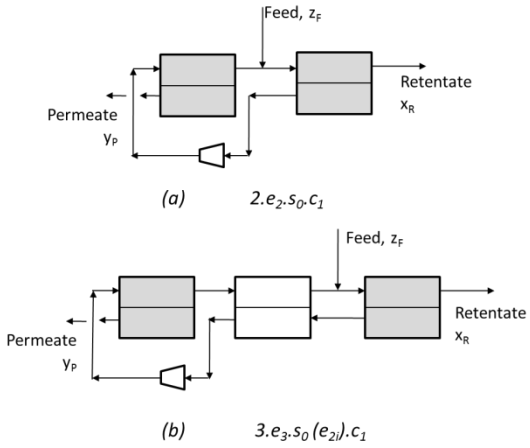

Figure 2-9: Configurations $3.e_3.s_0(e_2i).c_1$ and $2.e_2.s_0.c_1$ [17]

The configuration $3.e_3.s_0(e_{2i}).c_1$ is illustrated in Figure 2-9 alongside the classical configuration $2.e_2.s_0.c_1$ for reference.

Table 2-14: Results for configuration $3.e_3.s_0(e_{2i}).c_1$

$3.e_3.s_0(e_{2i}).c_1$								
Recovery %	Normalized Specific Energy Requirement	Recycle Composition	Pressure ratio stage e2	Pressure ratio stage e1/s1	Norm. Area stage e3	Norm. Area Stage e2	Norm. Area Stage e1	Total Norm. Area
95	1.8072	0.4831	60.17	17.29	0.0531	0.6957	1.4969	2.2457
93	1.5192	0.4077	45.06	16.96	0.0662	0.4523	1.5108	2.0293
91	1.3599	0.3560	36.41	16.65	0.0800	0.2961	1.5250	1.9011
89	1.2582	0.3188	30.73	16.34	0.0946	0.1828	1.5396	1.8171
87	1.1874	0.2908	26.65	16.04	0.1100	0.0945	1.5549	1.7594
85	1.1353	0.2693	23.56	15.74	0.1264	0.0221	1.5706	1.7192
84	1.1076	0.2628	18.97	15.44	0.1362	0.0000	1.5873	1.7235
83.7	1.1076	0.2626	15.13	15.22	0.1426	0.0000	1.5992	1.7418
83	-	-	-	-	-	-	-	-
81	-	-	-	-	-	-	-	-
79	-	-	-	-	-	-	-	-

Table 2-14 summarizes the results for $3.e_3.s_0(e_{2i}).c_1$ at varying recovery. The additional enriching stage e2 yields a recycle stream richer in oxygen than the feed stream. This is advantageous compared to the case of $2.e_2.s_0.c_1$ with no mixing loss allowed, where the feed stage e1 had to produce this high-oxygen stream. Indeed, $3.e_3.s_0(e_{2i}).c_1$ has a lower specific energy requirement than configuration $2.e_2.s_0.c_1$ with no mixing loss allowed for very high values of recovery (for example, a normalized energy requirement at 84% recovery of 1.1076 for $3.e_3.s_0(e_{2i}).c_1$ compared to an energy requirement of 1.1147 for $2.e_2.s_0.c_1$ with no mixing loss). However, as noted by Pathare[17], the contribution of the increasingly higher pressure ratios overpowers the effect of the mixing loss. As a result, the potential saving made by $3.e_3.s_0(e_{2i}).c_1$ over $2.e_2.s_0.c_1$ is fractional at values of recovery below 85%.Moreover, $3.e_3.s_0(e_{2i}).c_1$ allows production of nitrogen at recovery values above 85%, without incurring mixing loss due to recycle streams.

Interestingly, $3.e_3.s_0(e_{2i}).c_1$ has a higher specific energy requirement at all recoveries as compared with configuration $2.e_2.s_0.c_1$ with mixing loss allowed, showing that the savings made by the ISC arrangement of $3.e_3.s_0(e_{2i}).c_1$ are lower than the savings made by $2.e_2.s_0.c_1$ allowing mixing due to recycle streams. This is a counter-intuitive result: By visual examination, it may appear that configuration $2.e_2.s_0.c_1$ is a special case of the configuration $3.e_3.s_0(e_{2i}).c_1$ such that stage e2 performs an insignificant amount of separation. Thus, one may expect that $3.e_3.s_0(e_{2i}).c_1$ would have a specific energy requirement lower or equal to that of $2.e_2.s_0.c_1$, but not worse. However, this is not the case. This is due to the constraint that the retentate stream of stage e2 of configuration $3.e_3.s_0(e_{2i}).c_1$ is such that its composition exactly matches the composition of the feed

stream with which it is mixed. As a result, stage e2 is always constrained to perform appreciable separation. As a result, it is not necessary that configuration $3.e_3.s_0(e_{2i}).c_1$ should have a specific energy requirement lower or equal to that of configuration $2.e_2.s_0.c_1$ with mixing losses allowed.

In order to further investigate this point, calculations were performed with configuration $3.e_3.s_0(e_{2i}).c_1$ such that the retentate stream of stage e2 is allowed to have a different composition than the feed stream with which it is mixed. Such a calculation serves as a cross-check to the above results, as when the constraint on retentate stream of e2 is removed, the specific energy requirement of $3.e_3.s_0(e_{2i}).c_1$ is guaranteed to be lower or equal to that of configuration $2.e_2.s_0.c_1$. Indeed, Table 2-15 shows that, in this case, the solution to configuration $3.e_3.s_0\ (e_2).c_1$ is in-fact exactly equivalent to configuration $2.e_2.s_0.c_1$ with mixing losses allowed. The observation that both the feed and the retentate stream of stage e2 have exactly the same composition further shows that the solution is such that stage e2 is in-effective in performing any separation.

Table 2-15: Reduction of 3.e3.s0(e2i).c1 to 2.e2.s0.c1 with mixing losses allowed

	$2.e_2.s_0.c_1$ (mixing loss allowed)		**$3.e_3.s_0(e_{2i}).c_1$ (mixing loss allowed)**		
Recovery	Power	Retentate comp. e2	Power	Retentate comp. e2	Retentate comp. e3
83.5	1.108	0.209	1.107	0.207	0.207
85	1.130	0.223	1.131	0.223	0.223
87	1.171	0.250	1.171	0.250	0.250
89	1.226	0.283	1.227	0.283	0.283
91	1.308	0.326	1.308	0.326	0.326
93	1.437	0.385	1.438	0.385	0.385
95	1.672	0.468	1.672	0.468	0.468

The required membrane areas of the ISC arrangements examined in this section are generally fairly low. For the cases of cascades $3.e_3.s_0(e_{2i}).c_1$ and $3.e_2.s_1(e_{2i}).c_1$, which have recoveries over 79%, comparing Tables 2-12 and 2-13 with Tables 2-8 through 2-11 shows that a very small improvement in required area occurs across the board. Table 2-11 shows that the same small improvement is made at high recoveries for configuration $3.e_1.s_2(e_{1i}).c_1$. At very low recoveries, this configuration shows significantly smaller areas are required; for example, at 35% recovery it requires a normalized area of 1.8505, compared to 1.9854 for $2.e_1.s_1.c_1$ with mixing losses allowed, or 8.3723 for $2.e_2.s_0.c_1$ with mixing losses allowed. This confirms the finding of Pathare [17]: "Although the intermediate stage cascades use additional stages in comparison with the classical cascades, the membrane areas are not different, they are simply distributed strategically. This shows that the potential savings in specific energy consumption observed for the intermediate cascades do not come at the price of a drastically increased membrane area."

2.4.5 Summary of single-recycle cascade recovery variation study

For a case of nitrogen production from air, a number of single-recycle cascades were compared in terms of their energy requirement at various desired recoveries. The results are consistent with the findings of Pathare[17]:

- A feasible membrane cascade always exists which outperforms the single-stage process design

- No single membrane cascade is always the lowest in energy for all recoveries. Intermediate stages typically give the best results for most recoveries, especially those with a stripping stage.
- At low recovery values, the single-recycle ISC arrangement with one enriching stage is energy-efficient. However, the ISC arrangement still has an upper limit on recovery. At this upper limit, an ISC cascade with two enriching stages has the same capability, and the two-enriching stage cascade can then continue to increase the recovery. This configuration also has an upper limit on recovery. Beyond this value, a smooth transition is possible to a cascade with three enriching stages and zero stripping stages.
- At higher values of recovery, enriching stages were useful in reducing energy requirement. At high recovery, the advantage of the ISC configurations compared to the classical cascade was not as large as at lower recoveries.

.

CHAPTER 3. ENUMERATION OF DISTILLATION CONFIGURATIONS AND SCREENING USING GLOBAL OPTIMIZATION

3.1 Underwood's method for calculating minimum vapor duty of a distillation column

Advanced process simulation is advantageous when finalizing designs of a distillation column or configuration; the ability to examine the stage-by-stage behavior and utilize appropriate thermodynamic data allows the closest approximation of the real operating conditions of the separation scheme to be reached. However, when designing a multicomponent separation the computational effort associated with stage-to-stage calculations becomes massive when considering the hundreds or even thousands of process alternatives that are candidates for the best way to perform a separation. Therefore, before addressing the task of how to screen these numerous candidate configurations, it is first necessary to choose a simple but accurate way to model the separation occurring in each configuration.

Throughout the remainder of this dissertation, the model used for multicomponent distillation is based on the method proposed by Underwood in 1948.[29] For a column performing a single n_c-component split, a total of $2(n_c\text{-}1)$ equations are written to determine the minimum vapor flow while operating with an infinite number of stages and minimum reflux. One set of equations defines n_c-1 Underwood roots $\theta_{s,k}$ for split s as function of the component feed flowrates f, relative volatilities α, and thermal quality q:

$$\sum_{i=1,\ldots,n_c} \frac{\alpha_i f_i}{\alpha_i - \theta_s} = \sum_{i=1,\ldots,n_c} f_i(1-q_s) \tag{3-1}$$

This equation is a polynomial in θ_s which has a total of (n_c – 1) roots. Due to the nature of the polynomial equation, (n_c - 1) of the roots will always lie between two of the feed stream's relative volatilities, as follows for an n-component feed with α_1 being the largest volatility and α_n the smallest:

This equation is a polynomial in θ_s which has a total of (n_c – 1) roots. Due to the nature of the polynomial equation, (n_c - 1) of the roots will always lie between two of the feed stream's relative volatilities, as follows for an n-component feed with α_1 being the largest volatility and α_n the smallest:

$$\alpha_1 \geq \theta_1 \geq \alpha_2 \geq \theta_2 \geq \alpha_3 \geq \theta_3 \geq \alpha_4 \geq (\ldots) \geq \alpha_{n-1} \geq \theta_{n-1} \geq \alpha_n \tag{3-2}$$

Let k be an index that goes from 1 to (n_c - 1). Thus the Underwood feed equation can be solved n_c-1 times to obtain $\theta_{s,k}$. [30]

Once the values of the Underwood roots are calculated, the Underwood distillate equation defines the minimum vapor requirement for the column to achieve a given set of distillate products d.

$$\sum_{i=1,\ldots,n_c} \frac{\alpha_i d_i}{\alpha_i - \theta_{s,k}} \leq V_s^{\min}; \forall k = 1,\ldots,n_c - 1 \tag{3-3}$$

Consider the following example. An equimolar three component mixture *ABC* with a flow of 60 kmol/hr is separated into the streams *A* and *BC* in a sharp split separation, where recovery of *A* in the top product is assumed to be 100% and recovery of B in the bottom product is assumed to be 100%. Let *A* be the most volatile component

and *C* the least, with relative volatilities α_a=10, α_b=4, α_c=1 with respect to C. The feed is vapor (q=0). Equation 3-1 gives the following:

$$\frac{10(20)}{10-\theta_{s,k}}+\frac{4(20)}{4-\theta_{s,k}}=(60)(1-0) \tag{3-4}$$

Solving for $\theta_{s,k}$ gives two solutions: {7.5726, 1.7607}. These satisfy equation 3-2. Using these values with equation 3-3 yields two equations:

$$\frac{10(20)}{10-7.5726}\le V_s^{\min} \tag{3-5}$$

$$\frac{10(20)}{10-1.7607}\le V_s^{\min} \tag{3-6}$$

These combine to show that V_s^{min} is at least 82.4 kmol/hr to perform this sharp split separation at minimum reflux; from this, knowing D = 20 kmol/hr it is clear that the minimum reflux ratio needed is 3.12.

Though in this example the feed compositions were known, it is also possible to use the Underwood equations with unknown variables in the context of a larger problem which includes mass balances and product specifications for multiple distillation columns. When the overall problem is solved, the Underwood equations ensure that sufficient vapor is provided to each column for pure products to be produced; the advantage of using this method is that the separation governing equations fit within the framework of a nonlinear programming (NLP) problem with one set of $2(n_c - 1)$ equations per column feed stream rather than the multitude of (often differential) equations that would be required to obtain the separation performance of every stage in a column by any other method.

The results generated by the Underwood equations rely on several assumptions. First, the feed mixture does not form an azeotrope. Second, relative volatilities can be treated as constant throughout the column rather than being pressure independent. Third, it is assumed that in every column section the amount of molecules which evaporate and condensate in every column section (that is, in every collection of trays with no external streams entering and leaving) is equal; because of this the liquid and vapor flowrates remain constant. This assumption is known as constant molar overflow. It is also assumed that ideal phase behavior is valid and that latent heats of vaporization are constant for all components in the mixture.

3.2 Matrix Method for generating distillation search space

In order to design an energy efficient system for multicomponent distillation, it is vital that a full set of possible process designs be known. Research into finding a way of enumerating distillation process designs has been conducted for over 65 years.[31] Some such research focused only on generating the list of *sharp-split* configurations in which every column had zero overlapping components in the top and bottom product [32]; others included the arrangement with *non-sharp splits,* defined by having at least one component that appears in both the top and bottom product of a column. Two major approaches have been taken in this generation of possibilities; a *superstructure* method such as that favored by Sargent & Gaminibandara (1976) and Agrawal (2003), and *exhaustive combinatorial searching*, as favored by Fidkowski (2006) and Rong et al (2003). [33-36] Each of these options has advantages and disadvantages. The superstructure-based spaces are often comparatively less complete but are compact

spaces (subject to the assumptions made to generate them). Combinatorial searching often leads to more options, but a great number of them are non-useful configurations which utilize as many or more columns than there are components to be separated.

Many arrangements are possible, so first it must be determined what is practical. For example, it is possible for a five-component separations to use only a single distillation column, producing three of its five products as side draw streams. However, the difficulty of reaching high purity in product streams of such a column without prefractionation of this mixture will necessitate a huge number of stages and a prohibitively large reflux ratio. Similarly, it is possible to perform the same five component separation using ten distillation columns; however, with the high capital costs associated with such a scheme, it may also be undesirable.

There are several different classifications of distillation configurations to which a process design can belong:

- Subcolumn configurations – for an n component separation, those separation schemes which include less than (n-1) distillation columns
- Regular-column configurations – for an n component separation, those separation schemes which include exactly (n-1) distillation columns
- Plus-column configurations – for an n component separation, those separation schemes which included more than (n-1) distillation columns
- Sharp split configurations – separation schemes with no component ever contained in both the top and bottom product of any distillation column
- Nonsharp split configurations – separation schemes with at least one component contained in both the top and bottom product of at least one distillation column

- Thermally coupled configurations – separation schemes which have at least one reboiler or condenser replaced by a two-way transfer stream; for a top product thermal coupling, the condenser is replaced by a vapor stream which travels from the column in question (denoted column A) to a different column (denoted column B), plus a liquid stream which travels from column B to column A; for a bottom product thermal coupling the reboiler is replaced by a liquid transfer from column A to column B and a vapor transfer from column B to column A. The net molar transfer from column A to column B through this thermal coupling is always positive

Figure 3-1 and 3-2 demonstrate some three-component examples of each of these configuration classes. It is possible to embody any of the above classes at once, with the following exceptions: only one of sharp or nonsharp split can apply to a configuration; only one of subcolumn, regular-column, or plus-column can apply to a configuration. For example, Figure 3-2c is a thermally coupled, sharp split regular column configuration.

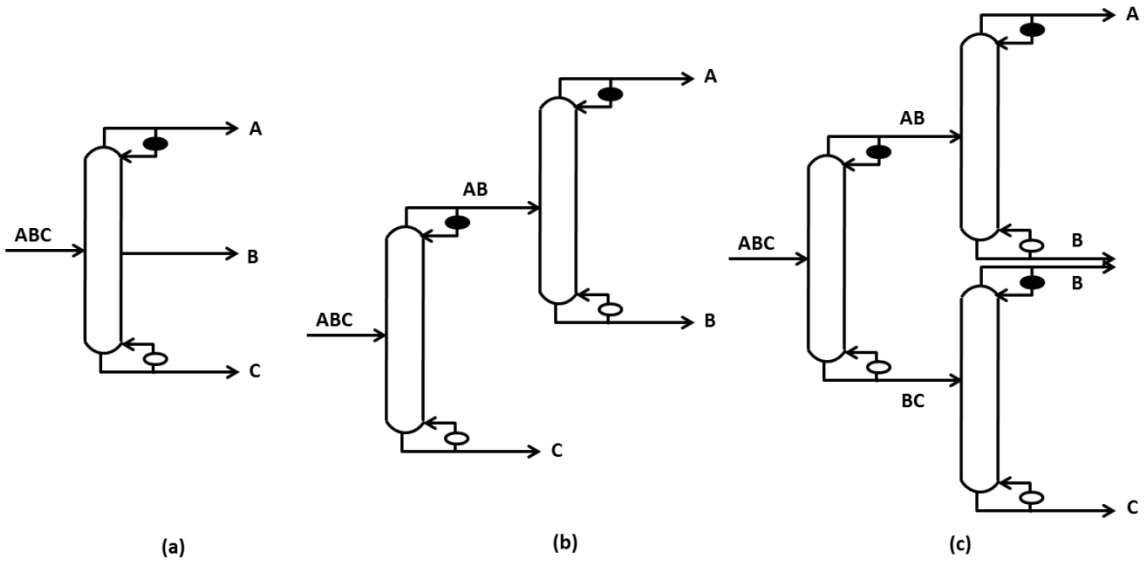

Figure 3-1: (a) subcolumn configuration, (b) regular-column configuration, (c) plus-column configuration

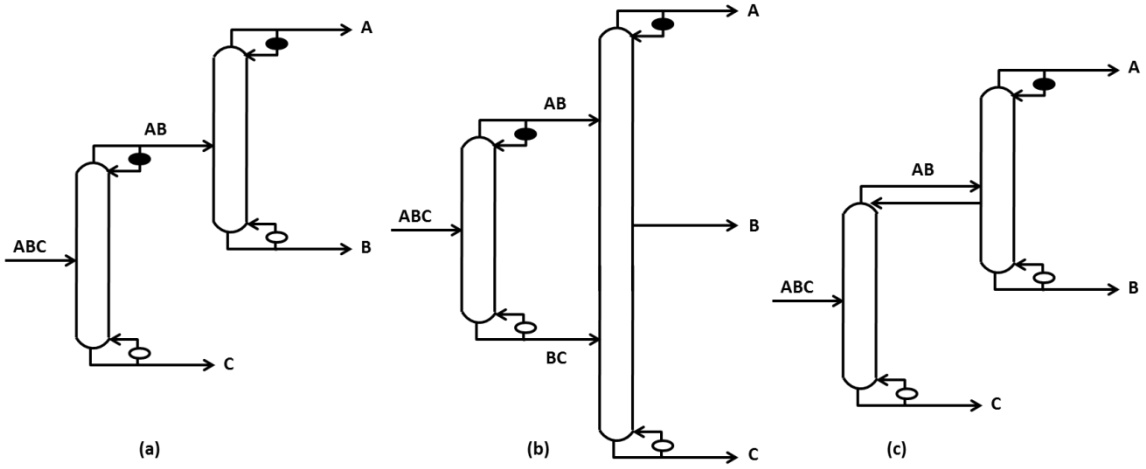

Figure 3-2: (a) sharp split configuration, (b) nonsharp split configuration, (c) thermally coupled configuration

Giridhar & Agrawal [37] introduced a method for determining what constituted a useful search space. Useful was defined as a search space that is as small as possible

while still including the optimal configuration for all feed conditions, and two criteria were considered in introducing it:

- The search space should include all configurations which can potentially be optimal for a given set of feed condition parameters. If a certain combination of feed parameters allows a given configuration to have a better performance measure than all other configurations for the same feed parameters, it must be included in the search space.
- The search space should not include configurations that can be demonstrated to never be useful for all sets of feed parameters, especially when such configurations are present in large numbers.

Giridhar studied a sampling of 120 different feed conditions in order to decide which configurations should be included in a search space. Comparing sharp split configurations to nonsharp split configurations showed that in 119 out of 120 cases, sharp splits were outperformed by nonsharp splits in terms of vapor flow requirement. It is clear that nonsharp splits are required as a part of the search space due to their possibility for low vapor requirement. However, sharp splits are also retained as a part of the search space due to their control simplicity and operability.

Comparing regular-column, subcolumn, and plus-column configurations showed that for all 120 feed conditions, the best regular-column configuration always performed better than the best plus-column configuration in terms of heat duty. As it is likely that plus-column configurations will also always have higher capital and installation costs due to their increased number of columns, this study was ruled to be sufficient to exclude

plus-column configurations from the search space based on the second criteria for a good search space.

Thermally coupled configurations were also chosen for inclusion into the search space after a number of papers on their potential for energy savings; Giridhar determined that for a range of 40 feed conditions that the regular-column fully thermally coupled (Petlyuk[38]) arrangement had on average a lower heat duty than the best sharp split configuration without thermal coupling by 26%, and a lower heat duty than the best nonsharp configuration without thermal coupling by 9%. Thus, thermally coupled configurations should be included in the search space as well. However, since "TC" configurations have a higher degree of operational and control complexity and can also sacrifice thermodynamic efficiency, it is also desirable to retain non-TC configurations in the search space.[39] Configurations that are regular-column and not thermally coupled are hereby referred to as "basic" configurations.

Thus, as a whole, the search space is reduced to including regular-column and subcolumn configurations, with both sharp and nonsharp splits, with and without thermal coupling. The topic of identifying energy-efficient subcolumn configurations using the search space of Giridhar has been examined by Shenvi et al [40]; however, the remainder of this dissertation will focus on identifying energy-efficient configurations in the search space of regular-column configurations.

Using the search space criteria outlined above, an algorithm for mathematically generating a list of feasible regular-column configurations was outlined by Shah & Agrawal. [41-42] This algorithm is known as the matrix method and is driven by the fact that a configuration without thermal coupling can be uniquely described by listing which

of the submixture streams which *could* be produced from an *n*-component feed are actually present.

Figure 3-3 demonstrates this unique description by drawing the three possible basic (non-TC) configurations for *n*=3. All three configurations contain the same feed ***ABC*** (where A is the most volatile and C the least) and same final products. Configuration (a) can be described as the only basic configuration which contains stream ***BC*** and does not contain stream ***AB***. Configuration (b) contains ***AB*** but not ***BC***. Finally, configuration (c) contains both possible submixture streams.

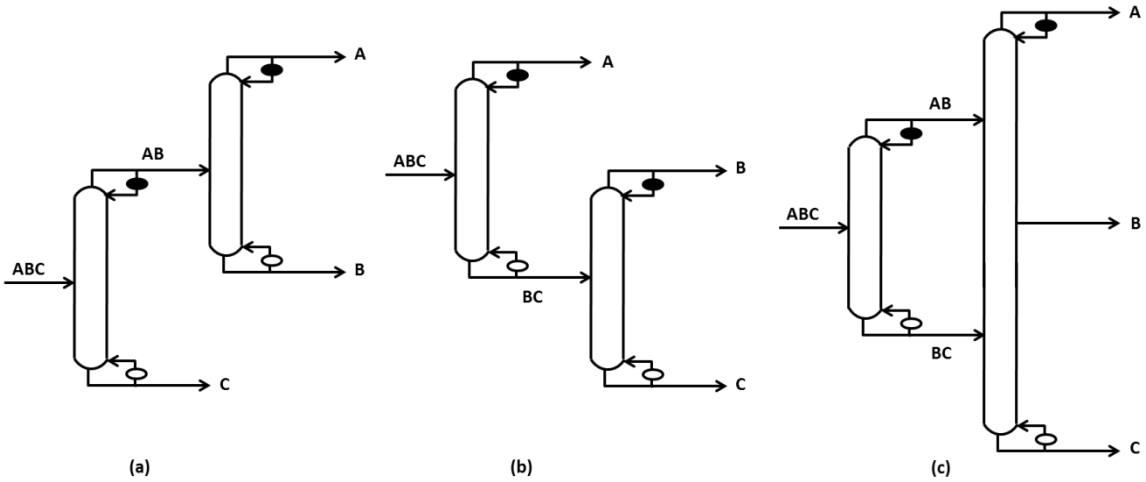

Figure 3-3: Basic configurations for n=3

Shah and Agrawal outlined a six-step procedure to generate all valid regular-column configurations in a search space:

1) Identify *n*, the number of components in the feed to be enriched to final products.

2) Generate an *n* x *n* upper triangular matrix. All elements below the diagonal are assigned a value of zero. All elements in the upper triangular section, including the diagonal, correspond to unique streams that may be present in the configuration. An example is shown for a five-component feed mixture (Figure 3-4) in which A represents the most volatile component and E the least volatile. Five final products, one for each component, comprise the final column. The feed stream is always placed in matrix position $X_{1,1}$. From any spot in the matrix, moving horizontally to the right, all streams encountered are possible top products which can be produced from the starting spot; all streams encountered diagonally to the right are possible bottom products produced from the starting spot. The opposite is also true. From any position, moving horizontally to the left, all nodes encountered represent streams which can yield the starting point as a top product; diagonally to the left are all nodes which can yield the starting point as a bottom product.

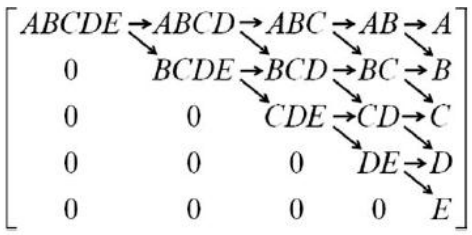

Figure 3-4: Matrix for a five component distillation.

3) Classify elements of the matrix as corresponding to the main feed stream , a submixture stream, or a final product stream. In Figure 3-4, the main feed is

ABCDE, the final product streams are A, B, C, D, and E, and all other streams are submixture streams. For an *n* component matrix the number of possible submixture streams is given by:

$$d = \left[\frac{n(n+1)}{2}\right] - n - 1 \tag{3-7}$$

4) Generate matrices representing all possible combinations of the presence and absence of submixture streams. Each submixture stream spot in the matrix of Figure 3-4 will be replaced by either a 0 (stream is absent) or a 1 (stream is present). The feed and final products will always be present. The presence or absence of a stream refers to its occurrence outside the distillation columns of a configuration. Since there are *d* submixture streams possible, there will be a total of 2^d unique matrices possible. Each of these matrices will correspond to a candidate basic distillation configuration.

5) Eliminate physically infeasible configurations. This is done using three checks. First, every stream that exists in a matrix (except the main feed stream) must have at least one existing stream that can act as its feed. Second, no component can disappear in a split, and a split can have only two products (for example, ABC cannot produce A and C as its products since B disappears; nor can it produce more than two products). Finally, at least n-2 submixture streams out of the total *d* possibilities must exist, to ensure that the configuration is a basic configuration. All three checks are implemented mathematically as described by Shah & Agrawal.[42] The matrices that pass these checks make up the complete search space of basic configurations.

6) From a given feasible matrix derived from step 5, translate the matrix to a drawing of the configuration. Figure 3-5 shows the translation of a five-component feasible matrix to a complete basic configuration utilizing four columns.

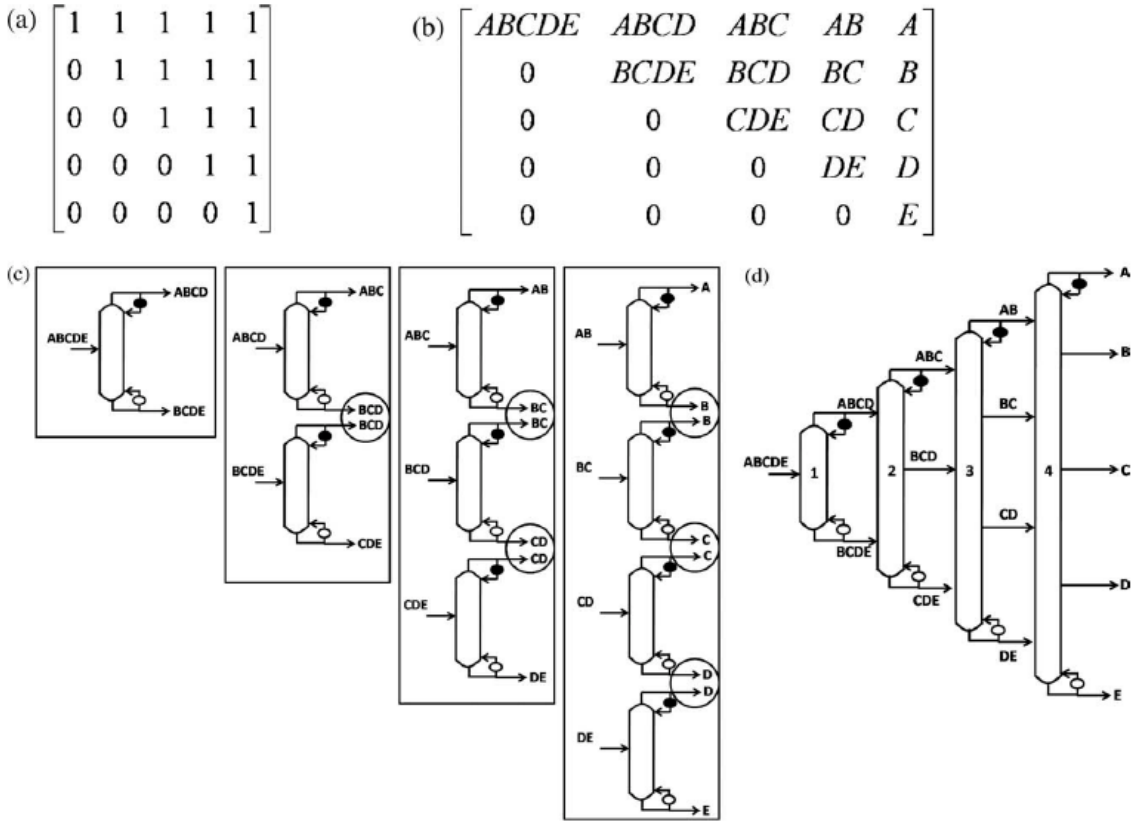

Figure 3-5: (a) A feasible 0-1 matrix; (b) replacing 0-1s by appropriate streams in the matrix; (c) drawing all possible splits and then grouping the splits that can be performed in the same distillation column; (d) assigning distillation column numbers and drawing as a regular-column arrangement [41]

As an optional final step, any configuration with submixture streams produced at the top or bottom of a column can have multiple thermally coupled variants. Figure 3-6

displays one possible thermally coupled variant for a 5 component basic configuration. In this case there are a total of 4 possible sites for thermal coupling in 3-6a; 3-6b is only one of 2^4-1 = 15 additional thermally coupled configurations that can come from the basic configuration in 3-6a.

The combination of basic and thermally coupled configurations is what is termed the complete search space of distillation configurations. As the number of components in the feed increases, the amount of separation alternatives increases rapidly. Shah and Agrawal [42] give the total number of regular-column configurations in the search space for three to eight component separations as ranging between 8 and 30,000,000:

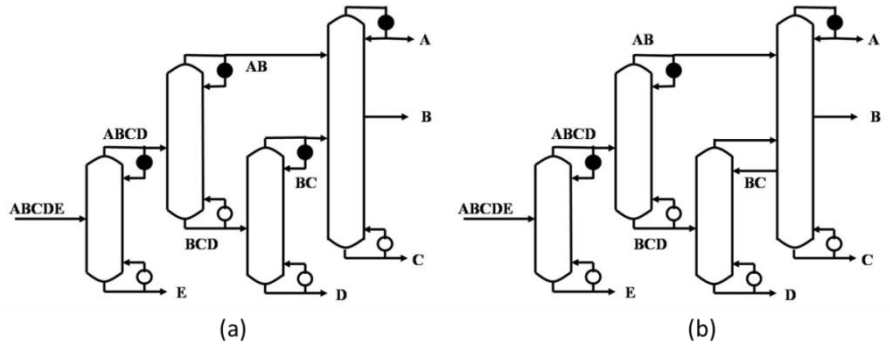

Figure 3-6: Basic and thermally coupled variants derived from a matrix

Table 3-1: The number of distillation configurations grows rapidly as the number of components in the feed increases [41]

Number of Components in the Feed	Number of Basic Configurations	Number of Additional Configurations with Thermal Coupling
3	3	5
4	18	134
5	203	5925
6	4373	502,539
7	185,421	85,030,771
8	15,767,207	29,006,926,681

Using Underwood's equations alongside the matrix method allows a complete and compact set of process alternatives to be evaluated quickly. It is clear that the large number of configurations in the search space makes stage-to-stage calculations impractical for separations of more than three components; however, the Underwood's equations can be solved for thousands of configurations using nonlinear optimization, and the resulting NLP problems can be adapted to learn many things about the search space, including what types of configurations have the lowest vapor requirement, thermodynamic efficiency, and estimated total cost.

3.3 Global optimization techniques for multicomponent distillation

Once a complete search space is available, there are many ways to use it for design of efficient separation processes. For small search spaces, such as the three component search space with 3 basic and 5 thermally coupled regular-column configurations, it is possible to perform complete process simulations of each of the 8 configurations to compare their strengths and weaknesses using real thermodynamic databanks and an equation of state appropriate to the system chemistry. It is possible to use previous knowledge of the problem to simulate only a precise few configurations; it is also common to look for a select few configurations which meet an operability or retrofit requirement.

However, for the greatest impact on energy and cost efficiency of the process design, all alternatives should be considered and a robust optimization problem should be solved to ensure the best possible solution is chosen. Several attempts have been made in the literature to minimize the vapor requirement of a configuration using Underwood's

equations and local optimization tools.[43-48] One method for performing such an optimization is the Sequential Minimization Algorithm (SMA). This method calculates the minimum vapor duty requirement for each individual split using the "transition split" or "preferred separation" for a single column.[49-51] The goal of this method is to find a good solution for the overall process by optimizing each individual column. For many configurations this is a valid method for reaching an optimal solution; for example, it calculates the exact minimum energy requirement for a three-component prefractionator configuration (Figure 1-3c).[52] However, this method disregards the effects that changing one column's operating conditions can have on another column – effects that only grow more prevalent as the number of columns increases.

Nallasivam et al suggested an alternative to the SMA method in which all distillation columns were optimized simultaneously using a global optimization solver. This method is the Global Minimization Algorithm (GMA).[53] GMA has the disadvantage of requiring far more computational time than SMA, but will always provide an equivalent or better solution. Using a set of 120 different saturated liquid feed conditions for a four component separation, the minimum total vapor requirement was calculated using both SMA and GMA methods for the 18 basic configurations identified by Shah & Agrawal. [37,42] It was found that for 10 out of 18 configurations, the SMA method produced solutions that (for all feed conditions) were within 4×10^{-6} percent of the solutions identified by GMA. The 10 configurations for which SMA was a valid global optimization technique were split into two categories: sharp splits configuration, and configurations with a nonsharp split in the first column in which the top and bottom products from the nonsharp split were fed into the same column. All configurations with

subsequent nonsharp splits or with single sharp nonsharp splits feeding two different columns had SMA solutions which were between 6.7% and 28.4% higher than the GMA global solutions for at least one feed condition. Extending this analysis to 5 components confirmed this heuristic for identifying whether SMA would provide a global solution.[53]

Further analysis showed that this heuristic did not apply to thermally coupled variants of a given basic configuration; introduction of thermal coupling ensures that SMA being either valid or invalid for a basic configuration is no guarantee that SMA will be respectively valid or invalid for the thermally coupled configuration.[53] Due to the unpredictability of methods that rely on sequentially calculating the preferred split without considering interactions between columns, it is necessary in many cases to expend the additional computational effort to ensure that the solution obtained for a distillation configuration is truly the best solution which can exist.

A detailed formulation that uses the Underwood's equations to optimize multicomponent distillation is presented in section 3-4.

3.4 Enumeration based Global Minimization Algorithm

When a series of discrete nonlinear equations is used to represent the separation performance of a distillation configuration, there are two ways to attempt finding a globally optimal solution. The first approach is to formulate the problem as a single mixed-integer non-linear programming (MINLP) problem solved by a local optimization solver.[54-55] In this approach the search space of distillation configurations is defined as a mathematical superstructure that contains all possible configurations meeting certain criteria. The MINLP approach attempts to find the globally optimal solution without fully

enumerating all the possible configurations in the search space. As pointed out by Caballero and Grossmann, This approach has three important challenges: 1) in most cases, a feasible solution is not found - singularities arise due to disappearing column sections, 2) Iterations are very time consuming and 3) even if a solution is found, it regularly corresponds to a poor local optimum and a much better solution exists.

To address these issues, Caballero and Grossmann developed a model that represents configurations using superstructures and solves with a logic-based outer approximation algorithm.[56] In this approach the MINLP problem is decomposed into an MILP master problem and an NLP sub-problem, with the master problem formulated by replacing nonlinear equations with their convex outer-approximations. Thus the master problem has less sensitivity to disappearing column sections, and also provides better initial guess values for the NLP sub-problem. The MILP master problem is solved to generate a feasible configuration. The NLP sub-problem is solved to optimize the variants of the feasible configuration generated by the MILP master problem. This process is repeated iteratively until the iteration steps begin to lead to a worsening solution. The best configuration discovered by the time the solution worsens is taken as the optimal solution. This procedure does not guarantee the global optimality of the solution it identifies.

Subsequently, Caballero and Grossmann presented a new iterative procedure to solve an MINLP problem that includes thermally coupled configurations in the search space.[57] In the procedure the integer variables associated with transfer-stream heat exchangers are given values of zero; this means that they are absent during each iteration of the master problem. This approach thus identifies a completely thermally coupled

configuration during each iteration of the master problem. In the sub-problem, the heat exchanger variables can be either zero or one, meaning they can be present or absent; the configuration structure is forced to be that of the solution generated by the master problem. These two steps are iterated until a stopping criterion is met in consecutive iterations. This procedure also does not guarantee a globally optimal solution. The limitation of both these procedures lies in the decomposition of the original problem into sub problems. To guarantee global optimality for an MINLP problem, all candidate solutions should be explored.

The second way to identify an optimal distillation configuration is to synthesize the complete search space and to generate individual nonlinear programming problems for each configuration in the search space; this is known as an enumeration based approach. The challenges of optimization using local solvers or sequential methods were noted in section 3.3. Some would recommend using multiple randomly generated initial guesses to achieve better local solutions, but this adjustment significantly increases computational burden without guaranteeing that it will achieve its desired results of global optimality. Furthermore, in a few cases, this solution methodology leads to a lack of feasible solutions.

For these reasons and those described by Nallasivam et al [53], it is necessary to have a general NLP-based formulation that can describe all basic and thermally coupled configurations, and can be solved to guaranteed global optimality. This algorithm is the fully-realized version of the Global Minimization Algorithm (GMA) introduced by Nallasivam et al [53]. The first part of the algorithm is using the matrix method to generate all possible regular-column configurations; in the second step an optimization is

performed for each basic and thermally coupled distillation configuration to calculate its corresponding globally minimum vapor duty requirement. This algorithm uses a bilinear reformulation of the Underwood equations. Optimization of each configuration provides a rank-list of distillation configurations in terms of their energy requirement. GMA is the first algorithm in literature to guarantee that all globally optimal distillation configurations for any ideal or near-ideal multicomponent separation process design will be identified. This approach does involve the increased computational effort of evaluating each individual configuration in the search space (compared to the MINLP approach), but is currently the only approach that is able to solve this problem to guaranteed global optimality. Details about the GMA formulation will be described in the following sections. Strategies for decreasing the computational time compared to the original GMA [53] will also be discussed.

3.4.1 GMA nonlinear programming formulation

Any optimization problem is described by: (i) the decision variables, (ii) the objective function, and (iii) the constraints. In the following sections, equations are presented for the objective function and the constraints to minimize the vapor duty of a distillation configuration. In all these equations, the components are numbered as 1, 2, …, *n* in the decreasing order of their volatilities. It is anticipated that in every distillation column the top products will be richer in the components with a lower index (1,2…) and the bottom products richer in the components with a higher index (..n-1, n). These equations can be automatically derived using the connectivity matrix.

The formulation in this section will be a formulation for minimizing total vapor duty of an *n*-component separation. Chapters later in this dissertation address the issue of using alternative measures of what constitutes a desirable distillation configuration.

Objective Function

The objective function is a mathematical expression describing the optimization goal. Since only basic and thermally coupled distillation configurations are part of the search space (meaning that all configurations have the same number of column shells and approximately the same amount of controls and piping), the capital costs of these configurations are not expected to be drastically different from one another. In general, the operating costs of these configurations can be significantly different. It is reasonable to assume that the operating cost of a configuration is proportional to the sum of the vapor flows generated at each reboiler of the configuration.[58] Furthermore, the diameter of a distillation column is proportional to the vapor mass flow rate through the column. Therefore, vapor duty may also be regarded as partially representative of the capital cost of a configuration. Further discussion of the role of capital cost in designing configurations will be examined in Chapter 4.

The sum of the vapor flows generated at each column steam reboiler in a configuration is referred to as the total vapor duty requirement of the configuration. When optimizing the equations for minimum reflux distillation, a *minimum* total vapor duty will be discovered. Using minimum reflux equations like Underwood's equations assumes infinite stages. While this is a theoretical simplification, it leads to a reasonable benchmark that is scalable with both capital and operating costs. More importantly, this

simplification makes the computation more tractable. A general representation for the objective function is

$$\sum_{s \in COLR} V_s^{bott}$$

where COLR lists all splits that have a reboiler. This function is minimized by the solver. Since the number of feasible configurations in the search space is very large for $n > 4$, the minimum reflux assumption is important since it avoids tray-by-tray computations; however solving this problem can still be thought of as similar to solving a tray-by-tray simulation. After identifying attractive configurations using the GMA, detailed process simulation can be performed on several of the most attractive.

Decision variables:

The formulation chosen includes a number of decision variables defined in a general manner, ensuring that they are capable of describing each feasible distillation configuration in the search space. On the other hand, the constraints, the objective function and variable sets are uniquely tailored to each distillation configuration based on the corresponding connectivity matrix.

(i) Stream flow rates (X_m): There are $n \times (n+1)/2$ upper triangular elements in an n x n matrix corresponding to an n-component separation. Each element in the matrix represents a potential stream in the configuration. Thus, $n \times (n+1)/2$ optimization variables for the total molar flows of these streams are declared. The subscript on each variable gives the stream number it is associated with. For a five component

separation, 15 X_m variables will be created since there are (5)(6)/2=15 streams possible.

(ii) Component flow rates ($X_{m,k}$): The molar flow rate of each component in each stream is declared as a decision variable. $n \times (n+1)/2 \times n$ optimization variables for the molar flow of each component in each stream are declared. These variables describe the flow of component *k* in each stream *m*. For a five component separation, 75 $X_{m,k}$ variables will be created since there are 5(15) individual component flows for the fifteen streams.

(iii) Liquid and vapor flow rates (L_m and V_m): These variables aid in determining the thermal quality of each stream. For each stream *m* a liquid (L_m) and vapor (V_m) flow are declared. For a five component separation, 15 of each variable will be created.

(iv) Minimum vapor duty requirements for splits ($V_s^{\min}$) and Underwood roots ($\theta_{s,r}$): The $X_{m,k}$, L_m and V_m variables can be used to formulate Underwood's equations. These equations relate the minimum vapor duty requirement, $V_s^{\min}$ to variables $X_{m,k}$ and $\theta_{s,r}$. The $\theta_{s,r}$ variables are the Underwood roots described in section 3.1. If the feed stream to a split *s* has *p* components, the corresponding Underwood's equation has *p*-1 Underwood roots.

(v) Actual split vapor flow at top (V_s^{top}) and bottom (V_s^{bot})**:** The minimum vapor required to perform a given split is $V_s^{\min}$. However, the actual minimum vapor flow at any point in a column also depends on the vapor flow at other points in the column. The actual minimum vapor flow in the column must at every point meet or exceed the minimum vapor flow requirement calculated by Underwood's equation. It is required only that V_s^{top} be greater than or equal to V_s^{min}, and that V_s^{top} is tied to V_s^{bot} through a molar balance on vapor in the column. When multiple splits exist in the same column, V_s^{top} of a lower section is linked with V_s^{bot} of the section immediately above it through another balance.

(vi) Split-specific distillate component flow rates **(** $\bar{X}_{s,k}$ **):** When a stream is produced by two splits (such as stream B in Figure 3-3c), it acts as the bottom product for one split and the top product for the other split; such a stream is always produced as a side draw. In this case, the feed streams of both splits can contribute to the composition of side draw stream. The flow contribution from the upper section cannot be used in the Underwood's distillate equation for the lower section. For this reason, the portion of the distillate component flows that are contributed only by the lower split is calculated and termed $\bar{X}_{s,k}$. If there are n_s splits in a configuration separating an n component mixture, $n_s \times n$ optimization variables are declared for the split-specific distillate component flow rates.

For a five component separation with the minimum four splits, the number of local distillate component flow rate variables will be 20; with the maximum ten splits there will be 50 variables for these flow rates.

Constraints

A distillation configuration has to be governed by both phase equilibrium and mass balances. In order to capture the effects of these governing equations in an optimization, a number of nonlinear and linear constraints are defined. The following sign convention is used for writing these constraints.

- For any $(i,j) < n$ the stream number of the stream which occupies spot (*i,j*) in the matrix method is given by $m_s = \binom{j}{2} + i = \frac{j(j-1)}{2} + i$. For the remainder of this chapter m_s is given by the above equation whenever *i* and *j* are defined; when *i* and *j* are not defined the stream number will be referred to by the more general *m* and defined specifically in the equation.
- For all splits in a configuration, the order of the splits is determined by the value of m_s. A split fed by a stream with $m_s = 10$ will have a higher split number than a split fed by a stream with $m_s = 4$.
- Every flow leaving a lower-numbered split as a product is either a pure final product or a feed to a higher-numbered split. A flow is considered positive when leaving the column containing the lower-numbered split that produces it. Such streams will always have a positive net flow. Liquid (or vapor) flow variables can be negative; that is, they can enter the column in a stream that has a net flow

leaving the column, but only if a larger opposing flow of vapor (or liquid) respectively exists so that the net flow is positive.

- In any molar balance around a particular envelope, terms associated with any stream whose net flow is entering the envelope are added to the left hand side of the molar balance; terms associated with any stream whose net flow is leaving the envelope are subtracted from the left hand side of the molar balance. The right hand side of the balance contains only accumulation terms and is always zero.

With this convention, a list of constraints is described below. The constraints are different for each configuration since each configuration has a unique set of streams and splits but the constraints always follow the format described.

(i) Material balance: The total molar flow entering a distillation column must equal that leaving the column; the accumulation term is zero. In the same way the flow of any component entering the column must equal the flow of that component leaving the column. These rules give rise to the following two types of linear equality constraints.

$$\sum_{m \in FEEDC_c} X_m = \sum_{m \in PRODC_c} X_m \quad \forall c = 1,...,n-1 \tag{3-8}$$

$$\sum_{m \in FEEDC_c} X_{m,k} = \sum_{m \in PRODC_c} X_{m,k} \quad \forall c = 1,...,n-1; \;\; \forall k = 1,...,n \tag{3-9}$$

$FEEDC_c$ is the set of all feed streams entering the distillation column *c;* $PRODC_c$ is the set of all product streams leaving distillation column *c*.

(ii) Total Stream flow constraints: Any stream has a net flow equal to the sum of its component flows.

$$X_m = \sum_{k=1}^{n} X_{m,k} \qquad \forall m = 1,...,n \times (n+1)/2 \tag{3-10}$$

(iii) Feed definition: The feed stream is always stream 1. The component flows in stream one are given by the parameter F_k, which is defined at the outset of the problem. q_f is the parameter for feed quality, which is used to define V_1.

$$X_{1,k} = F_k \qquad \forall k = 1,...,n \tag{3-11}$$

$$V_1 = \sum_{k=1}^{n} F_k(1-q_f); L_1 = \sum_{k=1}^{n} F_k(q_f) \tag{3-12}$$

(iv) Nonexistent streams have flows of zero: In a given configuration some streams may be absent. For such streams, the total stream and component flows must be set to zero.

$$X_m = 0 \qquad \forall m \in ABSENTS \tag{3-13}$$

$$X_{m,k} = 0 \qquad \forall m \in ABSENTS; \quad \forall k = 1,...,n \tag{3-14}$$

ABSENTS is the set of all feed streams that are absent in a given distillation configuration.

(v) Absence of components in streams: All the streams except the main feed stream have some components absent. For a four component separation, the main feed stream ABCD has some flow of each of the four components. Any other stream such as BC has some components absent (in this case A and D). In an actual

distillation, all components will be present in all streams, in at least trace amounts. However, because of assumption of infinite stages associated with minimum reflux operation, streams with trace amounts of components may be considered to be completely devoid of these components. The variables associated with the corresponding component flow rates are set to zero:

$$X_{m,k} = 0 \quad \forall j = 1,...,n; \;\; \forall i = 1,...,j; \;\; m = Z_{mat}(i,j); \;\; \forall k = 1,...,i-1 \tag{3-15}$$

$$X_{m,k} = 0 \quad \forall j = 1,...,n; \;\; \forall i = 1,...,j; \;\; m = Z_{mat}(i,j); \;\; \forall k = n+i-j+1,...,n \tag{3-16}$$

(vi) Net stream flow constraints: The sum of liquid and vapor flows in a stream must equal its net flow. In this model, it is assumed initially that all products are liquid, all intermediate streams associated with a condenser are vapor, and all intermediate streams associated with a reboiler are liquid. At later points in the dissertation it will be noted when this assumption is relaxed.

$$X_m = L_m + V_m \quad \forall m = 1,..., \frac{n(n-1)}{2} \tag{3-17}$$

$$\left.\begin{array}{r} X_m = L_m \\ V_m = 0 \end{array}\right\} \;\; \forall m = \frac{n(n-1)}{2} + 1,..., \frac{n(n+1)}{2} \tag{3-18}$$

$$\left.\begin{array}{r} X_m = L_m \\ V_m = 0 \end{array}\right\} \;\; \forall m \in REBOILERS \tag{3-19}$$

$$\left.\begin{array}{r} X_m = V_m \\ L_m = 0 \end{array}\right\} \;\; \forall m \in CONDENSERS \tag{3-20}$$

CONDENSERS and REBOILERS are the set of stream numbers of intermediate streams originating from exchangers.

(vii) Enrichment constraints: To ensure the final products produced are pure, the top product of a split must contain an increased amount at least one of the light components and the bottom product of a split must contain an increased amount in at least one of the heavy components, relative to the split's feed stream.

Each side of the constraint to ensure this involves a ratio of component mole fractions belonging to the same stream. Therefore, these mole fraction terms can be replaced by the corresponding component flow rate terms.

$$X_{m,k-1} \times X_{m_x,k} \le X_{m,k} \times X_{m_s,k-1} \quad \begin{array}{r} \forall s \in DISTC \\ i = ROW(DISTS_s) \\ j = COL(DISTS_s) \\ m \in FEEDS_s \\ \forall k = 3,\ldots,n-j+i \end{array} \tag{3-21}$$

These distillation constraints are applicable only when the product streams of a split have at least two overlapping components. FEEDS is the feed stream number for split *s*. DISTS is the distillate stream number for split *s*. DISTC is the set of splits which meet this criterion. ROW and COL give the i and j location of a stream number in the Z_{mat} matrix. *i* and *j* represent the row and column number corresponding to the distillate stream *m* under consideration in the *n* x *n* matrix. *n-j+i* corresponds to the last component in a stream at the location (*i*, *j*) in the matrix. When coupled with the previously described molar balance, this ensures that the bottom stream of a split is also enriched in at least one heavy component.

(viii) Thermal coupling definitions: There is no heat exchanger at locations where thermal coupling is introduced; therefore there can be no phase change. For a thermal coupling link at the top of a distillation column, the vapor portion of the

flow of the stream must be identical to the actual vapor flow at the top of the distillation column. For a thermal coupling link at the bottom of a distillation column, the vapor portion of the flow must be set equal to the actual vapor flow below the feed of the bottom split of the distillation column. These result in two types of linear equality constraints.

$$V_s^{bot} = -V_m \quad \forall m \in TCBOTT;\ \ c = CVECT(m);\ \ s = SBOT_c \tag{3-22}$$

$$V_s^{top} = V_m \quad \forall m \in TCTOP;\ \ c = CVECT(m);\ \ s = STOP_c \tag{3-23}$$

TCBOTT is the set of stream numbers associated with thermally coupled links at the bottom of a distillation column. TCTOP is the set of stream numbers associated with thermally coupled links at the top of a distillation column. CVECT is the number of the distillation column that produces stream *m*. SBOT and STOP give the split that produces (respectively) the bottom and top product *m*.

(ix) Underwood's equations: For the feed stream with *p* components, Underwood showed that *p*-1 Underwood roots are found between consecutive volatilities of the *p* components. The feed equation is written for each of these *p* components. After the feed equation is used to find θ, the distillate equation is written as described in section 3.1.

$$\sum_{k=i}^{n-j+i} \frac{\alpha_k X_{m,k}}{\alpha_k - \theta_{s,r}} = V_m \qquad \begin{array}{c} \forall s = 1,...,ns \\ m = FEEDS_s \\ i = ROW(m);\ j = COL(m) \\ r = 1,...,n-j \end{array} \tag{3-24}$$

$$\sum_{k=i}^{n-j+i} \frac{\alpha_k \bar{X}_{s,k}}{\alpha_k - \theta_{s,r}} \le V_s^{\min} \qquad \begin{array}{c} \forall s = 1,...,ns \\ m = DISTS_s \\ i = ROW(m); j = COL(m) \\ j_F = JVECT(FEEDS_s) \\ \forall r = 1,...,n - j_F \end{array} \tag{3-25}$$

In these equations i is to the first component of the stream under consideration and the term "n-j+i" is to the last component of the stream under consideration.

In cases where more than one component (i_1,..,i_2) appears in both the top and bottom products of a split, it has been shown[43] that the inequality constraint in the distillate equation is replaced by an equality constraint with the same terms for the left hand side and right hand side for all r from (i_1-i) to (i_2-i).

(x) Definition of distillate component flow: The definition of the term $\bar{X}_{s,k}$ is found using a vapor balance on all flows above the split in question.

$$\bar{X}_{s,k} = \sum_{m \in LPRODA_s} X_{m,k} - \sum_{m \in FEEDA_s} X_{m,k} \qquad \begin{array}{c} \forall s = 1,...,ns \\ m \in DISTS_s \\ i \in ROW(m) \\ j \in COL(m) \\ k = i,...,n - j + i \end{array} \tag{3-26}$$

$DISTS_s$ is the distillate product stream of split s. $LPRODA_s$ is the stream numbers that are above the split s within the same distillation column, plus the distillate product stream number of the split s. $FEEDA_s$ is the set of feed streams above the split s within the same distillation column. i is the first component in the distillate product stream under consideration and the term "n-j+i" is the last component in this product stream.

$$\bar{X}_{s,k} \le X_{m,k} \qquad \begin{array}{c} \forall s = 1,...,ns \\ m = DISTS_s \\ i \in ROW(DISTS_s) \\ j \in COL(DISTS_s) \\ k = i,...,n-j+i \end{array} \tag{3-27}$$

The distillate component flow of a split can be at most the component flow of the stream produced as a distillate of the split.

(xi) Vapor balance equations: Vapor balances are used to determine how much vapor is needed at each column's reboiler or thermal coupling. Vapor can be provided through feed streams, side draws or from the bottom of a column.

$$V_s^{top} \ge V_s^{\min} \qquad \forall s = 1,...,ns; \tag{3-28}$$

$$V_s^{top} = V_s^{bot} + V_m \qquad \forall s = 1,...,ns; \quad \forall m \in FEED_s; \tag{3-29}$$

$$V_i^{top} = V_j^{bot} + V_m \qquad \forall i \in TOP_c; j \in BOT_i; m \in SD_{i,j} \tag{3-30}$$

TOP is the list of all splits in column *c* besides the bottom split; BOT is the split immediately below split *i*.

The objective function of the set of constraints given here is a linear function; all constraints are linear save the enrichment constraints and Underwood's equations. The form of this problem is thus a nonlinear programming problem.

A number of additional techniques are used to improve the convergence speed and stability of the algorithm. These methods are expanded upon in the submitted work by Nallasivam et al[59], which also includes an example of the equations that would be

written for a given configuration. In short, the optimization is improved with the following techniques:

- It is known that the highest vapor duty in the search space is given by a sharp split with no thermal coupling.[37] The vapor duty of all sharp splits can be quickly calculated using the SMA method. The maximum of these serves as an upper bound on the objective function; it also serves as an upper bound on any given vapor flow in the configuration
- The fully thermally coupled is known to have the lowest vapor duty in the search space.[35,44,48] Since for the FTC configuration, the SMA method gives either the global optimum or a slightly higher local optimum, the SMA solution to the FTC configuration can be used as an upper bound on the objective function.
- Given a set of bounds on the component flows and vapor flows (which can be obtained from the feed specifications and SMA method), the Underwood roots can be bounded by inserting the already known variable bounds for component flows and vapor flows into the Underwood feed equation.
- In some cases, this improved bound of θ allows an improved bound on V_s^{min} through the Underwood distillate equation by a similar method.

3.4.2 Results of GMA – solver performance for a crude oil separation

Recall that there are 6,128 configurations which can separate a 5-component mixture using 4 columns. Heavy crude oil will be used as an example of a 5-component

separation. Though crude oil has a number of complex hydrocarbon compounds, it can be simplified into a 5 component mixture while still remaining fairly representative of the way it is processed in practice. The five fractions are naphtha (A), kerosene (B), diesel oil (C), fuel oil (D), and heavy ends (E). These can be represented as having the following constant relative volatilities and compositions, reported in Table 3-2. Let the feed flowrate be 100 kmol/hr.

Table 3-2: Feed specifications of a heavy crude with $q_F = 0.5607$

Component	**Symbol**	**Feed composition**	**Relative volatility**
Naphtha	A	14.4%	45.3
Kerosene	B	9.3%	14.4
Diesel Oil	C	10.1%	4.7
Gas Oil	D	3.9%	2.0
Residue	E	62.3%	1.0

In order to demonstrate the need for a global optimization algorithm, the results of ranklisting the search space will be compared for three different cases. The first case uses the solver GAMS/MINOS with general bounds and initial guesses set by estimation. The second case uses the solver GAMS/MINOS with bounds and initial guesses set using the SMA method, preferred split calculations, and the tighter bounds obtained by inserting known bounds into the Underwood's equation. The final case uses the solver GAMS/BARON with all of the improvements used in the second case. All three cases utilize the GAMS/MATLAB interface of Ferris et al.[60] In the interest of providing a quick screening tool, all three cases were allowed only 100 seconds of computational time on a Dell Precision T5500 with 2GHz Intel processor.

Table 3-3 demonstrates how the choice of algorithm leads to different results in generating a complete ranklist of the distillation search space.

Table 3-3: Optimization performance of GAMS/MINOS and GAMS/BARON

	Globally Optimal Solutions	Locally Optimal Solutions	No Solution Returned
Case 1	2,378	2,125	1,625
Case 2	4,447	1,336	345
Case 3	5,640	488	0

Implementing the improvements described in the latter part of section 3.4.1 allowed the local optimization solver MINOS to converge nearly twice as many solutions to the true global optimum in just 100 seconds. The nonconvexity of the problem still meant that hundreds of configurations could not be solved by MINOS, however, and thousands of process designs were only locally optimal in the solutions they proposed. Using GAMS/BARON as the primary solver for the search space allowed every configuration to be solved to a feasible solution; 5,640 of the configurations were certified to have an optimality gap of less than 2% and the remainder still had local solutions at least as good as those proposed by MINOS.

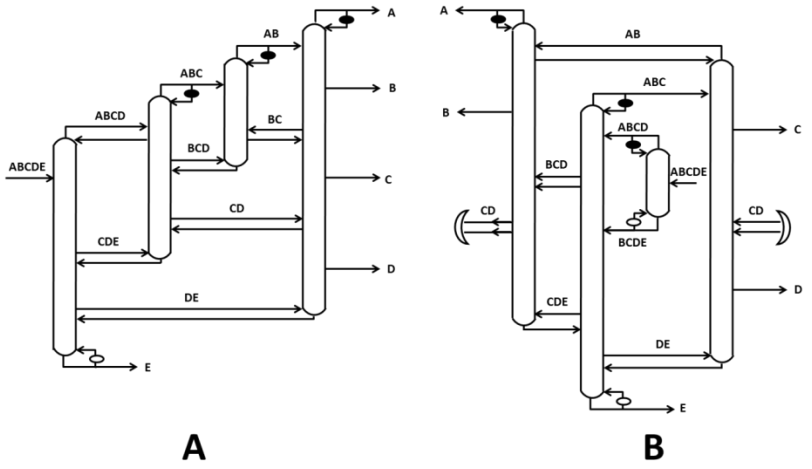

Figure 3-7: Two fully operable distillation columns for which GAMS/MINOS gets a locally optimal solution

Figure 3-7 shows an example of two configurations for which MINOS provides a solution much less efficient than that provided by BARON. The arrangement shown in Figure 3-7a has a certified minimum vapor duty of 0.6996 moles of vapor per mole of feed flow (hereby called a "normalized vapor duty" of 0.6996) according to GAMS/BARON. However, in the allotted computational time GAMS/MINOS from case 1 can only discover a local solution with normalized vapor duty of 1.3678, which is higher than the global optimum by 95.5%. When given the updated bounds in case 2, GAMS/MINOS can reach the global optimum.

Figure 3-7b likewise has a GMA solution with normalized vapor duty of 0.7352, which is reached in case 3. The first case can find only a normalized vapor duty of 1.4715, a 100.1% increase in vapor duty. In case 2, the use of better bounds and SMA guesses still only allows a solution of 1.2224 to be reached – a 64.3% increase beyond the solution from GAMS/BARON. Figure 3-7b is a satellite configuration, so the sequential

techniques used to generate good guesses are insufficient to fully bound the variables and will not give a good starting point for the solver. Many similar configurations suffer this problem even when using the improved bounds; this shows the importance of using a solver with range reduction and convex underestimation techniques even when good initial guess data is available. For this reason, the GMA and all modifications of it discusses subsequently always use the solver software GAMS/BARON.

3.4.3 Design uses of the enumeration strategy with GMA

For the heavy crude oil feed discussed in the previous section, the configuration in the search space with the lowest vapor duty is the fully thermally coupled arrangement (Figure 3-8), which has a normalized vapor requirement of 0.6996. Since the complete ranklist is available from case 3, it can be observed that a total of 175 configurations have a vapor duty within 0.0001 of the FTC configuration. Any of these configurations can be considered globally optimal for this separation.

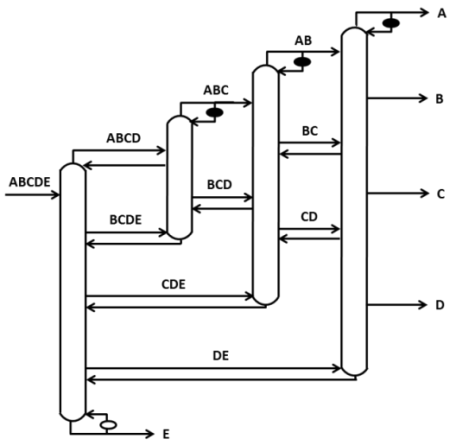

Figure 3-8: Fully operable arrangement of FTC configuration

It is possible that a practitioner would not want to build the FTC configuration because it has only one exchanger the vapor flow can be controlled from; adding additional exchangers can make the configuration simpler to control. A useful question to answer, then, is how many thermal coupling links can be removed from the column without sacrificing its low vapor flow requirement.

Consider a fresh example of an liquid equimolar mixture with relative volatilities of A,B,C, and D with respect to E being 39.0625, 15.625, 6.25, and 2.5 respectively. Again, the FTC arrangement turns out to be the global optimum, with a normalized vapor flow requirement of 1.0512. The six thermal coupling links in this configuration could make it undesirable to construct and operate. To solve this problem, the GMA can be applied to this feed.

In order to seek configurations falling within 5% of the global optimum, the upper bound on the objective function is set at 1.1041. GAMS/BARON will not fully solve a configuration if it can be proven that no solution better than 1.1041 exists; this saves much computational time compared to attempting to verify global optimality within 2% for all configurations.

If only the completely thermally coupled arrangements in the search space are solved, there are 26 such configurations (out of a possible 203) which have a vapor duty less than 1.1041. Addition of extra exchangers to a completely thermally coupled configuration is known never to decrease the vapor duty requirement.[35,44,48] Therefore it is clear that no derivative of the remaining 177 configurations will come within 5% of the FTC configuration's vapor duty. All variants of the 26 configurations with the same connectivity matrix are evaluated using the GMA and the same global

lower and upper bounds on the objective function. This yields a total of 340 configurations which come within 5% of the vapor duty of the FTC configuration. Solving only 340 configurations in the search space amounts to a massive decrease in computational complexity.

Of the 340 configurations, 338 are verified to be within 2% of global optimality; the remaining two configurations converged to within 4.6% of global optimality within 100 seconds. Of these 338 configurations, 82 have the same vapor requirement as the FTC (1.0516) while using less thermal couplings. Of these configurations, 10 use only three thermally coupled links (plus one side draw intermediate stream), compared to the six TC links (plus three side draw intermediate streams) used by the FTC configuration. One of these configurations is pictured in its most operable arrangement in Figure 3-9. Meanwhile, Figure 3-10 shows a configuration which requires only two thermally coupled links (plus one side draw intermediate stream) and comes within 2.7% of the optimal FTC solution. It will be shown in Chapter 5 that Figures 3-9 and 3-10 are not only easier to operate than the FTC solution, they also have an advantage in thermodynamic efficiency due to their structural properties.

This example illustrates how the use of a ranklist with the GMA method and GAMS/BARON solver can allow discovery of a suitably efficient column that still considers operability. Chapter 6 will discuss the use of graphical tools to further this selection process by allowing adaptive screening based on structural criteria.

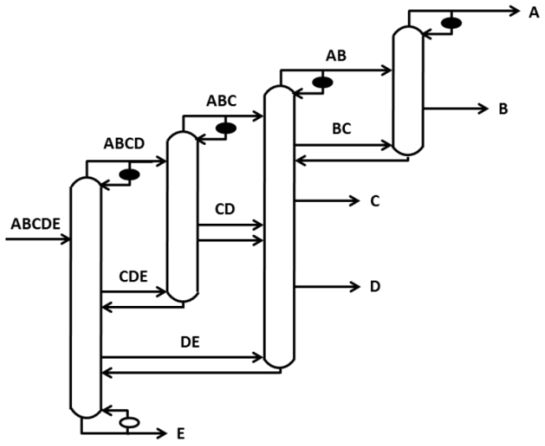

Figure 3-9: Fully operable arrangement of a configuration with only three TC links that reaches global minimum vapor duty

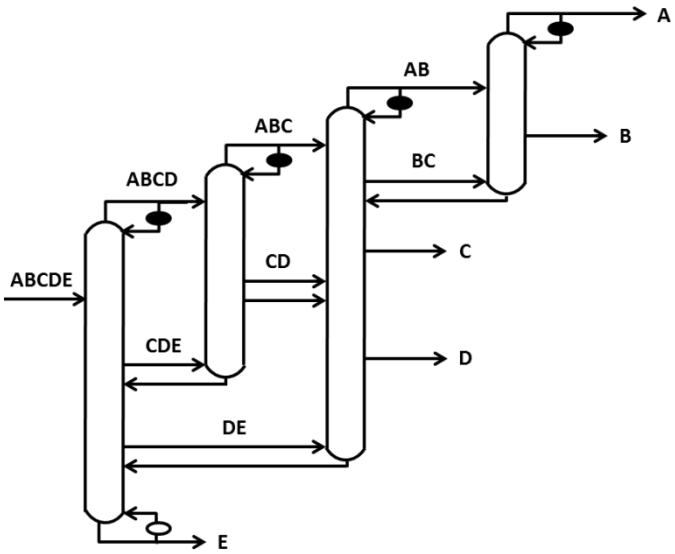

Figure 3-10: Fully operable arrangement of a configuration with only two TC links which reaches within 2.7% of global minimum vapor duty

In many situations, a column is required to be energy efficient not just for separation of a single feed, but for use with different feeds at different times. In such a situation, the global optimization-based rank list can be generated for a number of

representative feeds, and a configuration can be designed which is efficient and operable for all of the different feed conditions.

3.5 Assumption regarding multiple splits in a column

In order for the vapor balances and flow calculations in the GMA formulation to work, the following assumption must be satisfied.[59]

"When multiple splits share a column, the minimum vapor flow for each split can be found by solving the Underwood feed and distillate equations corresponding to each split, and then assuming a "mixing section" connecting the two splits; out of this mixing section a single stream is drawn with a composition calculated by completely mixing the products calculated individually for each split. The total vapor flow required by the column is equal to the greater of the two individual vapor flow requirements. This arrangement is assumed to be identical to a system that uses heat integration to arrive at the same total vapor requirement for performing two separate splits, followed by mixing."

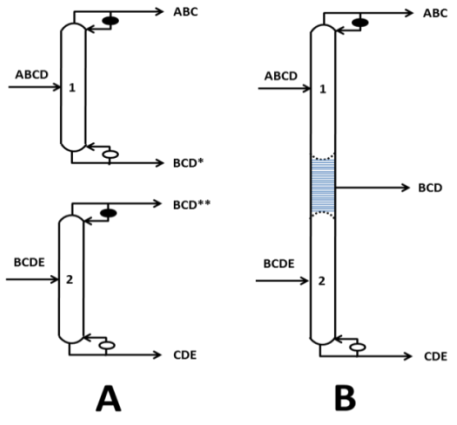

Figure 3-11: Process for calculating the mixed composition of a stream produced from two adjoining splits

A sample column arrangement is shown in Figure 3-11a.[59] The configuration contains two quaternary splits, S1 and S2; five components are present in the system. Each split produces a product BCD. However, when allowed to assume minimum vapor flows, the compositions of the two product streams may differ. They will be denoted BCD* and BCD**. In Figure 3-11b, the two splits are combined in one column. Rather than withdraw two product streams with different compositions, a single stream is withdrawn from the middle of the added section. It is assumed that its composition can be obtained by simply mixing the compositions of stream BCD* with those of BCD** to form product composition BCD. For the purpose of modeling, this takes place in the shaded mixing section with sufficient stages that the separation properties (such as minimum vapor requirement) of one split are unaffected by the presence of an adjoining split. While traveling up this mixing section from the bottom, the composition will move from BCD** to BCD*, eventually reaching BCD* with a large number of stages. BCD* is always the "lighter" of the two mixtures because it is produced from the top product of an earlier split, while BCD** comes from the bottom product.

If $V_1>V_2$, the configuration can be operated as shown in Figure 3-12a. The heat from the first column can provide part of the second column's duty through heat exchanger, resulting in a total vapor requirement from utility of only V_1 rather than V_1+V_2. If $V_2>V_1$, conversely, the configuration can be operated as that in Figure 3-12b. Part of the heat available in V_2 is used to vaporize all of V_1. Cold utility is used to condense the remainder of V_2. Again, this requires only V_2 generation of vapor rather than V_1+V_2.

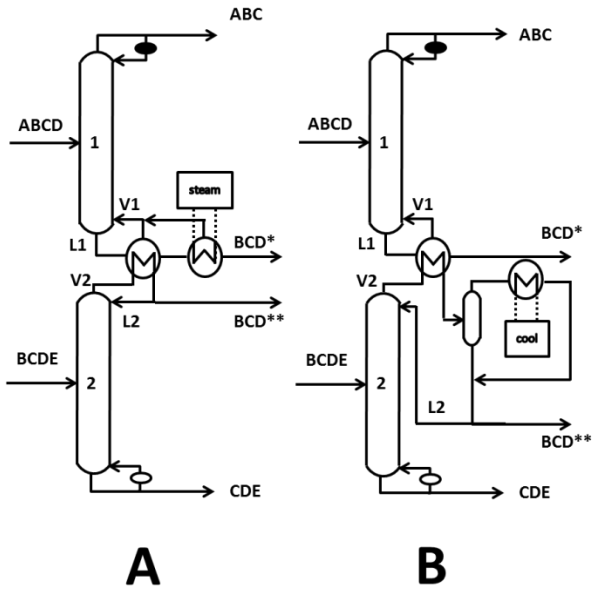

Figure 3-12: Possible heat exchanger options for operating adjoining splits using only the maximum of the two vapor flows rather than their sum

Thus, it is clear that many arrangements are capable of operating two adjoining splits at only the maximum of their vapor requirements (rather than the sum) if constant latent heat applies. In choosing to instead use the arrangement of direct transfer shown in Figure 3-11b, it should be expected that the separation performance of the system will either improve or remain the same since additional vapor is present in one of the sections. In order to express the separation performance of the system using only linear and nonlinear equations, it is thus assumed that the system in Figure 3-11b is functionally the same as those in Figure 3-12 if the product streams in Figure 3-12 were subsequently mixed. No optimization is performed considering different heat transfer arrangements; direct vapor transfer is the only arrangement considered. Mathematically, this is a strong inner approximation of the feasible set of heat transfer arrangements; if anything it underestimates the energy savings possible.

3.6 Further efforts into search space reduction and quick screening techniques

Section 3.4.2 described use of an upper bound on the objective function to restrict the search space to only those configurations which fall within 5% of a known global optimum. It is possible to further utilize the upper bound on the objective function to make complete screening of the search space possible, even if the global optimum is not known in advance. In particular, obtaining a guaranteed ranklist of a full search space is a computationally intense job. If it was instead desired to obtain a guaranteed ranklist of the top p configurations (where p might be something like ten, twenty, or fifty), adaptive system bounds could be used to reduce the search space that needs to be examined.

The procedure to quickly obtain the top p solutions to separate a given feed begins by solving any p configurations in the search space. Knowing in advance what configurations are favored might quicken the search; however a quick and efficient search can still be performed with the configurations examined in any random order. The GMA algorithm will provide global solutions for the first ten configurations, using an upper bound on the objective function equal to the worst sharp split configuration as calculated by the SMA method. The ten solutions are ranklisted and this is the basis for the top ten list. The solution currently identified as the p^{th} best is set as the global upper bound on the objective function. The next configuration, rather than necessarily being solved to global optimality, will be examined by GAMS/BARON for whether or not a solution exists less than the global upper bound. Often if no such solution exists the configuration can be discarded rapidly rather than requiring computational time to guarantee global optimality. If the configuration is discarded it is not a part of the set of best solutions. If a solution does exist less than the cutoff, the configuration is solved to

global optimality. It is inserted into the ranklist, and the solution previously occupying the p^{th} spot in the ranklist is discarded. The global upper bound is updated with the new p^{th} best configuration objective function value and all subsequent configurations must be tested against this new value.

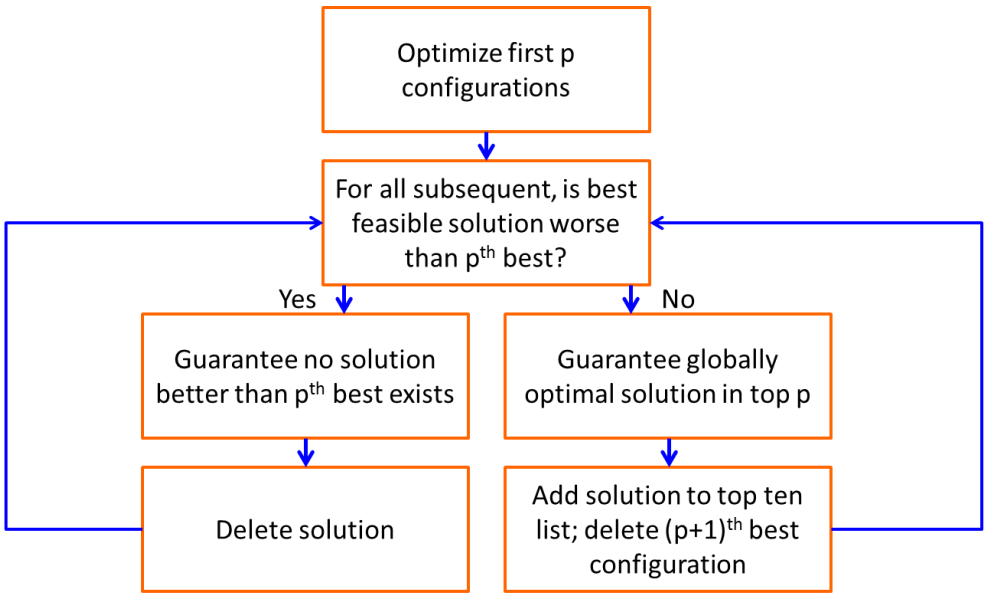

Figure 3-13: Procedure for reducing search space using upper bound cutoff for top p solutions

The procedure is summarized in Figure 3-13. The advantage of using this procedure is that for most search spaces the algorithm will very rapidly find ten solutions close to the global optimum. This allows an increasing proportion of the search space to be disregarded as the algorithm progresses.

Figure 3-14 demonstrates one example search space, for the heavy crude mixture considered in section 3.4 with p=10. In order to guarantee a complete ranklist of all possible configurations, a total of 6,128 optimization problem evaluations must be

performed. However, when following the procedure of Figure 3-13, a total of over 78% of this search space can be quickly guaranteed not to be in the top ten solutions without requiring global optimization. In most practical examples, these top ten configurations will be all that is needed for preliminary design – thus, the ability to eliminate 78% of the search space without sacrificing the knowledge that the solutions chosen are the best possible is extremely useful.

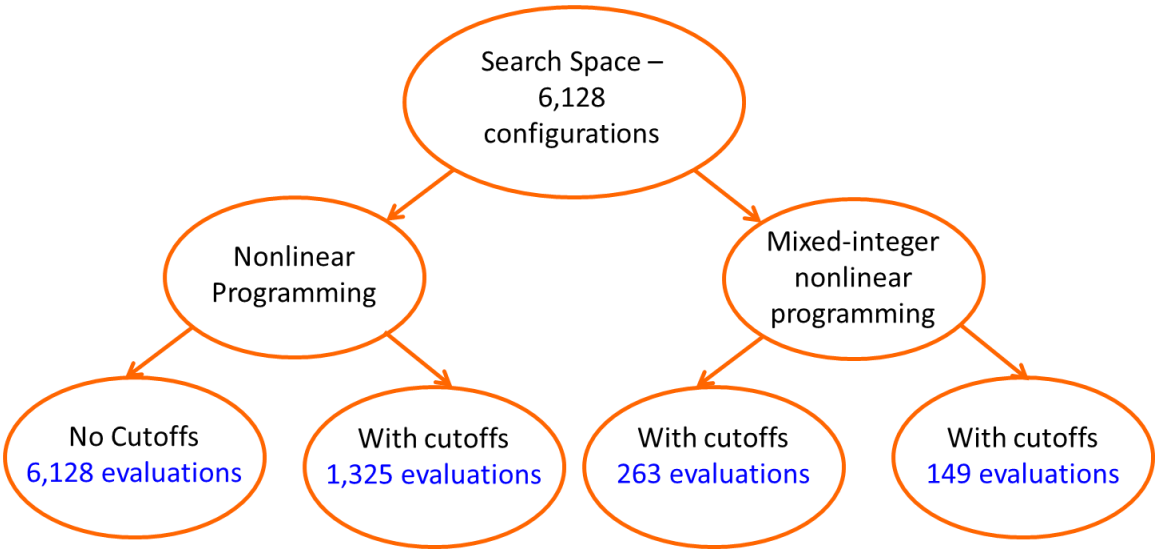

Figure 3-14: Number of problem evaluations required to completely evaluate various problem types

Not only can this algorithm decrease the search space size without any loss of global optimality, it can also be used with MINLP principles. For the heavy crude mixture, an MINLP procedure based on the matrix method configurations has 203 subproblems to solve. Note that 203 MINLP programs are not guaranteed to be faster to solve globally than 6,128 NLP programs; however, they still may be depending on how

they are formulated. In order to guarantee the top p solutions using an MINLP algorithm, the top p from the 203 subproblems must be identified, then all thermally coupled variants of the top p must additionally be solved as constrained MINLPs or regular NLPs. In this case, this requires an additional 60 evaluations leaving a total of 263 problems to solve. If the cutoff procedure is utilized *along with* an MINLP formulation, the total number of evaluations is reduced from 263 to 149; the remainder are quickly eliminated from consideration due to their solutions not approaching the global minimum for all configurations. Chapter 7 discusses further the possible implementation of MINLP problems.

Adaptive bound techniques improve the speed of screening for design of a multicomponent distillation. An additional layer of speed improvement can be added if it is known in advance which configurations are strong candidates for global optimality; if the upper bound of the objective function was quickly drawn close to optimality essentially all subsequent configurations would not require complete certification of their global solutions. Chapter 7 discusses additional opportunities to improve convergence speed including algorithm parallelization.

CHAPTER 4. TOTAL COST MINIMIZATION IN MULTICOMPONENT DISTILLATION

4.1 Introduction to Total Cost

While the minimization of vapor duty provides valuable insights into multicomponent distillation, it is also desirable to formulate a method by which the total cost, including capital and operating, can be optimized. Much data is available on how to estimate the cost of a configuration; some requires stage-to-stage calculations but methods are available to size columns and estimate their cost using only the vapor requirement of a configuration. Attempts to formulate such a minimization problem have been performed by Yeomans and Grossmann[61]; they formulated a state task network and state equipment network method using a superstructure approach and showed this representation could be solved mathematically in a unified manner with a logic-based outer approximation algorithm. The proposed modeling framework offers the capability of identifying optimal sharp-split configurations. Caballero and Grossmann [55,57,62] proposed a superstructure optimization approach which also includes both basic and thermally coupled configurations. This approach utilizes a two-step optimization procedure which first identifies the best fully thermally coupled (FTC) configuration and then identifies the best arrangement of heat exchangers for the connectivity identified in the first step. The solution obtained after these steps is considered to be the distillation configuration with the lowest cost in the search space. The model was formulated as a

generalized disjunctive programming problem and solved as a mixed-integer nonlinear program (MINLP). The primary drawback of this approach is that the sequential nature of the optimization makes it uncertain whether the true global optimum can be identified [55,57].

The vapor duty objective function of the GMA is thought to be loosely proportional to the capital cost of a given configuration since column diameter scales with the amount of vapor passing through it [35]. However, when multiple splits share one column, some column sections may operate substantially above the minimum reflux. The diameter of such a section may be larger than necessary. Such effects must be considered in addition to the energy cost for the GMA to give any true indication of total cost.

Therefore, it is useful to extend the GMA method to use total cost as the objective function. The new proposed method will be labeled the Cost Global Minimization Algorithm (CGMA). In order to verify the CGMA's efficiency and robustness, a separation system involving a five component ideal mixture is used as a case study. For n = 5, a total of 6,128 configurations (including both basic and thermally coupled configurations) constitute the search space. The detailed cost objective function formulated includes calculation of column height and diameter, tray size and number, and heat exchanger duty, and the annualized costs associated with each.

First, the global optimization techniques are applied to the sample problem and compared with a two-stage approach to demonstrate the need for the GAMS/BARON solver utilized by the CGMA. Subsequently, the effects of the weighting function used to balance capital and operating costs are studied using a set of sample weights. The results

demonstrate the usefulness of the CGMA as a tool to identify distillation configurations with potential to save energy while also being low in installation costs.

4.2 Methods for generating total cost

The GMA was created with the goal of minimizing the vapor duty of an individual configuration using the solver GAMS/BARON. GAMS/BARON is a branch-and-reduce solver which is derived from the class of branch and bound methods; it utilizes advanced range reduction and convex underestimation techniques to arrive at quick, globally optimal answers. As branch and bound methods are heavily influenced by the quality of variable bounds and the presence of nonconvex equations, the strategies introduced in Chapter 3 are retained for the cost formulation. The complete details of these three strategies are provided in a pair of articles by Nallasivam et al. [53,59]. In this study, the majority of the GMA framework has been retained; additional equations have been added to calculate all variables that are a part of the capital and operating costs of the system. Constraints will be described which calculate the column height and diameter, number of trays, and heat exchanger duties based on the vapor flows calculated in Underwood's equations. The distillation column diameter is calculated individually for each split, based on the largest vapor flow present within the envelope associated with that split. For example, in Figure 4-1, two splits (split 2 and split 3) are present in Column 2. The top split carries out the separation where A and B are produced from stream AB; the bottom split produces B and C from stream BC. The diameter (D2) of the top column section is calculated based on max{V2top and V2bot}. Therefore the column will likely have a different diameter for its top and bottom sections.

The two stage method used in this chapter formulates an optimization problem with total cost as the objective function. For an *n*-component separation problem, optimization is performed over a search space containing all feasible *n*-component regular-column configurations. The separation problem is formulated as a two-stage mixed integer nonlinear program (MINLP). In the first stage, all binary variables for heat exchangers associated with an intermediate stream are set to zero to indicate the absence of the exchangers. Intermediate streams are defined as any streams in the configuration which are not the main feed or final products.

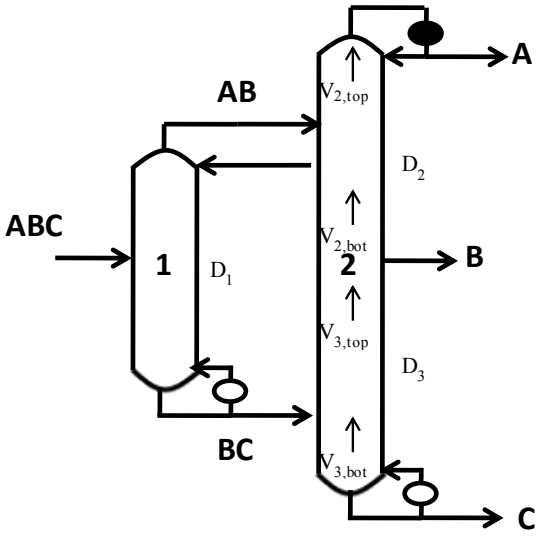

Figure 4-1: Diameter calculations for a column with two splits

With all heat exchangers absent, all possible connectivities will be optimized to obtain the completely thermally coupled (CTC) arrangement with the lowest total cost. In the second stage, the connectivity of the optimal solution from the previous stage is

forced to stay constant; the connectivity is solved for the optimal arrangement of heat exchangers. The optimal solution of the second stage is recorded. A different starting point is chosen and the process is repeated iteratively until the solution begins worsening. This method is termed the two-stage minimization algorithm (TMA).

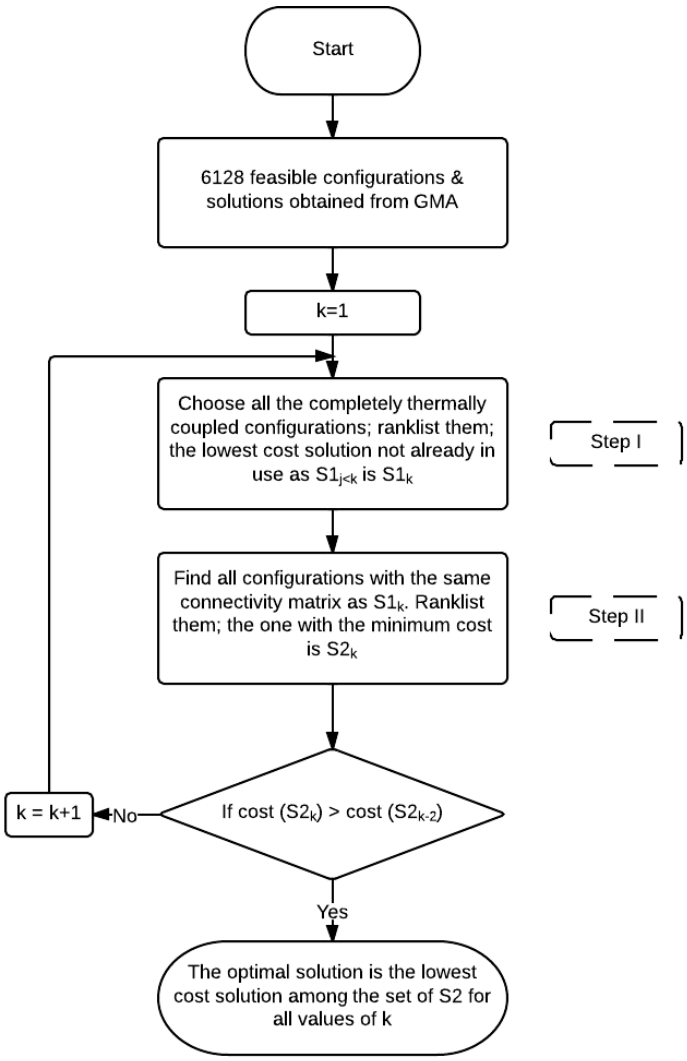

Figure 4-2: Flowchart of TMA Method

In order to compare results from the cost-based GMA method with the two-stage approach inspired by Caballero & Grossmann[55,57], both methods are applied to the regular-column search space proposed by Shah & Agrawal [42]. For n = 5, the matrix method gives a total of 6,128 configurations; of these, 203 are basic with no thermal coupling, 203 are completely thermally coupled (CTC), and 5,722 contain some degree of thermal coupling less than the CTC configurations. The CGMA algorithm generates a ranklist of all feasible configurations ranked by their combined total cost. The TMA method generates a series of solutions from different starting points; the series is terminated when an iteration gives worse results than the previous step. The flowchart of the TMA method is shown in Figure 4-2.

4.3 Formulation of total cost problem

The optimization problem formulated here is the same as that formulated in Chapter 3; however, a new objective function is used and additional constraints added to calculate the value of each term in the objective function. The objective function of the optimization is given by:

$$\min\left(\sum_{s=1}^{ns} Ccol_s + \sum_{s=1}^{ns} Ctray_s + \sum_{c\in REB} Creb_c + \sum_{c\in COND} Ccond_c + \sum_{c\in REB} Cst_c + \sum_{c\in COND} Ccw_c\right) \quad (4\text{-}1)$$

Here, the variables are Ccol (cost of column shell in split *s*), Ctray (cost of tray stages in split *s*), Creb and Ccond (cost of heat exchangers in column *c*), and Qreb (required heat energy in column *c*), Qcond (required cooling energy in column *c*). Cst and Ccw are parameters that give the cost per unit energy of heating and cooling. Reboiler

and condenser variables are only included in the objective function for those columns in the set of columns with heat exchangers (denoted as the sets REB and COND).

A feasible distillation column must satisfy phase equilibrium and mass balance relations. In addition to these constraints, the vapor flow requirement for carrying out a given separation operation in the given distillation section must satisfy Underwood's feed and distillate equations. The full set of constraints implied by these relationships is found in Chapter 3 and will be retained here with one exception. The Underwood distillate equation is modified in order to imply operation at a reflux ratio (L/D) 20% higher than minimum reflux. As with examples in literature [55,57], it is assumed that the vapor duty generated by Underwood's distillate equation is still valid at 1.2 times minimum reflux. Increasing L/D rather than L/V leads to an additional term subtracting 0.2 x D from the final vapor flow.

$$1.2\sum_{k=i}^{n-j+i}\frac{\alpha_k \bar{X}_{s,k}}{\alpha_k-\theta_{s,r}}-0.2\sum_{k=1}^{n}\bar{X}_{s,k}\le V_s^{\min} \qquad \begin{array}{c}\forall s=1,\ldots,ns\\ i=ROW(DISTS_s)\\ j=COL(DISTS_s)\\ j_F=COL(FEEDS_s)\\ r=1,\ldots,n-j_F\end{array} \tag{4-2}$$

As in the previously described formulation, FEEDS and DISTS give the stream number of the feed and distillate streams; ROW(m) and COL(m) give the values of *i* and *j* that satisfy $m=\binom{j}{2}+i\,;n\ge j\ge i$. The second sum term is an adjustment not present in any Underwood's equations-based total cost formulation previously in existence; existing formulations operate at (1+p) times the minimum (L/V) rather than (1+p) times the minimum (L/D)[55,57].

The Fenske equation [63] is used for determining the minimum number of equilibrium stages; in accordance with past models the actual number of stages NM_s will be taken to be twice the minimum [55,57]. In equation 4-3, α is the relative volatility of light key and heavy key components in the column section; β is the fractional recovery of the light key in the distillate; δ is the fractional recovery of the light key in the bottom.

$$NM_s = \frac{(2)ln\dfrac{\beta * \delta}{(1-\beta)(1-\delta)}}{\ln(\alpha)} \qquad \forall s = 1,\ldots,ns \tag{4-3}$$

For example, in a three component separation where A is the sole top product with 99.9% recovery in the top and 0.1% recovery in the bottom, the light key is A and the heavy key is B.

The height of the column (H_s, given in meters) and the area (A_s, in square meters) are given by the following:

$$H_s = 0.6(2 * NM_s) + 4 \qquad \forall s = 1,\ldots,ns \tag{4-4}$$

$$A_s = \frac{M_{AV} * \max(V_s^{top}, V_s^{bot})}{\sqrt{\rho_l \rho_v} * 0.6 * 329 * 0.8} \qquad \forall s = 1,\ldots,ns \tag{4-5}$$

where M_{AV} is the average molecular weight of components in the system, ρ_l and ρ_v are the average liquid and vapor density of the feed mixture, and the max term gives the larger of the actual vapor flows in the envelope of split *s*. The column shell and trays have a cost (in thousands USD) given by:

$$Ccol_s = (.6038 * A_s * H_s + 5.307) * 1.2 \qquad \forall s = 1,\ldots,ns \tag{4-6}$$

$$Ctray_s = (.5711 + .4068 A_s + .02283 A_s^2) * (2.5 + 1.72) \quad \forall s = 1, \ldots, ns \tag{4-7}$$

Costs for reboilers and condensers are fixed at US $15000 each when they exist in a given column. It is possible that with more detailed estimation of reboiler and condenser sizings, more favor would be given to those configurations that avoid using them; this should be investigated in future studies.

$$Creb_c = 15 \quad \forall c \in REB \tag{4-8}$$

$$Ccond_c = 15 \quad \forall c \in COND \tag{4-9}$$

The operating cost is the utility cost including cooling water and steam. Equation 4-10 through 4-13 demonstrate this. Heats (Q) are calculated in GJ/hr.

$$Qcond_c = \frac{(V_s^{top} - V_m)}{\sum_{k=i}^{n-j+i} X_{s,k}} \sum_{k=i}^{n-j+i} X_{s,k} \Delta H_k \qquad \begin{array}{c} \forall c = COND \\ s = STOP_c \\ m = DISTS_s \\ i \in ROW(m) \\ j \in COL(m) \end{array} \tag{4-10}$$

$$Qreb_c = \frac{(V_s^{bot} + V_m)}{\sum_{k=i}^{n-j+i} X_{s,k}} \sum_{k=i}^{n-j+i} X_{s,k} \Delta H_k \qquad \begin{array}{c} \forall c = REB \\ s = SBOT_c \\ m = BOTT_s \\ i \in ROW(m) \\ j \in COL(m) \end{array} \tag{4-11}$$

$$CCW_c = Qcond_c C_{CW} Op_{hrs} W \quad \forall c = 1, \ldots, n-1 \tag{4-12}$$

$$CST_c = Qreb_c C_{steam} Op_{hrs} W \quad \forall c = 1, \ldots, n-1 \tag{4-13}$$

In these equations, STOP and SBOT are the arrays which return the split number at the top and bottom of a given column respectively. The heat and cooling duty are calculated using the actual vapor flow at the top (for condensers) and bottom (for reboilers) as well as the amount of vapor that is passed to the next column through the product stream. Compared to the GMA, one difference in this formulation is that V_m is allowed to take any value for streams associated with an exchanger. C_{CW}, C_{steam}, Op_{hrs}, and W are parameters – the first two give heating and cooling per-unit costs; Op_{hrs} is the number of hours per year; W gives the number of years of operation desired for the analysis. The importance of the parameter W will be discussed later.

Many of the above equations are adapted from Grossmann[64]; cost estimation is based on Turton et al. [65]. Diameters of column sections are calculated using procedures presented by Stilchmair and Fair [66].

4.4 Case Study 1 – Comparison of TMA and GMA methods

To illustrate the reliability of the CGMA method, one example studied in Caballero & Grossmann [55,57] is studied. In this example, the five component feed mixture ABCDE is typically separated into the following products: Benzene (A), toluene (B), ethylbenzene (C), styrene (D), and α-methyl styrene (E). Table 4-1 shows the feed conditions and several parameter values for this example. The recovery factor has been fixed at 0.98 to give a reasonable number of theoretical trays.

Table 4-1: Feed data for case study 1

Component	Feed composition (mole fraction)	Relative volatility of component (α)	
Benzene (A)	0.3	10.5	
Toluene (B)	0.2	4.04	
Ethylbenzene (C)	0.1	1.76	
Styrene (D)	0.2	1.31	
α-Methyl styrene (E)	0.2	1.00	
Feed flow (kmol/h)			200
Pressure (atm)			0.5
Steam cost (US$/GJ)			5.09
Cooling water cost (US$/GJ)			0.19

With the CGMA method, there are in total 6,128 feasible configurations in the search space; each requires individual optimization using a deterministic global optimization package (BARON). All solutions are then ranklisted in order to find the final globally optimal solution for the system under study. In order to compare the CGMA's performance with that of the TMA, the complete search space is then analyzed for how it would perform using the TMA with the same cost model. Both models use a value of 1 for W.

The CGMA gives the lowest cost configuration in the search space to have an objective function value of $3,125,100. The configuration with this cost is displayed in Figure 4-3.

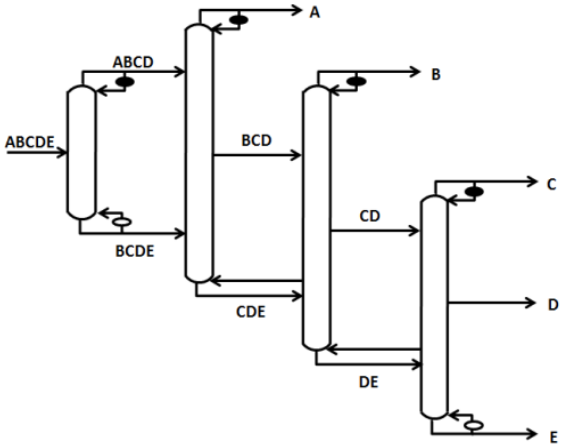

Figure 4-3: Globally optimal low-cost configuration

In the first step of TMA method, the lowest-cost CTC configuration is identified. The configuration is shown in Figure 4-4a and has a cost of US$3,183,000. Using this connectivity, the exchangers are varied until the lowest-cost exchanger arrangement is found; this has a total cost of US$3,140,100 and can be seen in Figure 4-4b.

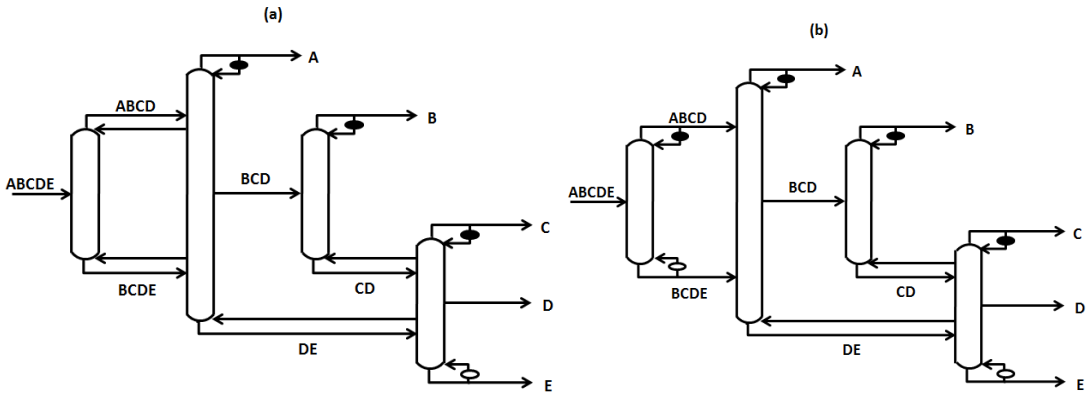

Figure 4-4: (a) Optimal configuration obtained at the first step of TMA method; (b) optimal configuration obtained at the second step of TMA method

In this case GMA identifies solutions with a cost lower than the TMA optimal solution by 0.5% - a small difference, but enough to show that the two-step method does not guarantee finding the global optimum. TMA does not initially identify the configuration in Figure 4-3 because the FTC variant of Figure 4-3 has a higher cost than Figure 4-4(a); thus the best configuration is filtered out in the first step and may only be found with repeated iteration. Only 219 (203+16) configurations are actually considered by TMA in the first iteration; that of Figure 4-3 is not one of them. This is why the two stage method does not guarantee the global optimality of the solution. The main difficulty is that many topologically different configurations with thermal couplings have very similar objective function values. Some of the nearly globally optimal configurations could prove more attractive when thermal couplings are replaced by exchangers. Further, when considering factors not captured using Underwood's equations or the cost objective function, other configurations may be even more advantageous. Therefore, it is desirable to identify not just the single best globally optimal configuration, but several configurations which reach nearly optimal cost.

CGMA has the ability to rank list alternative configurations according to a chosen criterion, which is quite useful for a practitioner to assess benefits of the parameters that are not easily expressed in mathematical form. For example, in this five component case, we find 33 configurations within 3% of the lowest objective function value. A practitioner can pick a configuration from these based on other factors like control and operability, manufacturability, safety, or retrofit while still guaranteed a low-cost solution.

4.5 Case Study 2 – Insufficiency of TMA method

Consider another example introduced by Caballero & Grossmann[55,57]. In this example, the feed mixture ABCDE contains five alcohols and is typically separated into the following products: ethanol (A), isopropanol (B), 1-propanol (C), isobutanol (D), and 1-butanol (E).

Table 4-2: Feed data for case study 2

Component	Feed composition (mole fraction)	Relative volatility of component (α)	
Ethanol (A)	0.2	4.10	
Isopropanol (B)	0.3	3.60	
1-Propanol (C)	0.2	2.10	
sobutanol (D)	0.2	1.42	
1-Butanol (E)	0.1	1.00	
Table 4-2 continued			
Feed flow (kmol/h)			200
Pressure (atm)			1.0
Steam cost (US$/GJ)			5.09
Cooling water cost (US$/GJ)			0.19

Compared to the first study, all separations in this case study are relatively difficult to carry out according to their relative volatility values. Table 4-2 shows the feed data for this example. The recovery has again been fixed at 0.98 and W at 1.

In this example, focus is given to the solutions resulting from repeated iteration of the TMA method. The stopping criterion is relaxed so that it will never be stopped, and indefinite iteration is allowed until the full search space has been covered. Figure 4-5 shows the first 42 steps of the iteration process. The top green points represent the top 42

fully thermally coupled configurations in the rank-list of 203 possibilities. The upper data point associated with each iteration will be the solution to the first stage of the two-stage method. In the second stage, each configuration from stage 1 is allowed to have any combination of heat exchangers; the combination with the lowest cost is represented by the lower point in each iteration. For example, the best possible CTC configuration has a cost of $8,250,000; the best configuration derived from it has a cost of $7,530,000. These correspond to the leftmost two points on the graph.

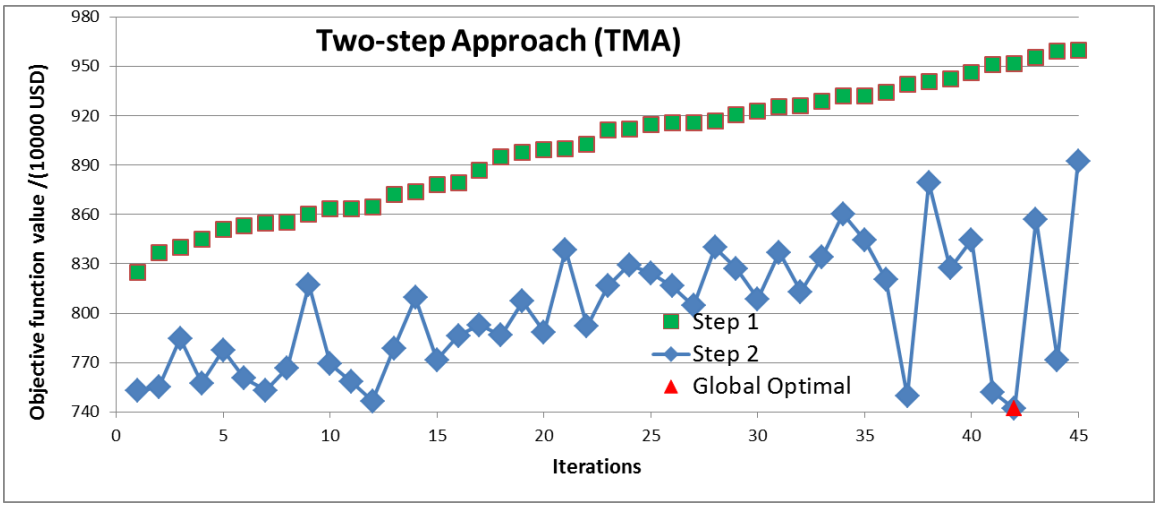

Figure 4-5: Solutions of the first 45 iterations of TMA method

It follows that having a better solution in Step 1 does not always translate to identifying a lower-cost solution in step 2. For example, the solutions of the ninth and tenth best completely thermally coupled configurations are US$8,605,000 and US$8,633,000 respectively. But when intermediate heat exchangers are allowed, the connectivities can yield costs as low as $8,173,000 and $7,692,000 respectively.

The global optimum (confirmed to be so by CGMA) is identified only when considering the 42nd best completely thermally coupled configuration (equivalent to 42 iterations of the TMA). Based on the stopping criterion, TMA will terminate the process in the very early stages and conclude that the initially identified stage 2 solution of $7,530,000 is the optimal solution; the true globally optimal configuration (red point on the graph) can yield a cost with savings of about $113,000. In total, the CGMA can identify 7 solutions with lower cost than that identified by the TMA. This again demonstrates that CGMA is more reliable for identifying the single most cost effective distillation configuration; the lack of correlation between first and second step successes in TMA leaves it uncertain if and when it will identify a global solution.

4.6 Case Study 3 – Comparison of different objective function weights

Returning to the feed data in Table 4-1, it becomes of interest how the CGMA reacts to changes in the weight of capital and operating cost; also of interest is a comparison with the vapor duty objective function of the GMA. For this reason three cases are considered for the 5 component search space, which contains 6,128 configurations.

- Scenario A: Configurations optimized by vapor duty only using the GMA algorithm. This scenario can be loosely held to represent W >> 1. This is used rather than actually using the CGMA with W >> 1 for the purpose of evaluating the GMA itself as a measure of total cost; it is, however, found that the lowest vapor configuration in this case does also have the lowest operating cost.

- Scenario B: Configurations optimized on total cost using the CGMA with W = 1.
- Scenario C: Configurations optimized by capital cost alone using the CGMA with W = 0.

For each of the three scenarios, a complete ranklist of all configurations is generated. Figure 4-6 shows a configuration deemed to be globally optimal for each of the three scenarios. Figure 4-6a shows the fully thermally coupled configuration, which has a globally minimum vapor requirement of 419.1 kmol/hr of vapor to handle 200 kmol/hr of feed input. For this case there are 263 configurations within 2% of the FTC solution.

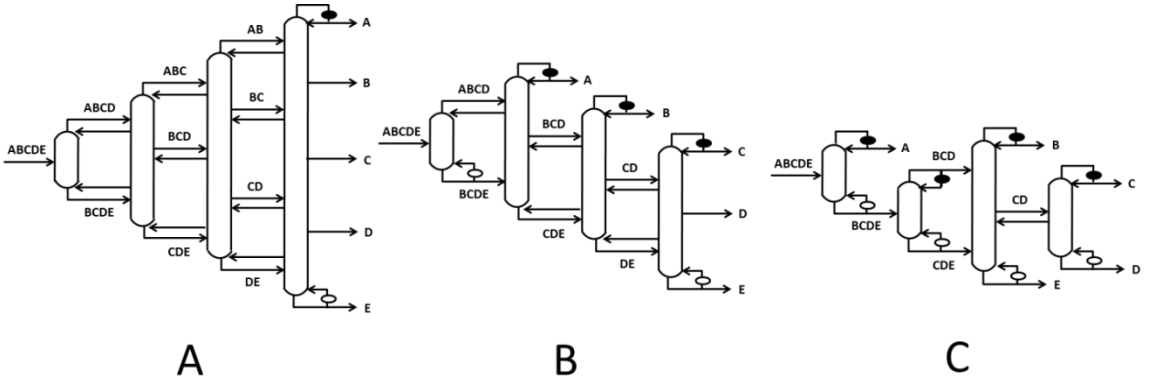

Figure 4-6: Optimal configurations for each scenario

When optimized for cost with W=1 (scenario B), the FTC configuration has a total cost of $3,612,000 and the lowest operating cost in the search space. Figure 4-6b demonstrates the configuration with the lowest combined cost for scenario B, estimated to cost $3,125,000 in combined capital and weighted operating costs. There are 13 configurations within 2% of the cost of Figure 4-6b; two of them also belong to the set of

configurations within 2% of the vapor duty of the FTC solution. Figure 4-6c shows a basic configuration which, without considering operating cost, becomes the lowest-cost configuration to build (at an estimated $953,000 – it has an associated operating cost of $3,366,000). There is only one configuration within 2% of the capital cost of this configuration; twelve configurations fall within 10%.

When the entire search space is examined, plotting the results of any of the above scenarios against one another further demonstrates that none of the three yields the same configurations as the most efficient. Figure 4-7 demonstrates the difference between the search space results of scenario A and scenario B.

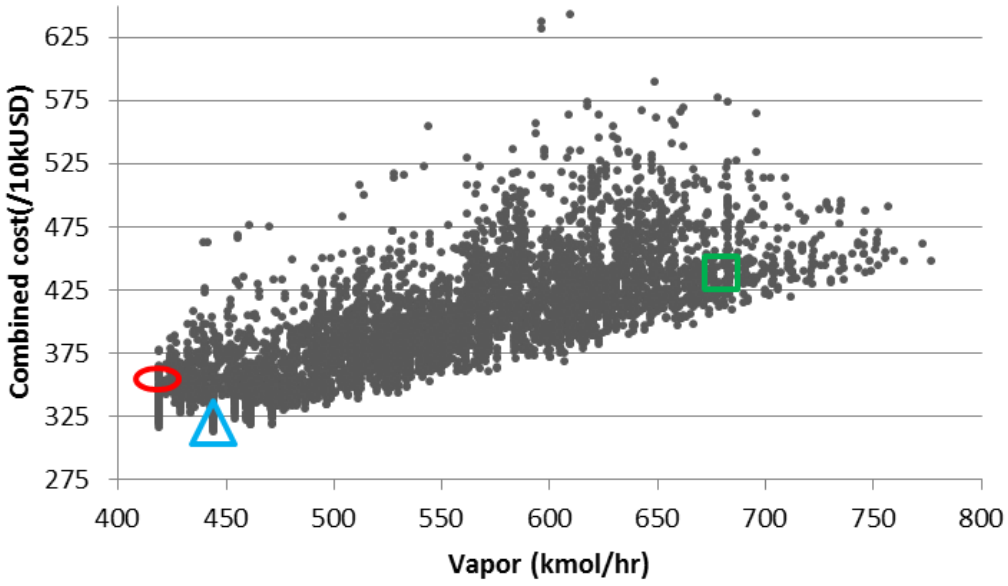

Figure 4-7: Vapor vs. total cost plot

Three highlighted shapes on the plot represent the three configurations in Figure 4-6. The FTC configuration (Figure 4-6a) has the lowest possible vapor flow, but has approximately 15% more total cost than several other process alternatives; it is thus represented by the leftmost circle. The configuration in Figure 4-6b is represented by the bottommost triangle; it has a slightly higher vapor flow than the FTC, but allocates the vapor in such a way that column diameters are reduced and the overall total cost is reduced. The rightmost square is Figure 4-6c – by focusing exclusively on reduction of capital cost, it has incurred a fairly high vapor flow since no vapor is shared between columns through thermal coupling; this translates to a high operating cost and high total cost. As a whole the graph demonstrates that the lowest total cost configuration is likely to have a low vapor flow – but the lowest vapor flow is not guaranteed to be the lowest possible cost.

In order to determine whether minimizing capital cost can ever be a viable strategy for finding a low total cost, the comparison of capital cost with total cost is shown in Figure 4-8.

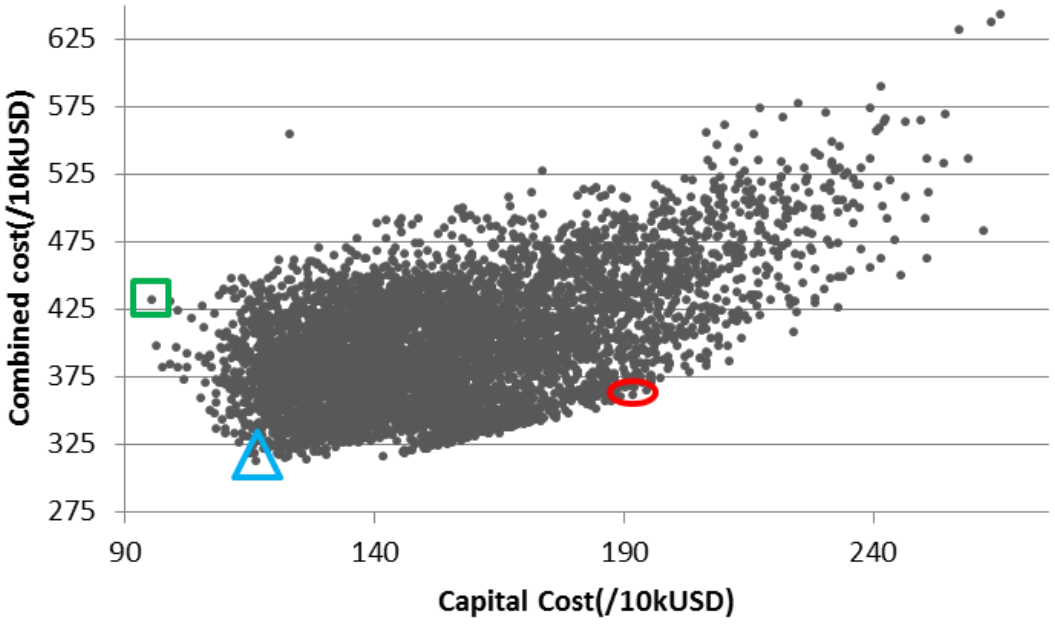

Figure 4-8: Capital cost vs total cost plot

Here, the lowest capital cost point (Figure 4-6c) is given by the leftmost square; as expected, its high vapor flow leads to a relatively high total cost despite its extreme capital savings. The configuration with the lowest cost (Figure 4-6b) does indeed possess a fairly low capital cost as well as its low vapor duty; this enables it to be a much stronger performer in total cost. The FTC configuration, while lower than average in total cost due to its globally minimum vapor duty, does require an above-median capital investment.

One final way to study the three scenarios in the above case is to look at how their operating cost relates to their total cost. By taking the ratio between the two at W=1, it can be noted which configurations are likely to become more favorable with increasing W and which are likely to be favored by decreasing W. This is demonstrated in Figure 4-9.

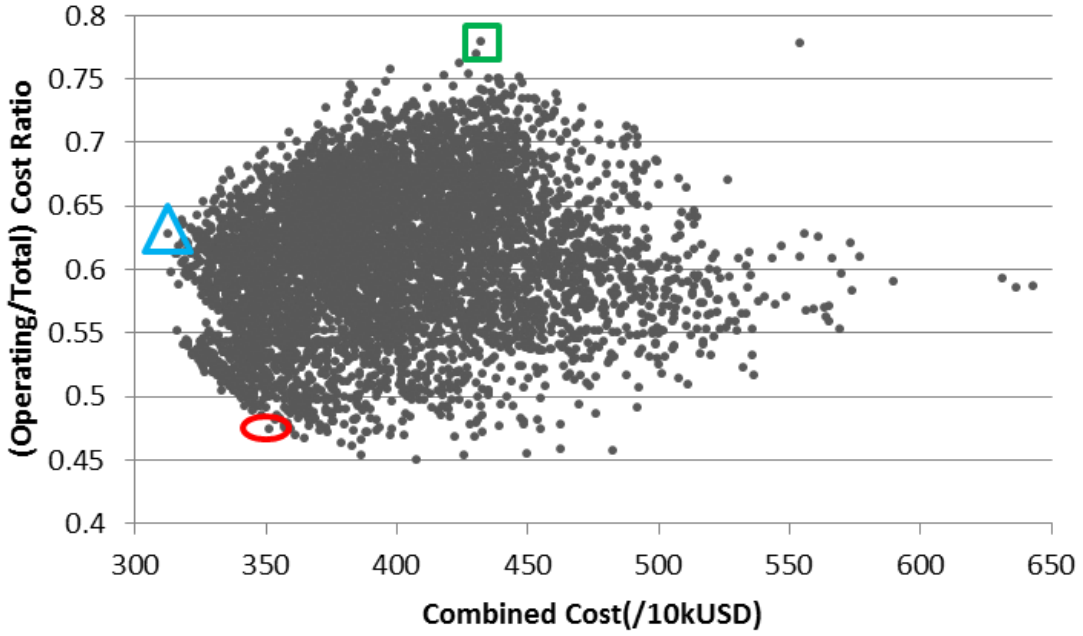

Figure 4-9: Many different ratios of operating to total cost exist in the search space

Once again Figure 4-6a (bottom circle) and Figure 4-6c (top square) present two widely contrasting pictures, with Figure 4-6b (leftmost middle triangle) operating somewhere between them as a low-cost alternative. As expected based on its low capital costs and relatively massive operating costs, Figure 4-6c would become increasingly favored in a scenario where W decreased from 1; it would shift to become more undesirable if W increased, which would represent an increased desire to reduce operating costs. As Figure 4-6a was identified as capital-heavy with extremely low operating costs, the FTC arrangement will be favored by a design strategy which is willing to incur capital costs on behalf of energy efficiency; the FTC will be seen as undesirable when capital installation becomes the determining factor in decision-making.

Figure 4-6b stands as a moderate option which would likely be a strong design choice under a number of different economic scenarios.

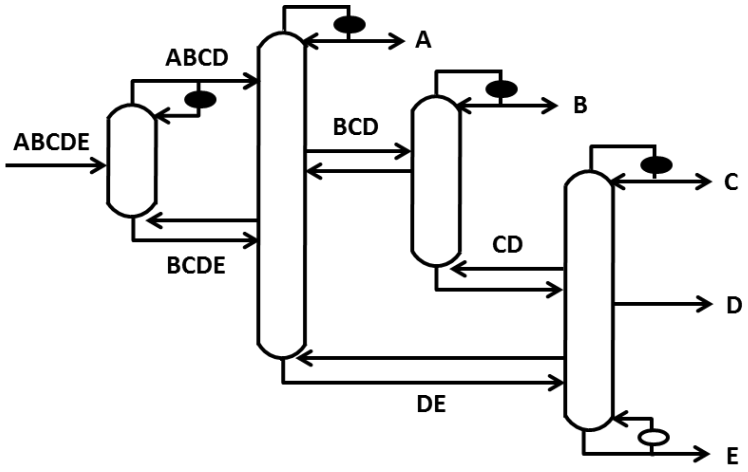

Figure 4-10: Low-vapor configuration with near optimal cost

This analysis has focused on the three configurations in Figure 4-6; however it is clear that in Figures 4-7 through 4-9, there exist a large number of alternate configurations that would provide very similar benefits as any of these three configurations. For example, a configuration with an almost identical vapor duty to that of the FTC configuration can be found which, rather than incurring 15% more total cost than Figure 4-6b, would incur only an additional 1.2% cost increase. This configuration is demonstrated in Figure 4-10; it requires about 26% less capital investment than the FTC configuration. This demonstrates that choosing a design by considering the full search space and how each configuration fares in multiple metrics may be a superior method of design compared to choosing the single best configuration by any one objective function.

It may allow insights that were not clear in a search space with only one dimension of results.

It is additionally possible to use identified optimal configurations as starting points in searching for similar configurations which are easier to operate and control while remaining cost effective. For example, the configuration pictured in Figure 4-6b contains two thermal coupling links – it is possible to include variants of this configuration which contain less thermal coupling in the comparison in order to create a simpler system which is still low-cost. Table 4-3 demonstrates the normalized objective function values of the three configurations already studied, plus three additional configurations with the connectivity of 4-6b, but with the thermally coupled links at stream CDE, stream DE, or both replaced with reboilers. It is clear that the location of the thermally coupled links are important; by choosing to retain the coupling at stream DE, an additional reboiler for use in vapor control can be implemented with only a 1.7% increase in cost; removing the thermal coupling at stream CDE comes at a substantially higher cost.

Table 4-3: Comparison of multiple options for designing a low-cost separation

	% Increase from globally optimal solution		
	Vapor	Capital	Total Cost
4-6a	0%	101.3%	15.6%
4-6b	6.1%	21.9%	0%
4-6c	60.7%	0%	38.2%
4-6b - CDE coupling only	22.1%	19.5%	9.4%
4-6b - DE coupling only	12.5%	20.6%	1.7%
4-6b - no coupling	27.4%	13.4%	11.3%

The analysis in this section has focused on several of the extreme points of the parameter W. When designing a practical system, it is important to set W to reflect the needs of the designer and the current economic conditions. The objective function in this paper does not directly account for depreciation of capital or time value of money but could easily be adapted to do so without losing the guarantee of global optimality and ability to quickly screen the full search space without ignoring potential options.

CHAPTER 5. A METHOD FOR THERMODYNAMIC EFFICIENCY MAXIMIZATION OVER THE FULL SEARCH SPACE OF REGULAR-COLUMN CONFIGURATIONS

5.1 Introduction to exergy

Using minimum vapor as the objective function has the advantage of approximating both capital cost and operating cost; conversely, the temperature level at which vapor is generated is not considered. This could lead to a distillation configuration being regarded as more efficient despite requiring generation of vapor much higher in temperature than a rival configuration, driving down its true efficiency. While the objective function presented in Chapter 4 gives a clearer estimate of the monetary cost to build and operate a configuration, it still assumes that the same temperature steam and coolant are used in all exchangers throughout the configuration; there is no distinction between a unit of energy applied to heat a mixture to 350 K and the same unit of energy applied to heat a mixture to 500 K. This could lead to "cost-saving" configurations being recommended that actually prove to be inefficient due to the high-pressure steam or extreme refrigerants required to operate the configuration.

While there is no simple way to completely account for the pressure and temperature of heat exchange utilities without performing detailed process simulation, accounting for temperature levels in a distillation to derive a thermodynamic efficiency for a separation process has often been don through exergy analysis. Analysis based on

thermal efficiency can often provide useful insights for design that would not be apparent otherwise. This is particularly true for cryogenic distillations, which operate below ambient temperatures and use work rather than heat to drive separation. Exergy analysis is also a useful tool in analyzing systems with heat integration.[67-70]

The exergy of any material stream is the maximum amount of work that can be generated by bringing the stream into equilibrium with a heat reservoir. Figure 5-1 demonstrates an ideal procedure for extracting thermal work from a material stream; the maximum amount of work possible if no losses occur in the conversion procedure is given by $Q\left(1-\frac{T}{T_{surroundings}}\right)$. In this expression T is the initial temperature of the stream, $T_{surroundings}$ is the ambient temperature of the heat reservoir, and Q is the heat generated by the ideal engine. This, then, is the exergy of this material stream. While energy cannot be destroyed, only converted from one form to another, exergy can be destroyed or lost in processes that are not isothermal.

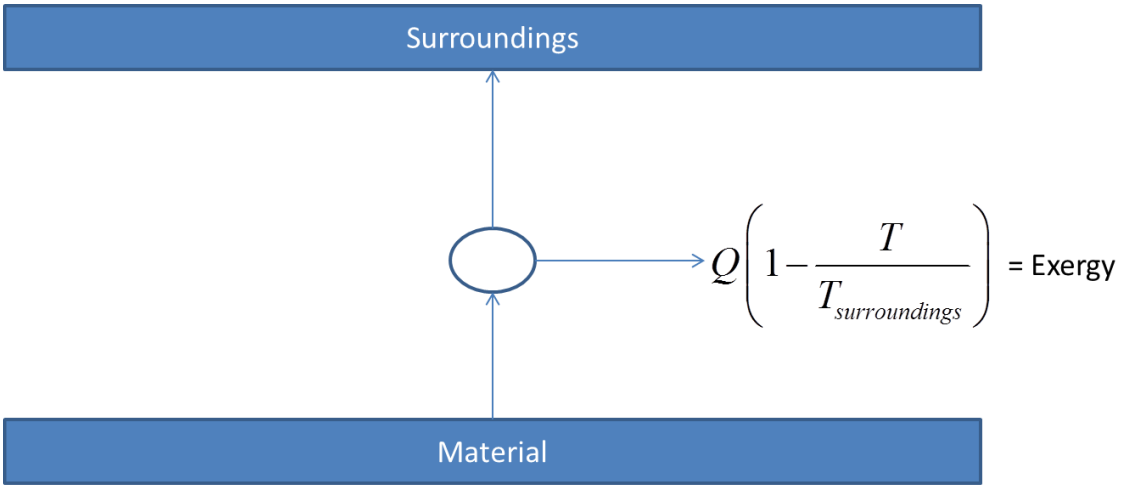

Figure 5-1: Definition of exergy of a material stream

Equations for calculating exergy loss and thermodynamic efficiency of a distillation column are described by Agrawal and Herron.[71-73] The thermodynamic efficiency of a separation is given by

$$\eta = \frac{\text{minimum work of separation}}{\text{total exergy loss} + \text{minimum work of separation}} \tag{5-1}$$

When the total exergy loss of the system is calculated, any given distillation configuration's attractiveness can then be measured in terms of minimizing the loss of exergy in the system – a system which creates the least loss of ability to do work by the material streams is the most desirable. Coupling this method with the matrix method described earlier in this dissertation should allow the complete search space of basic and thermally coupled configurations to be screened using an exergy-based objective function – one which will provide a new lens through which to view the attractiveness of these configurations. This minimum-exergy formulation is useful both as a stand-alone measure of energy efficiency and as a deciding factor between configurations which have already been found to have similar vapor duties or similar capital costs.

5.2 Exergy equations for a multicomponent distillation

Figure 5-2 shows a sample distillation configuration for a four-component separation. The liquid and vapor flows at the top and bottom of every column are represented on the diagram.

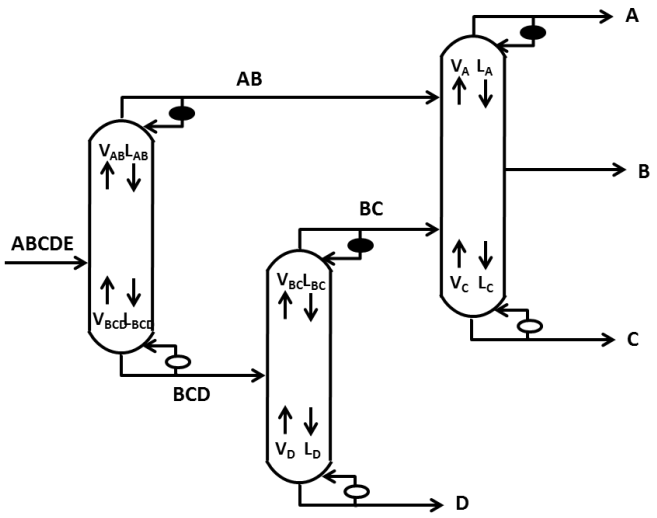

Figure 5-2: Sample distillation configuration with n = 4

This specific configuration will be used to derive equations for the exergy change associated with heat exchangers in a distillation column; these equations can be expressed generally for any configuration in the search space. Determining the exergy loss for this separation can be achieved through a balance on the exergy entering and leaving the configuration. To ensure consistency, the boundary of the area for which the balance is performed is drawn such that each stream entering an exchanger is taken to be leaving the system, and each stream leaving an exchanger is taken to be entering the system. For this specific example the following lists of streams are taken to be entering and leaving the configuration:

<u>Entering</u>:

- F_{ABCDE} (liquid)
- L_{AB} (liquid)
- L_{BC} (liquid)

- L_A (liquid)
- V_{BCD} (vapor)
- V_C (vapor)
- V_D (vapor)

Leaving:

- F_A (liquid)
- F_B (liquid)
- F_C (liquid)
- F_D (liquid)
- L_{AB} (vapor)
- L_{BC} (vapor)
- L_A (vapor)
- V_{BCD} (liquid)
- V_C (liquid)
- V_D (liquid)

Assume liquid feed and liquid final products for the time being; in addition, all condensers save those producing final products are partial condensers for the time being (therefore, all submixture streams produced as a top product are vapor). The exergy exiting the combined columns can be written as

$$\in_{in} = \in_{feed} + L_{AB}e_{AB} + L_{BC}e_{BC} + L_A e_A + V_{BCD}E_{BCD} + V_D E_D + V_C E_C \qquad (5\text{-}2)$$

$$\in_{out} = L_{AB}E_{AB} + L_{BC}E_{BC} + V_{BCD}e_{BCD} + L_D e_D + V_A E_A + L_C e_C + F_B e_B \qquad (5\text{-}3)$$

where E represents the exergy of a vapor stream and e represents the exergy of a liquid stream. ∈ is the exergy of a stream without a specific thermal quality known. All liquid flow variables can be eliminated via mass balance:

$$L_i = V_i + F_i \text{ (bottom products)} \tag{5-4}$$

$$L_i = V_i - F_i \text{ (top products)} \tag{5-5}$$

The overall exergy change in the column can be expressed as

$$\begin{gathered}\Delta \in = \in_{in} - \in_{out} = \in_{feed} -(F_A e_A + F_B e_B + F_C e_C + F_D e_D) \\ +(V_{AB} - F_{AB})(e_{AB} - E_{AB}) + (V_{BC} - F_{BC})(e_{BC} - E_{BC}) - V_{BCD}(e_{BCD} - E_{BCD}) \\ +V_A(e_A - E_A) - V_D(e_D - E_D) + V_C(e_C - E_C)\end{gathered} \tag{5-6}$$

For a liquid feed, the feed exergy is the sum of exergy of mixing and thermal exergy given by

$$\in_{feed} = RT_0 \sum_{i=A,B,C,D} z_{F_i} lnz_{F_i} + e^T_{feed} \tag{5-7}$$

Let

$$\delta = E^T_{feed} - (F_A E_A + F_B E_B + F_C E_C + F_D E_D) \tag{5-8}$$

$$\mu = (e^T_{feed} - E^T_{feed}) - \begin{pmatrix} F_A[e_A - E_A] + F_B[e_B - E_B] \\ +F_C[e_C - E_C] + F_D[e_D - E_D] \end{pmatrix} \tag{5-9}$$

This allows part of the exergy equation to be expressed using the terms δ and μ:

$$\in_{feed} -\left(F_A e_A + F_B e_B + F_C e_C + F_D e_D\right) = RT_0 \sum_{i=A,B,C,D} z_{F_i} lnz_{F_i} + \delta + \mu \tag{5-10}$$

Assume that the thermal component of the exergy of the vapor mixture is approximately equal to the sum of thermal exergies of the individual components in a saturated vapor state, so

$$\delta \approx 0 \tag{5-11}$$

Agrawal and Fidkowski[39] found through extensive numerical integration for various mixtures, that for a liquid feed,

$$\mu \approx 0 \tag{5-12}$$

Additional numerical integration with multiple mixtures was performed; the results confirmed that this assumption is valid for liquid feed cases. In all feed conditions used, the contribution of the μ term to the total exergy change in the system was 3% or less. Therefore for the sake of computational efficiency, the function for minimizing exergy loss will assume that the two terms above are always zero. The exergy loss of the system is now given by

$$\begin{aligned}\Delta \in = \in_{in} - \in_{out} = RT_0 \sum_{i=A,B,C,D} z_{F_i} lnz_{F_i} + \left(V_{AB} - F_{AB}\right)\left(e_{AB} - E_{AB}\right) \\ + \left(V_{BC} - F_{BC}\right)\left(e_{BC} - E_{BC}\right) - V_{BCD}\left(e_{BC} - E_{BC}\right) \\ + V_A\left(e_A - E_A\right) - V_D\left(e_D - E_D\right) + V_C\left(e_C - E_C\right)\end{aligned} \tag{5-13}$$

The difference in exergies between a liquid and vapor is given by

$$e_i - E_i = \Delta H\left(\frac{T_0}{T_i} - 1\right) \quad (pure\ component) \tag{5-14}$$

$$e_{mix} - E_{mix} = \Delta H \int_{q=0}^{q=1} \left(\frac{T_0}{T_{mix}} - 1\right) dq \quad (mixture) \tag{5-15}$$

By mass balance, the term V_D can be eliminated:

$$V_D = V_{AB} + V_{BC} + V_A - V_{BCD} - V_C - F_{AB} - F_{BC} \tag{5-16}$$

Substituting these equations into the exergy loss, the term now involves a number of integrals over the thermal quality of the streams:

$$\begin{aligned}\Delta \in = RT_0 \sum_{i=A,B,C,D} z_{F_i} lnz_{F_i} + \left(V_{AB} - F_{AB}\right)\Delta HT_0 \int_{q=0}^{q=1} \left(\frac{1}{T_{AB}} - \frac{1}{T_D}\right) dq \\ + \left(V_{BC} - F_{BC}\right)\Delta HT_0 \int_{q=0}^{q=1} \left(\frac{1}{T_{BC}} - \frac{1}{T_D}\right) dq \\ - \left(V_{BCD} - F_{BCD}\right)\Delta HT_0 \int_{q=0}^{q=1} \left(\frac{1}{T_{BCD}} - \frac{1}{T_D}\right) dq + \\ V_A \Delta HT_0 \int_{q=0}^{q=1} \left(\frac{1}{T_A} - \frac{1}{T_D}\right) dq - V_C \Delta HT_0 \int_{q=0}^{q=1} \left(\frac{1}{T_C} - \frac{1}{T_D}\right) dq\end{aligned} \tag{5-17}$$

Since relative volatility can be defined by equation 5-18 for pure component and equation 5-19 for mixtures:

$$\Delta HT_0 \left(\frac{1}{T_i} - \frac{1}{T_D}\right) = RT_0 ln\alpha_i \tag{5-18}$$

$$\Delta HT_0 \int_{q=0}^{q=1} \left(\frac{1}{T_{mix}} - \frac{1}{T_D}\right) dq = RT_0 \int_{q=0}^{q=1} ln\left(\sum \alpha_i x_{i,mix}\right) dq \tag{5-19}$$

it is possible to express the integral terms in the balance as

$$\begin{aligned}\frac{\Delta \in}{RT_0} = \sum_{i=A,B,C,D} z_{F_i} lnz_{F_i} + \left(V_{AB} - F_{AB}\right) \int_{q=0}^{q=1} ln\left(\sum \alpha_i x_{i,AB}\right) dq \\ + \left(V_{BC} - F_{BC}\right) \int_{q=0}^{q=1} ln\left(\sum \alpha_i x_{i,BC}\right) dq \\ - \left(V_{BCD} - F_{BCD}\right) \int_{q=0}^{q=1} ln\left(\sum \alpha_i x_{i,BCD}\right) dq + V_A \ln \alpha_A - V_C \ln \alpha_C\end{aligned} \tag{5-20}$$

Finally, the liquid phase composition $x_{i,j}$ (the fraction of component *i* in any stream *j*) can be expressed implicitly (using as an example stream AB):

$$z_{i,AB} = q x_{i,AB} + (1-q)\left(\alpha_i x_{i,AB} / \sum_{k=A,B} \alpha_k x_{k,AB}\right) \tag{5-21}$$

When this implicit expression is written for every component in every submixture stream, the resulting set of equations can be inserted into the exergy balance to give an exergy loss term involving only variables that can be determined from Underwood's equations for minimum reflux distillation. The relationship between relative volatility and temperature turns out to be very important in constructing this model; most crucially, because of the substitution of relative volatility values, the final equation for exergy loss does not contain temperature! The thermodynamic efficiency of the system can thus be found without utilizing detailed stage-to-stage calculations.

In all exergy calculations performed in subsequent sections, the assumption of liquid bottom products and vapor top products is removed. In order to truly calculate the minimum exergy loss for a given configuration, all reboilers and condensers (save those associated with final products) have the ability to produce column products which are liquid, vapor, or two-phase. The objective function suggested is adjusted accordingly.

Due to equation 5-1, the maximum thermodynamic efficiency occurs at the minimum value of the exergy loss term. The objective function given above is specific to the example shown, but any general configuration will yield an exergy loss equation where each reboiler and condenser will yield a temperature-independent term with the same form as one of the terms given in the sample objective function. Thus, through an exergy balance around any given configuration, an objective function is derived that measures overall thermodynamic efficiency of a distillation configuration without performing stage-to-stage calculations or relying on temperature variables. The objective function is integrated numerically through three-point Gaussian quadrature in order to preserve the NLP form of the problem rather than involving differential equations.

5.3 Comparison of exergy objective function to vapor duty objective function: single configuration

For the regular-column search space of Shah & Agrawal[42], a set of equations can be generated containing all of the constraints in section 3.4.1. The goal, then, is to solve a series of problems of the form

$$\begin{gathered}\min \Delta\varepsilon(x) \\ \text{subject to:} \\ h_i(x)=0 \\ g_i(x)\leq 0\end{gathered}$$

where h and g represent all linear and nonlinear constraints on a distillation configuration being solved by Underwood's method. The methodology used to solve this problem is very important; drawing accurate conclusions relies on solving the problem to global optimality for all configurations in the search space. For the reasons outlined in Chapter 3 of this dissertation, the solver GAMS/BARON is chosen for these nonconvex NLP problems. The GMA formulation is extended to include the equations calculating exergy loss in a configuration; together with the set of equations presented in Chapter 3 these form the Exergy Loss Global Minimization Algorithm (ExGMA). The global optimality can still be ensured by BARON as the objective changes from minimizing vapor flows to minimizing exergy loss; the increased nonconvexity of the problem may lead to increased computational time demands.

In order to study the effect of exergy minimization using multiple feed conditions, the following three cases will be used.

Table 5-1: Case studies for exergy minimization

	Case A	Case B [Kim & Wankat][74]	Case C [heavy crude]
# Components	4	4	5
Component A	α=64	α=13.432	α=45.3
Component B	α=16	α=5.891	α=14.4
Component C	α=4	α=2.19	α=4.7
Component D	α=1	α=1	α=2.0
Component E	n/a	n/a	α=1
Feed fraction A	0.25	0.30	0.144
Feed fraction B	0.25	0.40	0.093
Feed fraction C	0.25	0.25	0.101
Feed fraction D	0.25	0.05	0.039
Feed fraction E	n/a	n/a	0.623

The first question to answer in order to determine the effect of exergy loss on design of a distillation process is the following: when exergy loss is minimized in a configuration with a specific connectivity, will this ever provide a different result than minimizing vapor flows? In Figure 5-3, a configuration is demonstrated.

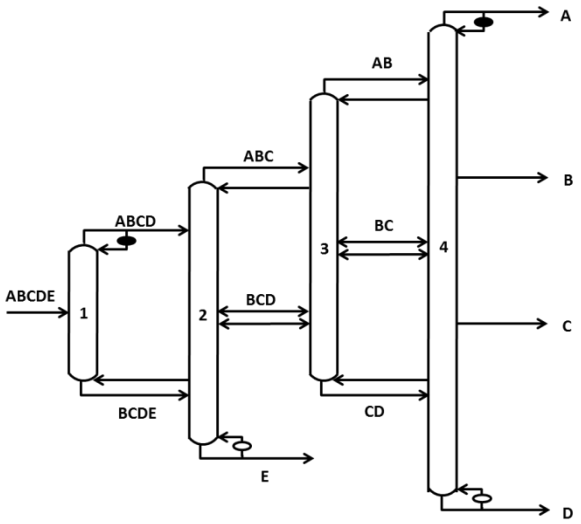

Figure 5-3: Configuration for heavy crude separation

When this configuration is used to separate a mixture of heavy crude oil (case C in Table 5-1) and optimized using total vapor flow as the objective function, this configuration requires a vapor flow of (0.836)F, where F is the molar flow rate of the feed stream. Henceforth this vapor requirement will be referred to as simply "a normalized vapor duty of 0.836". This vapor flow is such that the configuration in Figure 5-3 ranks among the top 16% of configurations used for separating this feed mixture into its pure components. However, there are still more than 900 configurations that have the same total vapor requirement or less. The configuration also has an exergy loss of $3.148(RT_0)$, henceforth referred to as a normalized exergy loss of 3.148.

When the configuration in question is optimized with the objective of minimizing the configuration's exergy loss, there is no doubt that the vapor duty of the configuration will have to increase to see any improvement in the system's thermodynamic efficiency. In fact, the configuration's normalized vapor requirement does increase to 0.852, an increase of 1.9%. Surprisingly, though, this small increase in vapor requirement is able to produce a fairly large shift in the configuration's exergy efficiency. The normalized exergy loss of the system drops to 3.042, a decrease of 3.5%.

In order to explain this effect, the total (normalized) vapor or liquid duties handled by the system's four heat exchangers are compared in Figure 5-4. In both cases, a large amount of vapor is generated by the reboiler of column 2, and a much smaller amount by the reboiler of column 4. Since the configuration is assumed to have liquid feeds and products, all vapor generated in a reboiler must be condensed elsewhere in the configuration. Thus, the primary variables that affect exergy are the total vapor flow and the way in which a given total vapor flow is distributed between reboilers and condensers.

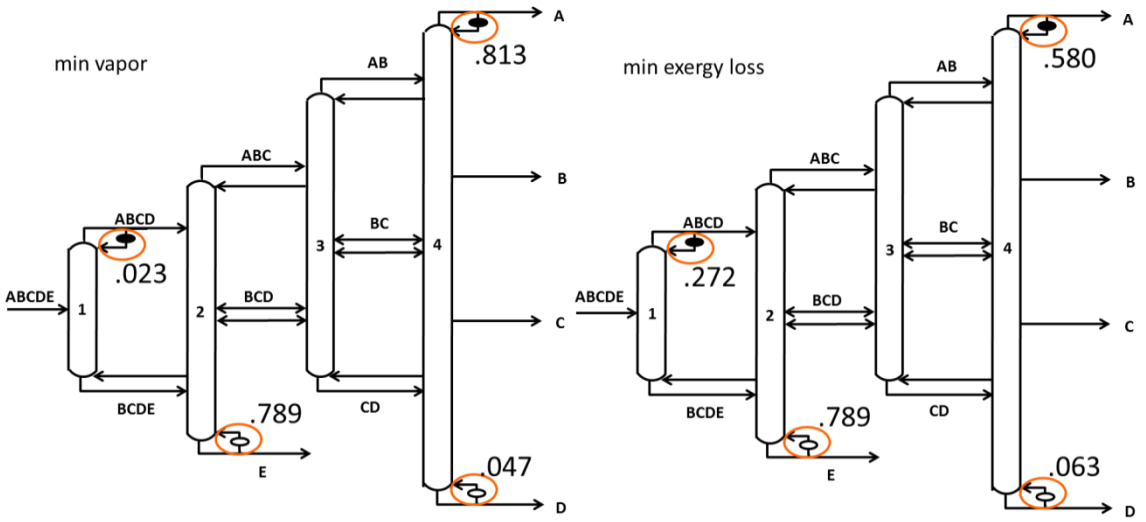

Figure 5-4: Comparison of vapor distribution for different objective functions

In this case, the first configuration in Figure 5-4 places a very high load on the condenser at the top of the final column. This condenser must operate at a much lower temperature than the condenser in column 1. This is because the volatilities of the components which must be condensed out in column 4 (mostly component B) are much higher than those in column 1 (mostly component E). The exergy objective function was developed to account for temperature considerations, so it will favor exchangers with high condenser temperatures, all other things being equal.

Just as each exchanger can have a vapor duty associated with it, each exchanger can have an exergy change associated with it. Figure 5-5 demonstrates the comparison presented in Figure 5-4 in terms of exergy. Indeed, as condenser vapor duty moves from column 4 to column 1, exergy loss also moves with it. But the combined exergy loss decreases; the two condensers in the figure optimized for exergy loss have notably less exergy loss than the same two condensers condensing a lesser amount of vapor in the

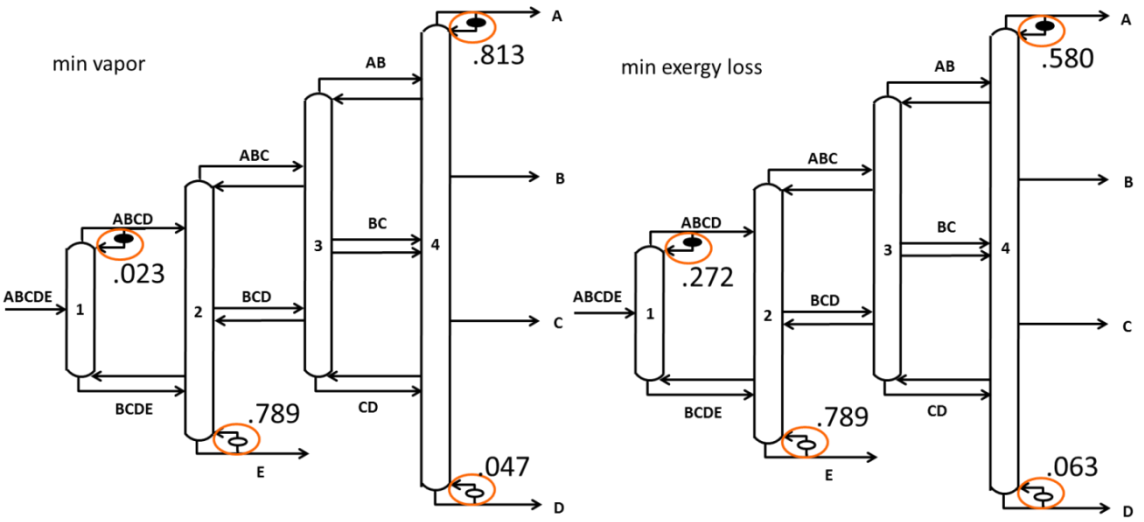

Figure 5-5: Comparison of exergy loss for different objective functions

leftmost arrangement. The total exergy loss decreases by 3.5% when shifting to the operating conditions in Figure 5-4(b); however, the shift also increases vapor duty by 1.9%.

As a whole, this comparison allows the following to be observed.

Observation 1: "Optimizing a configuration for minimum vapor duty can produce a different set of operating conditions than optimizing it for minimum exergy loss."

Note that there are still many configurations where the two objective functions do produce the same operating conditions.

5.4 Comparison of the vapor and exergy properties of the regular-column search space

It is clear that using exergy as an objective function can produce a different set of operating parameters than using vapor flow as an objective function for design of a single configuration. It then becomes of interest to observe this difference across all possible

configurations, producing a two-dimensional map that includes both the minimum total vapor flow and the minimum exergy loss of a configuration. Of particular interest is the following question: is a configuration that is exergy efficient necessarily low in total vapor requirement, and vice versa? This mapping of the search space will be performed for all three feed conditions in Table 5-1. All listed relative volatilities α are relative to that of the heaviest component in the feed, which is assigned a relative volatility value of 1.00.

The first case study is a general case that represents a very easy separation to perform. For a system with four components in the feed, there are 152 possible configurations for carrying out the separation.[42] Each of these 152 configurations is optimized twice: the total vapor flow of the configuration is minimized and subsequently the total exergy loss is minimized. This configuration can be represented as a point on a graph where the x coordinate represents the normalized vapor flow requirement of the configuration when optimized for minimum vapor flow, and the y coordinate represents the normalized exergy loss of the configuration when optimized for minimum exergy loss. After performing this for all configurations in the search space, the results are shown in Figure 5-6.

It seems that there exist many configurations high in vapor duty without necessarily being high in exergy loss. The data allows the formulation of Observation 2.

Observation 2: "Not all configurations with low vapor requirements have a low exergy loss; likewise, not all configurations with a high vapor requirement are thermodynamically inefficient."

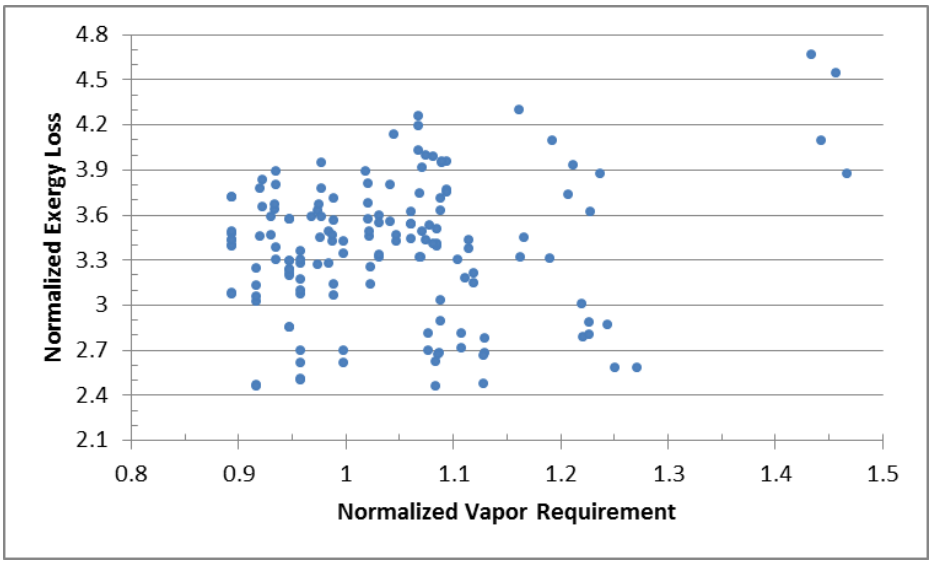

Figure 5-6: Exergy vs. vapor duty plot, Case A

To see whether this observation holds for another feed condition, the 152 configurations in the 4 component search space are subjected to the same procedure using an example considered by Kim & Wankat (Table 5-1).[74] This example represents the separation of an alkane system with constant relative volatilities. This is a more difficult separation than Case A due to volatilities which are closer together; it should be expected that vapor duty optimization will yield a higher value of the objective function for all cases relative to the feed amount.

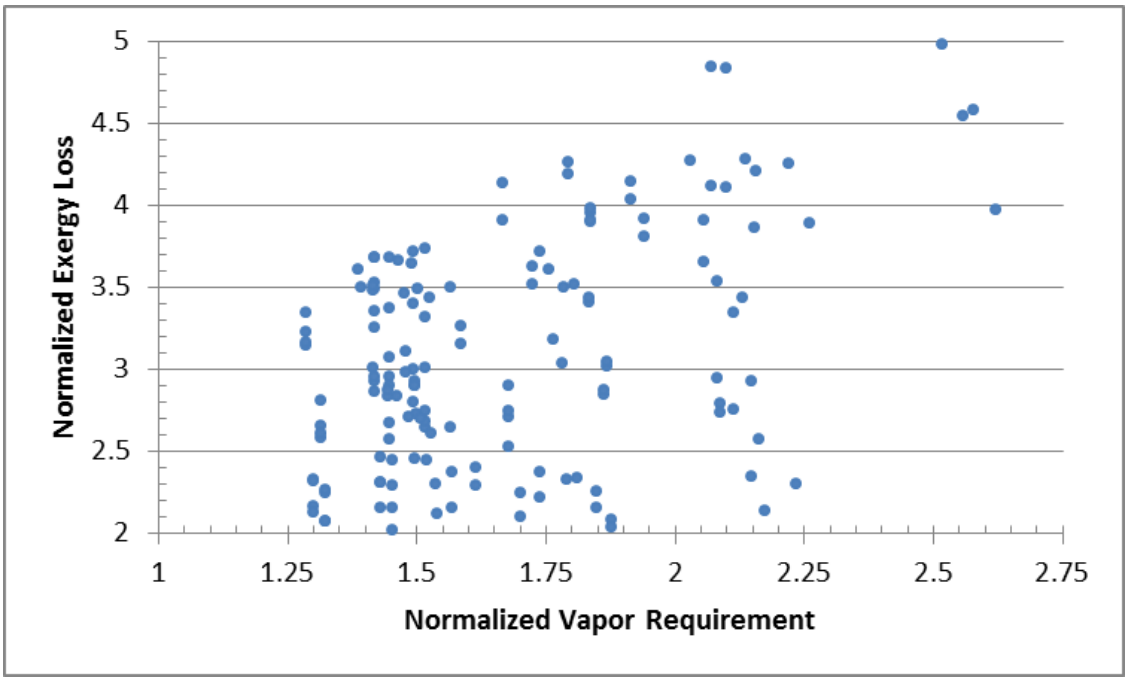

Figure 5-7: Exergy vs. vapor duty plot, Case B

Figure 5-7 shows the distribution of vapor duties for all 152 configurations in the search space. Indeed, higher vapor requirements are observed across the board. Once again it is observed that Observation 2 describes the behavior of the system. Low exergy loss and low vapor requirement do not necessarily go hand-in-hand; likewise, high exergy loss does not automatically translate to high vapor requirement.

It is important that this observation be shown true for an example with more than four components. For this, Case C is used. This mixture represents a typical heavy crude oil separation with constant relative volatility assumed (Table 5-1). The total number of configurations for which exergy and vapor objective functions must be compared is now 6,128; these configurations are shown in Figure 5-8.

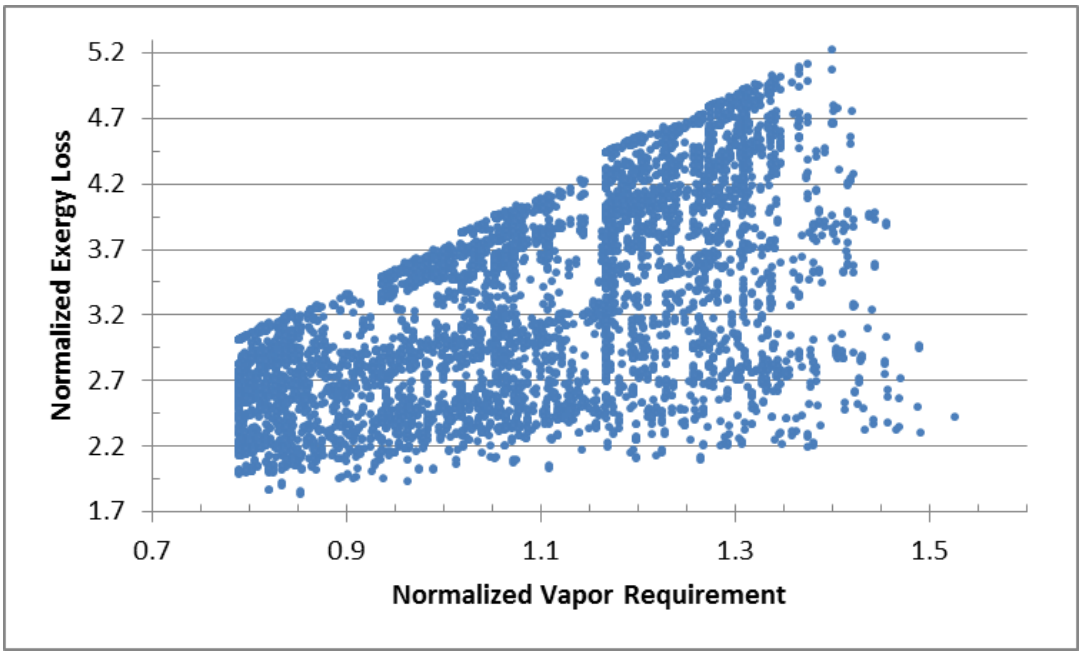

Figure 5-8: Exergy vs. vapor duty plot, Case C

Now it is clear over a large sample size that while a very slight positive correlation may exist between exergy loss and vapor requirement, Observation 2 is true for this 5-component separation. A number of configurations with a low vapor requirement have a high exergy loss; many configurations with high vapor duty also happen to be thermodynamically efficient (low exergy loss).

5.5 What differentiates exergy efficient configurations and low-vapor configurations?

It has been shown that low vapor duty and high thermodynamic efficiency do not necessarily go hand-in-hand. To proceed, two cases will be presented as a demonstration of how the exergy loss and vapor duty relate. Both of these configuration pairs will come

from the 5 component Case C presented in Figure 5-8, with data from Table 5-1. This represents several configurations capable of separating a mixture of light crude oil, which is treated as a 5 component mixture.

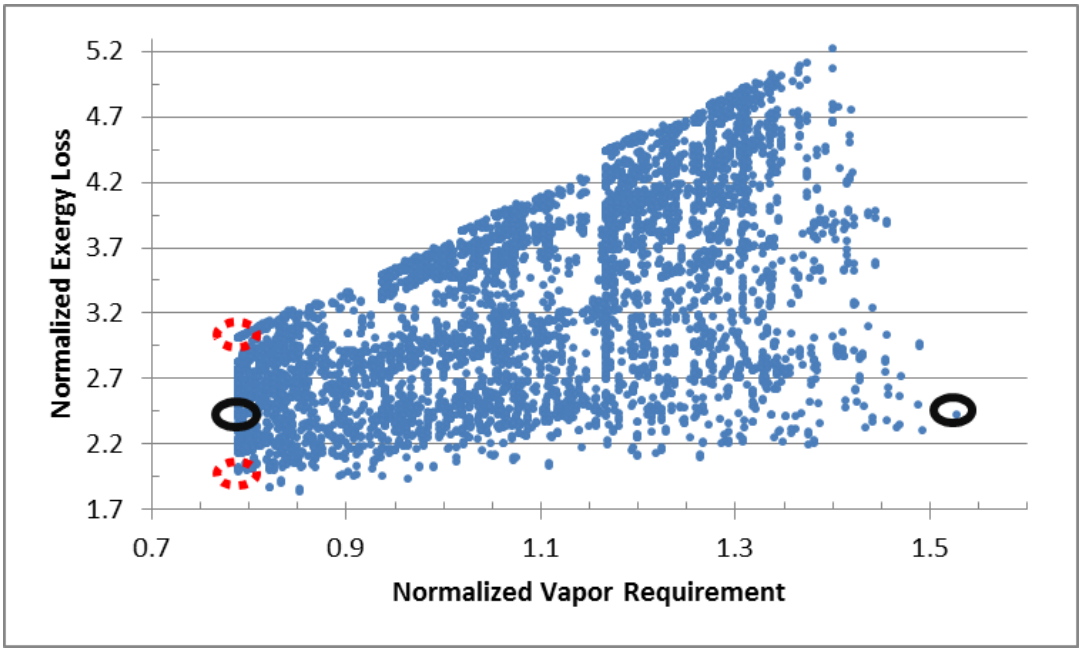

Figure 5-9: Points under consideration for comparison (5 components)

In terms of Figure 5-8, two configurations near global minimum in vapor consumption that have vastly different exergy losses will be examined. Then, two very different configurations in terms of vapor requirement that both have an identical exergy loss will be studied. These points on the graph are shown in Figure 5-9.

The two points on the graph with a dashed circle each represent a configuration (Figure 5-10). Both are systems with only one reboiler and multiple thermal coupling links. By the standards of minimum vapor duty used in Chapter 3, these configurations

would be very similar in terms of usefulness due to their identical required vapor flow (b has a vapor requirement approximately 1.3% higher than a). The way the system's exchangers are arranged, while not affecting the vapor duty, does change the exergy loss of the system substantially.

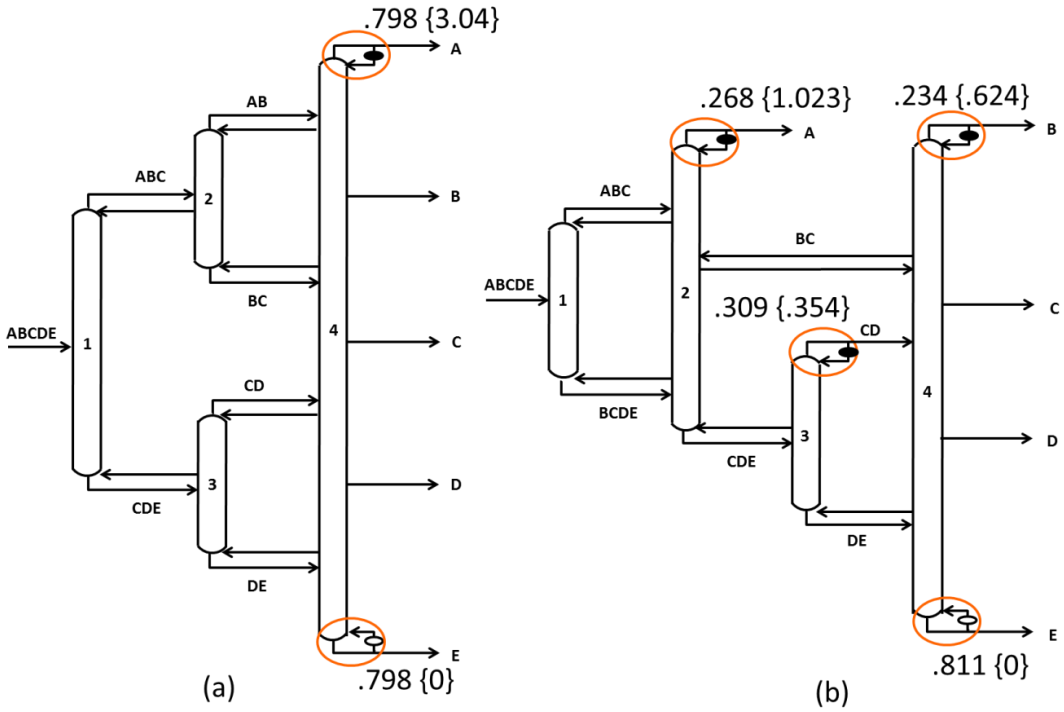

Figure 5-10: Comparison of two cases with similar vapor requirements

For these two configurations, normalized vapor condensed or vaporized at each condenser is listed first, with the bracketed numbers reflecting the normalized exergy loss associated with this phase change operation. Because these cases are defined as having liquid feeds and liquid products, by definition two configurations with similar total vapor generation will also have similar total liquid generation at their condensers. These are two

such configurations; the primary difference between them is how the condensation requirement is distributed. The leftmost case is a fully thermally coupled system where all heat exchanger operations are performed in the final column. The configuration on the right generates its entire vapor requirement in the final column, but performs condensations at three separate points within the configuration.

In total, the normalized exergy loss of the first configuration is 3.04. Without adding a substantial amount of vapor, the second configuration reduces this exergy loss to 2.00, a 34% decrease in exergy loss. This decrease in exergy loss is due to the higher temperatures in the condensers of the third and fourth columns; though the total amount of vapor handled in condensers may be nearly identical, handling it at temperatures which allow for a milder utility selection will be reflected favorably in the total exergy loss of the system.

As another example of how utility selection can drive exergy loss in different configurations, consider the points circled in a solid line in Figure 5-9. These configurations are demonstrated in Figure 5-11. The configuration on the left has no thermal coupling, so all vapor required in a given column must be produced completely at the column's reboiler and condensed at the column's condenser. With a total vapor flow of 1.527, this configuration would be deemed highly inefficient if the only criteria were total vapor flow. The configuration on the right uses thermal coupling to supply vapor to multiple columns; as a consequence the left configuration requires 93% more vapor than the right.

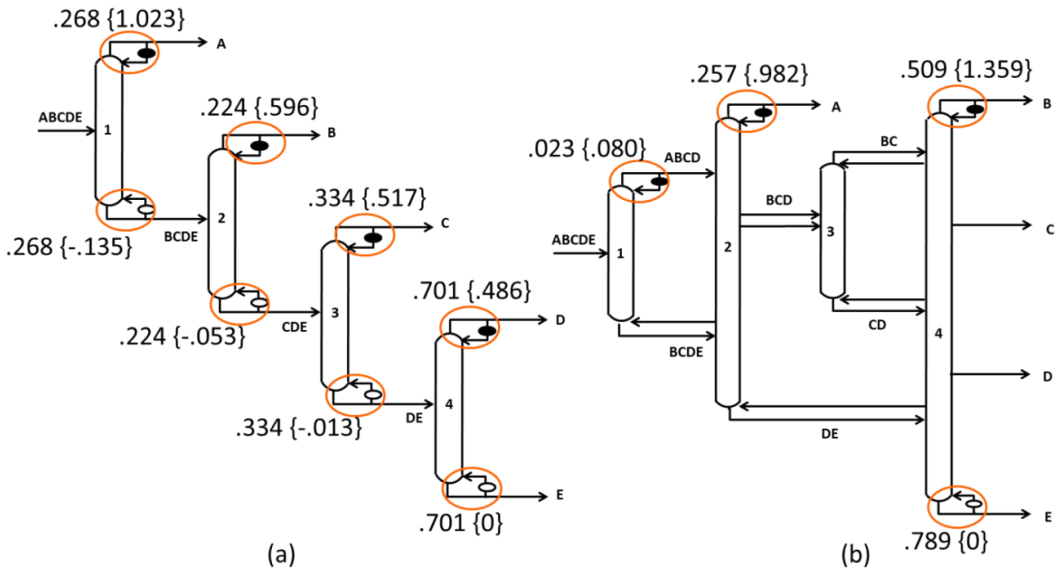

Figure 5-11: Comparison of two cases with similar exergy loss

In terms of exergy loss, differences in the location at which the vapor is handled makes these two configurations equal in thermodynamic efficiency. In the configuration on the right, a total of 0.766 normalized vapor flow is condensed by the exchangers associated with streams A and B (the two condensers in the system with the coldest required utility due to the high volatility of the A-rich and B-rich streams they are handling). In the configuration on the left, only 0.492 normalized vapor flow is handled by the equivalent A and B condensers. Much of the load in the leftmost configuration is handled by the condenser for pure product stream D, which operates at the highest utility temperature of all condensers in this system.

The exergy balance around the system favors more than just high-temperature condensers; in the configuration on the left, the overall exergy loss of the system is reduced by its use of low-temperature reboilers such as the one associated with stream

BCDE. This does not demonstrate that the configuration on the left is superior to that on the right. Rather, it shows that the left configuration, thought to be far inferior by the measure of total vapor generated, can actually perform just as well as the right configuration in terms of thermodynamic efficiency due to the distribution of its heat exchangers. Of course, to take advantage of a configuration such as this, hot utilities at different temperatures should be beneficially available, and similarly, heats rejected at warmer temperatures should find beneficial use at the plant under consideration.

This type of comparison can be applied to any of the points in Figures 5-6 through 5-8. In all of these cases, optimizing based on exergy loss will favor those configurations that allow the exchangers with mild temperature requirements, and will discriminate against those systems such as the fully thermally coupled configuration (highest-exergy point on the lowest-vapor left border in all three diagrams). Considering all this, one final observation can be formulated.

Observation 3: "A screening tool using minimum exergy loss as its target will favor selection of configurations using efficient, mild-temperature reboilers and condensers when possible."

This screening tool can be used on its own, to simply rank list every configuration in the search space in terms of exergy loss. Instead of providing a single answer for "best configuration", this system is easily able to identify the top 10 most thermodynamically efficient configurations for further study, or any other number of efficient configurations. However, for the most effective design the screening criteria can be made two-dimensional by selecting a region from an exergy-vapor plot like that of Figures 5-6 through 5-8 for further study of the configurations contained within.

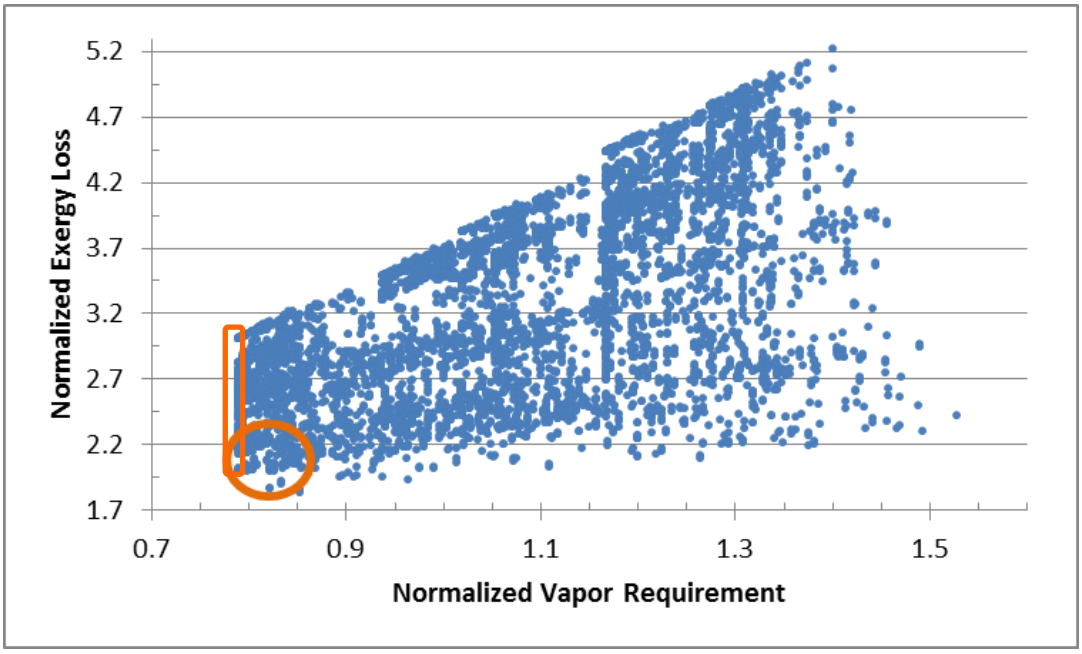

Figure 5-12: Demonstration of two-dimensional screening criteria for design

Figure 5-12 demonstrates one such region selection; the circled region contains around 50 points that all fall within the top 4% of configurations in terms of exergy loss and within the top 12% of configurations in terms of vapor requirement. The rectangular bar contains all minimum vapor configurations. Considering both as design options allows the positive aspects of the minimum vapor objective function to be retained (such as the vapor requirement's impact on the diameters of columns, a capital cost consideration) while utilizing thermodynamically efficient columns. As a reminder, any of the configurations in Figure 5-12 have the same feed, and produce the same final products; the only difference between them is which splits they select and where they position reboilers and condensers. The configurations within the indicated space should be evaluated in detail for capital and operating cost, availability of hot and cold utilities, heat integration with the rest of the plant, and any other pertinent design criteria.

5.6 Summary of exergy loss minimization study

In this study, equations were developed that express the exergy loss of a distillation configuration in terms of its operating parameters. This allows minimization of exergy losses for any given configuration. When coupled with the matrix method of Shah & Agrawal[42], this enables a ranklist of the entire search space of configurations for any liquid feed mixture producing liquid products. A comparison of this ranklist with the ranklist produced by minimizing total vapor flow yielded several observations. First, a given configuration often (but not always) requires different operating conditions to achieve minimum exergy loss than to achieve minimum total vapor generated. Second, not all configurations with low vapor requirements have low exergy losses, nor do all high vapor requirements lead to high exergy losses. In fact, graphing the exergy and vapor requirements for all configurations in the search space (such as in Figure 5-12) shows no clear trend. Finally, these graphs (and the previous observation) can be explained by the fact that minimizing exergy loss tends to favor configurations that perform their heat exchange at mild temperatures. While using thermodynamic efficiency for design is not infallible, this system provides a quick-to-generate design criterion that can be utilized alone or in conjunction with minimum vapor flow to select an energy-efficient distillation configuration from the massive search space of possible configurations for any given mixture. This design method is highly useful when utilizing heat pumps to drive the distillation.[75]

CHAPTER 6. DISTVIEW GRAPHICAL INTERFACE FOR MULTICOMPONENT DISTILLATION SCREENING

6.1 Need for a graphical screening interface

In Chapter 3, one example was presented in which it was required to identify configurations with a vapor duty within 5% of that of the FTC configurations; after such configurations were identified, the only information present for each one was its connectivity matrix and final operating parameters. If the number of candidate configurations was limited to a handful, sorting and screening possibilities might be a relatively simple thing to do drawing each configuration by hand using the methods of Shah and Agrawal.[42] However, when many process design options are available (as with the 340 options identified in the aforementioned study), it becomes desirable to develop automated methods for assessing and visualizing the properties of configurations more complex than a mere objective function value.

The following considerations should be included in the development of a graphical screening interface that utilizes the regular-column configurations of Shah & Agrawal:[42]

- Capacity to display the vapor duty, total annualized cost, or thermodynamic efficiency of any configuration that has been formulated as an NLP and solved using GAMS/BARON

- Displays available operation parameters such as vapor flow and compositions throughout the configuration
- Way exists to screen based on structural criteria
- Multiple criteria can be used in conjunction to narrow the list of desirable configurations
- Flowsheets developed using this interface (including applicable process data) can be printed, saved, and shared

6.2 Features of the DistView graphical interface

In response to the need for a graphical screening interface to interpret results from the optimization tools presented throughout this dissertation, the software DistView has been developed. Technical assistance has been rendered by the Rosen Center for Advanced Computing at Purdue University.

In order to draw regular-column distillation configurations, the program accepts a number of inputs. First, for the entire search space, the components, stream numbers/labels, and variables must be defined. For example, a four-component alkane separation will be represented by the following notation:

Components {Naphtha Kerosene Diesel Gas-Oil}
Base_Configuration {
Stream -Label ABCD -Number 1
Stream -Label ABC -Number 2
Stream -Label BCD -Number 3
Stream -Label AB -Number 4
Stream -Label BC -Number 5
Stream -Label CD -Number 6
Stream -Label A -Number 7
Stream -Label B -Number 8

Stream -Label C -Number 9
Stream -Label D -Number 10
Sortables {
Vapor_Duty numerical {Vapor Duty} {Total amount of vapor generated in the configuration}
Total_Cost numerical {Total Cost} {Estimated combined cost to build and operate the configuration}
Number_Thermal_Couplings numerical {#TC} {Number of thermally coupled transfers replacing exchangers}
}

Using this notation, DistView first reads the names of the four components. All 10 possible streams in the configuration are given both a number and a label. Three sortable columns are defined for data storage; the intention is that for every configuration defined, a value for each of the three sortables will be provided. The description at the end of each sortable line is used in a hover-over tooltip so that users will have clear descriptions of each variable.

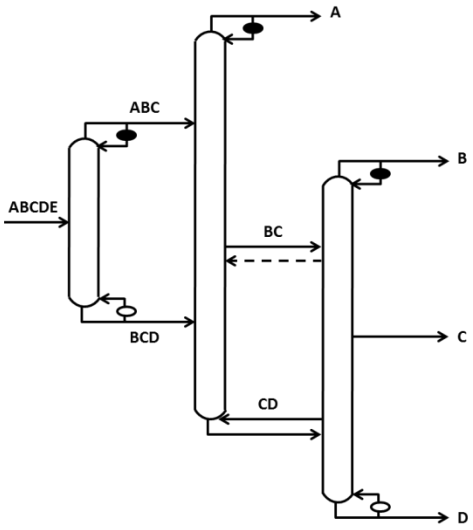

Figure 6-1: Sample configuration for creation in DistView

This introductory block defines the general parameters which are under study for the configuration. The next input into the DistView program is a list of splits performed by the separation scheme. To demonstrate how the configuration is defined, interpreted, and created, take the example of a four-component configuration shown in Figure 6-1. If this configuration is optimized for the total minimum annualized cost for the feed shown in Table 6-1, a set of compositions, stream flows, and vapor flows is calculated. A feed flow of 250 kmol/hr is taken.

Table 6-1: Feed conditions for DistView flowsheet creation

	Component	Feed Mole Fraction	Relative Volatility
Case 2	**A** N-butane	0.3	29.07
	B N-pentane	0.4	12.81
	C N-heptane	0.25	2.35
	D N-octane	0.05	1

In this case, the estimated combined annualized capital and operating costs sum to $127,350 to achieve pure products. The estimated vapor flow required to perform this separation under operating conditions optimized for total cost is 201.9 kmol/hr. Each of the splits present in the configuration must be specified; this is expressed to the DistView input file as

Solution 1 {
Split -Feed 1 -Top 4 -Bottom 6 -Column 1
Split -Feed 4 -Top 7 -Bottom 8 -Column 2
Split -Feed 6 -Top 9 -Bottom 10 -Column 3
Vapor_Duty 437.059393
Total_Cost 155.392454
Number_Thermal_Couplings 0

Next, the vapor flow in each column section is obtained and listed from the bottom section sequentially up to the top for each column. Each stream flowing is specified by listing first the net flow, then the *n* (here, 4) mole percentages of each component in the stream. Finally, the reboiler and condenser duties (in kmol/hr) are set for each column.

Column_1_vapors {178.484 178.484 }
Column_2_vapors {155.242 251.128 }
Column_3_vapors {103.333 103.333 }
Stream_1_flows {200.000 30.000 40.000 25.000 5.000 }
Stream_4_flows {140.000 42.857 57.143 0.000 0.000 }
Stream_6_flows {60.000 0.000 0.000 83.333 16.667 }
Stream_7_flows {60.000 100.000 0.000 0.000 0.000 }
Stream_8_flows {80.000 0.000 100.000 0.000 0.000 }
Stream_9_flows {50.000 0.000 0.000 100.000 0.000 }
Stream_10_flows {10.000 0.000 0.000 0.000 100.000 }
Reboiler_Duty {178.484 155.242 103.333 }
Condenser_Duty {82.599 251.128 103.333 }
}

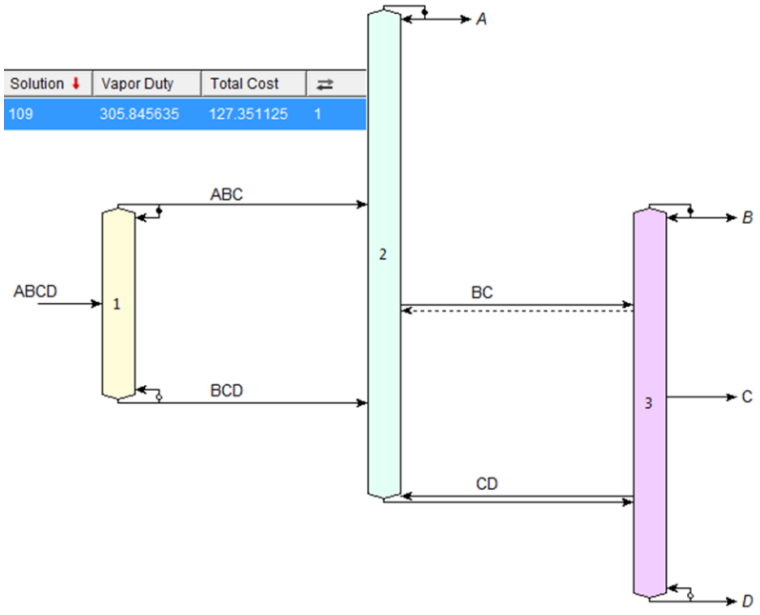

Figure 6-2: DistView representation of configuration

The diagram produced algorithmically from the specifications provided is shown in Figure 6-2. All of the flow specifications calculated by the Cost GMA algorithm are available to DistView, and the program represents them as mole percent flows for any stream upon hovering over that stream.

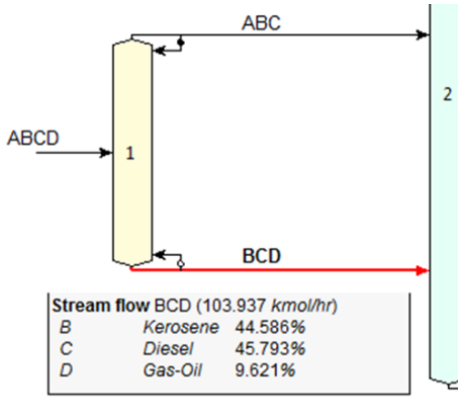

Figure 6-3: Representation of stream flows

Likewise, the vapor flowing at any point in the configuration is identified to the DistView interface, allowing tooltips to present the vapor flow in any column section upon hovering over that section. Any exchanger in the configuration has a specific number of moles of vapor condensed or generated; this information can be viewed by hovering over an exchanger icon. Both these features are demonstrated in Figure 6-4.

For any configuration, the stream flowrates and compositions as well as all vapor flows in the configuration are known by the program through the input. DistView can use

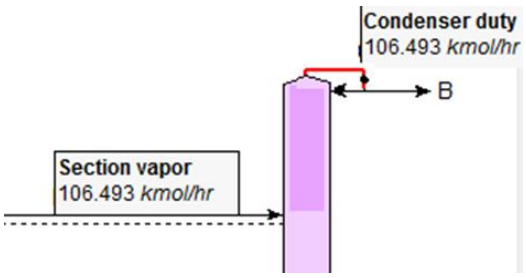

Figure 6-4: Representation of section vapor flows and exchanger duties

this information to generate a .PDF or .JPEG file that includes both the drawing of the configuration (Figure 6-1) and a complete stream tables/vapor flows table (Table 6-2 and 6-3).

Table 6-2: Stream flows and compositions calculated by Cost GMA for Figure 6-1

Column Variables (kmol/hr)						
Column	Reb. Duty	Cond. Duty	Section Vapor Flow (Bottom to Top)			
1	208.55	8.55	104.613	104.613		
2	n/a	190.803	22.437	126.374	94.739	190.803
3	97.296	106.493	97.296	74.858	74.858	106.493

Table 6-3: Vapor flows and exchanger duties calculated by Cost GMA for Figure 6-1

Stream Variables					
Stream	Net Flow (kmol/hr)	%A	%B	%C	%D
ABCD	200	30	40	25	5
ABC	96.063	62.46	35.04	2.503	
BCD	103.937		44.59	45.79	9.621
BC	92.607		86.39	13.61	
CD	47.393			78.9	21.1

Note that the reboiler duty is not equal to the bottom section vapor flow for column 1 – this is an indication that in order to reduce capital cost, additional vapor has been created at the reboiler of column 1 and passed to column 2 directly rather than flowing to column 1.

With the ability to rapidly generate complete process flowsheets with flow and vapor duty data, it becomes quite simple to compare different configurations within the search space. For example, Figure 6-5 demonstrates a configuration that is identical to Figure 6-2 save for one design difference: rather than producing stream CD at the bottom product of column 2, the new configuration produces pure component D in a sharp split; due to this, column 3 performs only one split, that of BC producing pure B and pure C. Compared to Figure 6-2, which has an estimated total cost of $305,900, the configuration in Figure 6-5 has an estimated total cost of $327,100. The vapor flows for the latter configuration are shown in Table 6-4, giving some idea of how this additional cost was incurred.

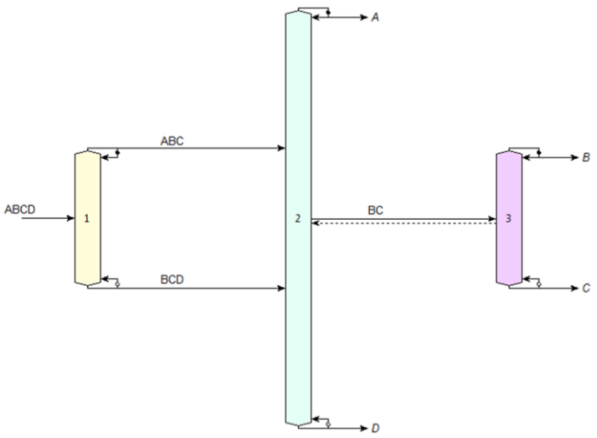

Figure 6-5: Alternate configuration for cost comparison to Figure 6-2

Table 6-4: Vapor flows for Figure 6-5.

Column Variables (kmol/hr)						
Column	Reb. Duty	Cond. Duty	Section Vapor Flow (Bottom to Top)			
1	205.268	8.55	104.613	104.613		
2	52.149	190.803	52.149	152.803	94.739	190.803
3	69.667	127.731	69.667	127.731		

It can be observed that the first column and top half of the second column have vapor flows unchanged from those given in Table 6-2. The primary difference comes in the flows in the third column and the bottom part of the second column. With a complete separation of C and D required in the second column, the vapor flow in the bottom column section increases by about 26 kmol/hr; with no available thermal coupling link to supply part of this requirement, an extra reboiler with a duty of 52 kmol/hr vapor handled must be added to the configuration. Some of this vapor is passed to the third column to help fill vapor duty requirement through side draw stream BC. However, now that column 3 is required to perform a complete sharp split between B and C rather than creating B and C from prefractionated mixtures BC and CD, the vapor requirement of the third column increases to a maximum across the entire column of 127.7 kmol/hr, compared to the previous maximum of 106.5 kmol/hr for the third column in Figure 6-2. This leads to a column with a higher diameter, which along with the additional reboiler and increased maximum vapor flow in column 2, does more to increase the total cost of the system than the removal of a separation section does to reduce the cost. The end result of this change is that Figure 6-5 has a total cost more than $22,000 higher than Figure 6-2. Thus it is clear that with the abundance of information available through the

process flowsheets, increased understanding can be gained of why certain configurations are favored by the global optimization performed on the search space in Chapters 3, 4, and 5 of this dissertation.

Table 6-5: Feed characteristics of light crude oil, n=5

Component	Letter	α	composition
Naptha	A	45.3	0.461
Diesel	B	14.4	0.195
Kerosene	C	4.7	0.073
Gas Oil	D	2	0.114
Heavy Ends	E	1	0.157

Another tool for screening through the multicomponent search space incorporated into DistView is the use of a filter system. Data for a light crude oil mixture is shown in Table 6-5 to provide an example of a separation that has a "real-life" design currently present in a number of refineries. Figure 6-6 shows the default configuration for performing this split; it is a sharp split configuration where the heaviest component is removed in each successive column. As a first level screening tool, assume that it is desired to identify configurations with lower total vapor flow required than the normalized vapor flow requirement of Figure 6-6, which is 0.681. It is already known that the FTC configuration will provide the lowest vapor requirement (in this case, 0.352, a reduction of 51.7%). However, FTC contains only two heat exchangers; conversely it contains 6 thermally coupled links at the top and bottom of columns. Such a configuration may be considered difficult to operate. It is also essentially impossible to retrofit from Figure 6-6.

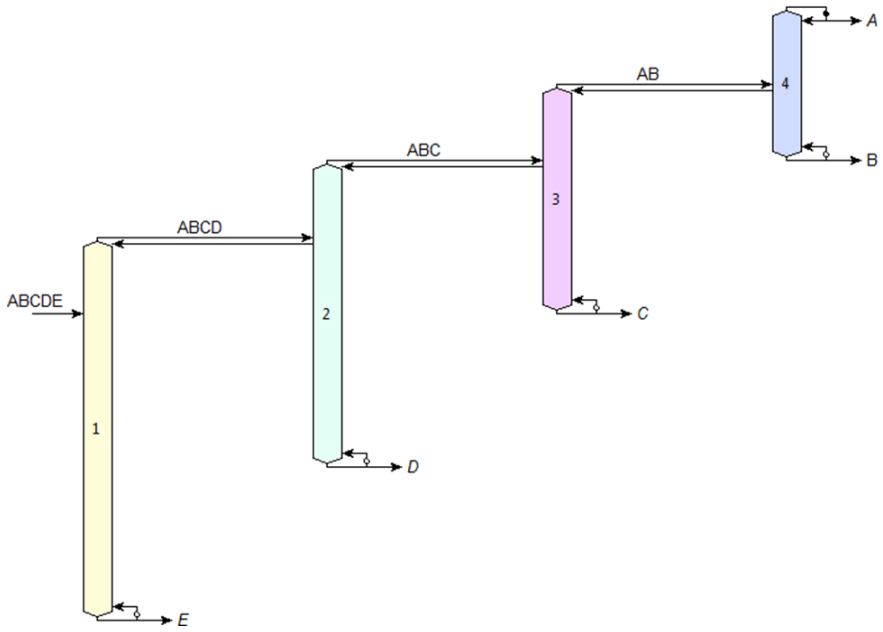

Figure 6-6: Traditional configuration for crude oil separation

Thus, it may be desirable to find a configuration that offers some of the energy savings of the FTC configuration, but in a manner that is simpler to control and could be partially retrofitted from Figure 6-6. The filter tool enables such a search. Filters can be placed on the number of thermal couplings, number of total streams, vapor duty, exergy loss, or capital cost of the configuration; also, filters can be created to only view designs which contain a particular split. For the example of light crude separation, let a filter be used so that the first column always performs the separation "ABCDE to ABCD/E", the first split in Figure 6-6. This will allow quick removal of the heavy petroleum products and waxes that can make operating separations more difficult in any column they enter. In addition, let a filter be used limiting solutions to having at most four thermally coupled links for simpler control systems; finally only solutions with a lower vapor than Figure 6-

6 are allowed. This combines to yield a set of filters that can be implemented as shown in Figure 6-7.

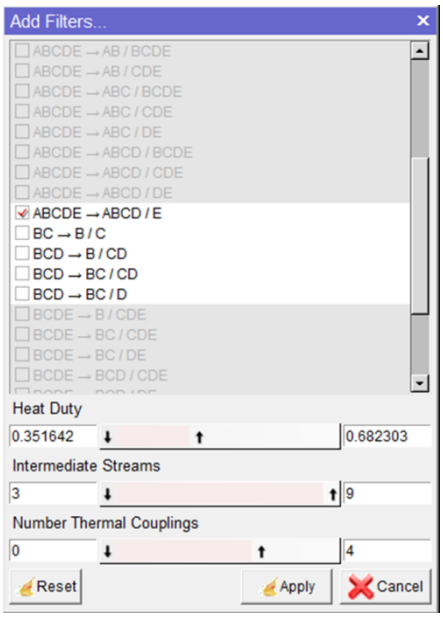

Figure 6-7: Filters applied to identify attractive option for light crude distillation

Table 6-6: Top 8 solutions following the filters of Figure 6-7; light crude oil case

Solution	Heat Duty		
3731	0.547895	5	3
3733	0.547895	5	4
3790	0.547895	6	3
3791	0.547895	6	4
3794	0.547895	6	4
3179	0.570880	5	3
3180	0.570880	5	4
3181	0.570880	5	4

After all filters have been applied, the number of configurations being considered is narrowed from 6,128 all the way to 58 (including the original configuration on which the filters were based). The top few configurations are listed in a form seen in Table 6-6.

With these restrictions on the space it is no longer possible to achieve a vapor duty of 0.352; however a vapor duty as low as 0.548 can be achieved (19.6% potential energy savings). Figure 6-8 shows a configuration that achieves this savings. This configuration shares characteristics in common with both the FTC configuration and the classic configuration.

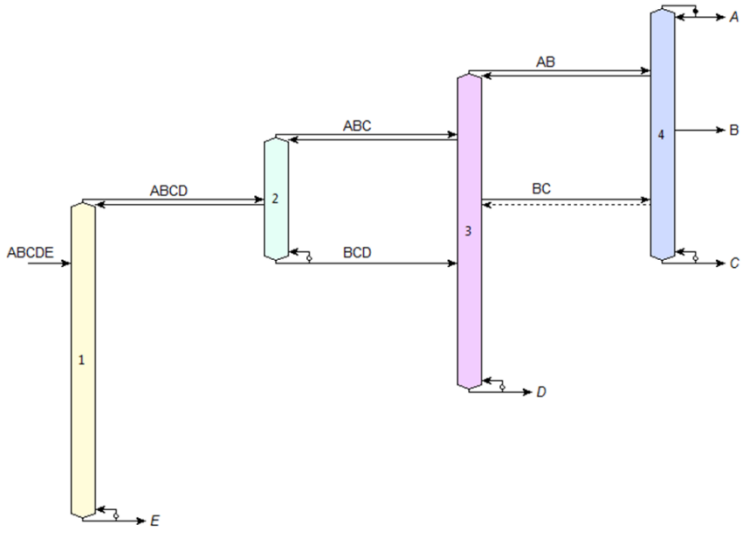

Figure 6-8: Identified configuration which can save almost 20% compared to classical configuration for crude oil separation

Like the classic configuration, it removes the heaviest products before the final column and utilizes a reboiler for every column. Like the FTC configuration, it utilizes multiple nonsharp splits to reduce vapor duty and has only a single condenser. Combining some of the useful properties of an efficient configuration with those of an existing, practical

configuration can lead to a solution which displays efficiency, operability, and potential for retrofit all at once.

Further exploring the space generated by the filters, configurations can be identified meeting the criteria that reduce vapor duty using as little as a single thermal coupling link; in fact, Figure 6-7 itself can still provide up to 1% energy savings with all of its TC links replaced by condensers save the link at stream AB. In addition, if it were desirable to maintain the low number of transfer streams in Figure 6-6, inserting a single transfer stream (CD) to the classical structure can still achieve nearly 8% reduction in vapor duty, yielding a configuration shown in Figure 6-9.

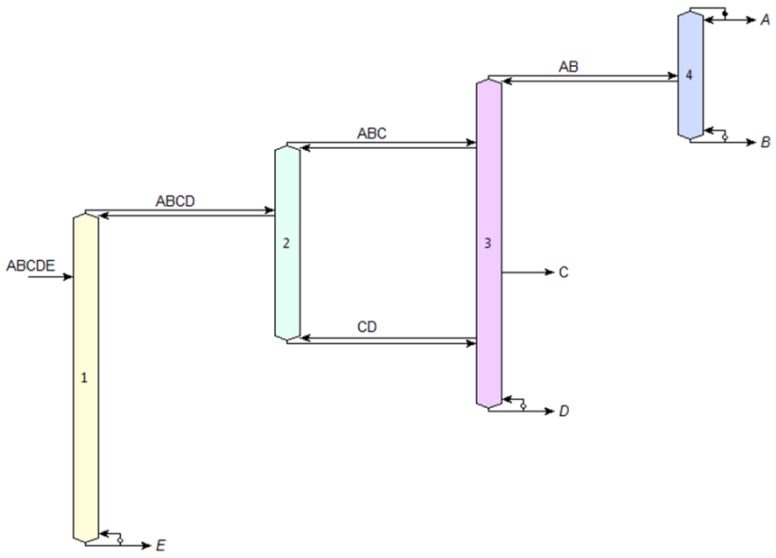

Figure 6-9: 8% vapor reduction using only 4 intermediate streams

6.3 Versatility of DistView for sharing results of multicomponent distillation design

The above two examples demonstrate the utility of the DistView program in designing systems for multicomponent distillation; programmed into the software tool is

the ability to display and interpret results from all of the different tools for design contained in this dissertation. It also makes sharing discussions about multicomponent distillation very straightforward between two practitioners (especially when both possess the software); all of the following methods of sharing results are supported by DistView:

- A table of all solutions can be exported as a CSV file; if sharing this CSV file with someone without the DistView input file, the solutions can still be visualized by opening the example file with the same number of components. All configuration numbers listed in the CSV file will be drawn exactly the same in the example file as in the input file; the only functionality lost is the ability to interact with the stream/vapor flow results and filter based on objective function
- A document containing both the image of a configuration and the stream/vapor tables of Table 6-2 and 6-3 can be generated for sharing. For image files, JPEG, PNG, and GIF versions are available; for full page documents, PDF, PS, and EPS formats are available.
- If user modification of the flowsheet is desired, an Asymptote file can be generated, allowing all aspects of the configuration to be rearranged in a drawing editor.
- DistView creates its representations of the distillation search space using TXT documents. The GMA algorithm and its exergy/cost modifications all include the procedure for writing such TXT documents after each optimization is performed. For $n < 6$ the Inputfile.txt document can be directly transferred with ease, allowing access to the full search space and information on every configuration therein to anyone opening the input file on DistView.

- Any of the image or PDF files created by the viewer can be inserted into reports or papers as examples of the configurations discussed therein.

In summary, the DistView software system has been developed to aid in research into multicomponent distillation such as that discussed in Chapters 3, 4, and 5 in this dissertation. The software instantly generates flowsheets for up to 20,000 distillation configurations at one time, including vapor flows, stream compositions, and exchanger duties. The complete space of configurations drawn by the software can be individually examined, reproduced in image or PDF form, and screened using filters. Filters are available to specify heat duty, exergy loss, capital cost, number of exchangers replaced by thermal coupling, or number of column sections or splits; any of the above filters can be used simultaneously to narrow a large search space and quickly find configurations which meet very strict requirements. If starting with a particular configuration, these filters enable finding an energy efficient solution which still is easy to retrofit from the starting design. If looking for a configuration with certain operational parameters, like a minimum number of exchangers, filters also enable subdividing the search space based on the complexity of the separations. Taken all together, the DistView software is thus a valuable research tool which can be applied to multicomponent separations regardless of how the user defines what a “desirable configuration” is.

CHAPTER 7. CONCLUSIONS AND FUTURE WORK

7.1 Summary

Multicomponent separations are extremely important to design well because of their large share of overall plant costs. Both capital expenditures and energy operating cost should be considered in order to choose the best separation system. Therefore, the research focus of this dissertation is the design of energy and cost efficient separation processes; this includes optimization of membrane separation schemes based on operating costs, as well as optimization of distillation separation schemes based on vapor requirement, thermodynamic efficiency, operating costs, and capital expenditures. Systematic tools are used both to generate the possible options for performing separations and to identify the ideal operating conditions to achieve the most desirable version of a given option. Using these tools together enables a ranklist of all possibilities; this ensures that no good option is skipped in crafting a process design. In order to avoid missing out on excellent solutions, it is vital that the optimization technique be a guarantor of global optimality and that all possible options be either exhaustively enumerated and evaluated or exhaustively enumerated and confirmed not to have a solution superior to a known solution. All of these criteria are met by the GAMS/BARON tool; therefore, all separations in this dissertation are evaluated using GAMS/BARON to optimize a nonlinear or mixed-integer nonlinear programming problem.

Chapter 2 describes methods for identifying the most energy-efficient methods to separate a mixture of nitrogen and oxygen using a cascade of polymeric gas separation membranes. Two major studies were performed; the first related to the use of intermediate stage cascades (ISC) and the second to the effect of varying recovery on the energy requirement of a cascade system.

ISCs are a method by which a membrane cascade (classically restricted to having only one more membrane stage than there are recycle compressors) can be arranged to have substantially fewer recycle compressors than there are membrane stages. The usefulness of ISCs was demonstrated by producing nitrogen at 99.9% purity and 58.5% recovery. The ideal number of recycle compressors was found to be $p = 4$ for this nitrogen case study when ISCs are not used. The ISC configurations were found to provide a marked improvement in energy efficiency for configurations with $p < 4$; however, with p close to 4 it was also observed that not all possible intermediate stages are required to derive the full energy benefit of utilizing intermediate stages. When $p = 4$, there was no identifiable energy benefit to using intermediate stage cascades. Therefore the primary use of intermediate stage cascades in gas separation problems is to improve energy efficiency when there is a desire to use less recycle gas compressors (usually for capital cost related reasons).

Due to the tradeoff between permeability and selectivity in membrane separations, reducing the recovery of the permeate product does not necessarily reduce energy requirement. For the nitrogen production example, a number of different separation schemes were tested to determine the relationship between recovery and energy requirement. No single configuration was always optimal across the entire range of

recovery values. Many arrangements, particularly those with few stages, were heavily restricted in what recoveries they could produce. Multiple enriching stages were valuable for producing high recoveries of nitrogen in an energy efficient way. One definite finding of the study was that a suitable membrane cascade could always be found which was superior to the single stage cascade.

Chapter 3 describes the work done on vapor duty minimization for multicomponent distillation configurations. Using the matrix method to generate the complete search space for multicomponent distillation, each configuration is then individually optimized to have the minimum possible vapor duty after meeting a number of constraints. Chapter 3 gives the full formulation for this nonlinear programming problem; the problem includes material balances, problem definitions like the feed and product flowrates, individual balances on liquid and vapor, definition of thermally coupled streams, assurance that proper enrichment of light and heavy components occurs in every split, and Underwood's equations for minimum vapor flow calculation. A number of specific techniques are used to more tightly bound the variable values as well as provide strong initial guesses. The formulation presented in this chapter is known as the Global Minimization Algorithm (GMA).

The need for global optimization in solving this problem is demonstrated by comparing the optimization of a heavy crude mixture using GAMS/BARON, GAMS/MINOS without bounding efforts, and GAMS/MINOS with bounding efforts. Without bounding efforts, local solver MINOS failed to solve over 26% of the search space; it reached optimality for only 39% of configurations. With bounding efforts, over 5% of the search space was still unsolvable and only 72% reached optimality.

GAMS/BARON was able to provide a feasible solution for every configuration in the 5 component search space; it guaranteed global optimality for 92% of configurations in just 100 seconds of computational time and would be likely to guarantee 100% optimality given additional computational time. For many process designs, the solution using GAMS/BARON required less than half the vapor flow than the feasible solution constructed by GAMS/MINOS. For this reason, GAMS/BARON was chosen as a suitable solver for all work in this dissertation. To demonstrate a potential use of GAMS/BARON with the Global Minimization Algorithm, a case was presented for which the best configuration was assumed to be known and all configurations within 5% of this best configuration in vapor duty were sought. The GMA identified 26 completely thermally coupled configurations and 177 total configurations which were within 5% of the fully thermally coupled solution. The application of this technique is the case where a known efficient configuration is deemed insufficient for reasons of complexity, operability, or retrofit and additional process alternatives with similar energy efficiency are desired.

Chapter 4 dealt with a formulation modification of the GMA algorithm to account for total annualized cost. A series of equations were presented to explain the Cost Global Minimization Algorithm (CGMA). Studying the performance of the CGMA using a series of enumeration based nonlinear programs compared to the performance of a two-stage based method known as TMA, it because clear that limiting the search space by means of TMA had the potential to ignore configurations with great potential to be low-cost solutions. In addition, it was observed that the answer found by the first stage of TMA had very little correlation on the final answer achieved after the second step. One

example showed that it required 42 iterations of the TMA, run well past its stopping criteria, to identify the solution shown to be best by the CGMA. The solution obtained by TMA after stopping criterion were met was only the eighth lowest cost configuration in the search space according to GMA.

The CGMA was also compared to the vapor duty based GMA to observe the difference in the type of configuration put forward as efficient. A third case, that of the CGMA stripped of all operating costs and reduced only to equipment capital costs, was also included in the comparison as a demonstration of how changing the relative weights of capital and operating portions of the CGMA could yield different configurations identified as strong candidates. Traditionally low in vapor duty configurations like the FTC configuration fared well in operating cost metrics while requiring a high capital cost. Simple configurations with sharp splits and a low degree of thermal coupling were favored when optimizing only based on capital expenditure. When a weighted combination of the two was considered, it yield a nonsharp split configuration with both thermally coupled links and heat exchangers present; this balanced configuration has both low capital expenditure and low energy operating cost, making it a strong candidate to perform separations under a wide variety of economic and feed conditions.

In Chapter 5, the question of temperature was considered. The vapor duty formulation did not calculate temperatures of steam, nor did it account for differences in latent heat between components. The cost GMA formulation included latent heat calculations, but still did not calculate temperatures of steam. This could lead to a configuration being viewed as more desirable despite requiring costly steam high in vapor quality. To address this inefficiency, the Exergy Global Minimization Algorithm

(ExGMA) was introduced. The thermodynamic efficiency of the system was calculated using an exergy balance; because of the relation between relative volatility and temperature, the equation for exergy loss in a system contained only variables which could be calculated from Underwood's equations. Using this new exergy objective function, several observations were made. First, different operating conditions are often (but not always) adopted by the exergy minimization of a configurations compared to its vapor minimization. Second, configurations that are low in vapor duty are not necessarily thermodynamically efficient, nor are configurations that are high in vapor duty necessarily inefficient. Third, the ExGMA favors those configurations where large amounts of the required phase change operations were performed in the mildest conditions; that is, shifting of vapor handling to reboilers with lower steam temperatures and condensers with higher coolant temperatures is encouraged by the formulation. The exergy formulation can be used independently or in conjunction with either of the other formulations presented in this dissertation to identify desirable configurations. For example, for a five component heavy crude separation there are around 50 configurations immediately identifiable on an exergy-vapor plot which fall within 4% of the lowest exergy loss in the search space and within 12% of the lowest vapor requirement in the search space.

Chapter 6 described a graphical screening tool to aid in the design of multicomponent distillation sequences. DistView was developed in order to immediately visualize the results of any of the algorithms from Chapters, 3, 4, and 5. By inputting a text description of the configuration layout and operating parameters, a complete, interactive flowsheet is created for every configuration which has been enumerated. Up

to 20,000 configurations can be drawn by the program in a few seconds. Each flowsheet can contain information about total vapor requirement, exergy loss, capital cost, operating cost, number of thermally coupled streams, and number of intermediate transfer stream; in addition, the flowrate and composition of any stream can be found by hovering over the stream on the interactive drawing; likewise the vapor handled by any reboiler or condenser is shown on the flowsheet. The vapor flow in any column section is also available. Filters are available which enable viewing of only those configurations which meet certain numerical of structural criteria; an example was presented of how to use the filters to identify the 57 configurations which could improve on the vapor duty of a traditional crude separation scheme while retaining the same first column and using at most 4 thermal couplings. This set of configurations included schemes with up to 19.6% potential energy savings.

7.2 Future Direction

7.2.1 Mixed-integer formulation improvement/6 component separations

An MINLP formulation has been partially developed with the potential to evaluate the search space for the globally optimal configuration using fewer problems than a complete enumeration. If the global optimum of this problem can be reliably found, it represents a vast potential decrease in computational time to arrive at the best possible configuration. The current formulation is inadequate to converge 5-component problems to global optimality for configurations with a large number of sites for potential thermal

coupling. This is because of the heavy involvement of the integer variables in the highly nonlinear Underwood equation constraints.

The difficulty of optimality verification would only become more difficult if the MINLP algorithm was adapted to include cost and exergy considerations in the way that the GMA algorithm was. The long term goal for creating an MINLP is to be able to optimize the massive search space for $n = 6$ components without requiring the evaluation of all 506,912 configurations in the search space; if the current MINLP were made to converge for this system it would require only 4,373 evaluations to tackle this massive problem.

It is possible that improving bounds and optimization techniques may improve the MINLP sufficiently to converge for $n = 5$, currently an elusive task. However, for attacking the search space of $n = 6$, it is likely that either a complete reformulation of integer constraints or a new method of subdivision of the search space would be required. The most likely reformulation to achieve the desired ends would be introducing a continuous variable that achieves the results of the integer variable in capturing all thermally coupled analogs of a connectivity without actually requiring integer constraints.

7.2.2 Optimization of Dividing Wall Columns using Underwood's method and a modified GMA

A number of thermally coupled configurations in the search space derived by Shah & Agrawal [42] can be directly rearranged to produce dividing wall columns with the same total vapor requirement. For example, the FTC arrangement for $n = 3$ can be rearranged into the DWC in Figure 7-1 with an identical total vapor flow requirement.

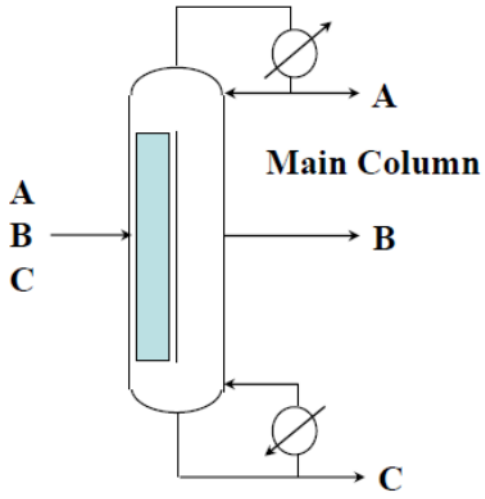

Figure 7-1: Divided wall column derived from FTC for n = 3

A simple way to draw a number of divided wall columns is to begin from a thermally coupled configuration in the NLP search space (such as the above Petlyuk configuration). However, this does not incorporate ALL possible ways to use a divided wall column. Ramapriya et al [76] proposed new rules for creating dividing wall configurations; some of these represented configurations not directly derived from the search space used throughout this paper. Results supporting the energy efficiency of such DWCs were generated using ASPEN Plus® simulations. However, the vast number of thermally coupled alternatives possible with $n > 4$ suggests it would be very difficult to evaluate all DWC process alternatives using such a process simulator. For options directly derived from a thermally coupled regular-column configuration, the GMA can be used to calculate directly the minimum vapor duty of the DWC. However, since there are DWC arrangements not corresponding to a regular-column configuration, it is important that future work define a way to calculate minimum vapor flows (and thermodynamic efficiencies) for such dividing wall arrangements for the purpose of quickly screening the

search space. Once this is complete, DWCs can be considered a part of the complete search space and the toolbox available to the practitioner of multicomponent distillation design would be even more versatile and robust.

7.2.3 Retrofit optimization

Several options were presented throughout this dissertation which could be used to tentatively identify configurations which could be retrofitted from an existing column configuration. The DistView tool can identify configurations which share common structural characteristics with the starting configuration. However, without being able to quantify what makes a retrofit possible, DistView can only go so far in identifying opportunities to improve energy efficiency without spending the capital to completely replace a configuration.

Because of this, it would be useful to create a more detailed way of determining a configuration's suitability for retrofit. The simplest way would be to impose additional constraints in all NLPs in the search space based on the properties of the starting configuration. For example, if the starting configuration had an existing first column with 55 stages and a 15 m^2 area, it would be possible for the CGMA to only examine operating conditions that led to a number of stages in the range $50 < NM_s(1) < 57$, $10 < A_s(1) < 18$. Alternately conditional constraints could be used; if a column had identical stages and diameter to one already in existence, it would register zero cost in the objective function; otherwise a new column must be used and fully paid for.

One more abstract way to consider retrofit in the optimization is to assign a retrofit score to the configuration based on how many columns, column sections, and heat

exchangers could be reused in the new configuration. After calculating a retrofit score for a configuration, two options are available. The first is to create a weighted objective function where the efficiency indicator is coupled with the retrofit score. The weight could be adjusted based on whether retrofit was a mere possibility or an imperative. The second use of a retrofit score would be as a cutoff constraint; in other words, if r(x) calculates the retrofit score of a configuration, the nonlinear program would be modified with $r(x) < k$, where $r(x) = 0$ represents using the original configuration and $r(x) > k$ represents creating a new configuration with no potential for retrofit at all.

Using one of these techniques to quantify retrofit ability in multicomponent distillation would further increase the strength and versatility of the design toolbox for performing effective separations.

7.2.4 Problem parallelization

All the series of nonlinear programming problems presented in this dissertation are performed on a single computer in series; that is, for a search space of 6,128 configurations ($n = 5$) a total of 6,128 problems are solved in succession, with only one problem active at a given time.

There is no interdependence between NLP problems in the GMA or any of its derivatives (save in the case where NLP solutions are used to continuously update the upper bound of the objective function, when only a subset of best solutions is desired). This makes the GMA and its derivatives good candidates for parallelization. Each processor or core devoted to a single NLP problem would be responsible for the algorithmic generation of all constraints, bounds, and initial guesses using MATLAB

followed by the solution of the problem using GAMS/BARON. In theory for a five component search space up to 6,128 parallel problems could be simultaneously solved.

For any future endeavors to move into the six component search space, which contains over 500,000 configurations, each of which is more complex than a 5 component NLP problem, parallelization is an absolute must if any chance to fully optimize the search space is desired.

LIST OF REFERENCES

LIST OF REFERENCES

1) Humphrey, J. L., & Siebert, A. F. (1992). Separation technologies; An opportunity for energy savings. *Chemical Engineering Progress;(United States)*,*88*(3).
2) Coker, D. T., Freeman, B. D., & Fleming, G. K. (1998). Modeling multicomponent gas separation using hollow-fiber membrane contactors. *AIChE journal*, *44*(6), 1289-1302.
3) Baker, R. W. (2002). Future directions of membrane gas separation technology. *Industrial & Engineering Chemistry Research*, *41*(6), 1393-1411.
4) Favre, E. (2007) Carbon dioxide recovery from post-combustion processes: Can gas permeation membranes compete with absorption? *Journal of Membrane Science,* 294(1-2), 50-59.
5) Lokhandwala, K.A., Pinnau, I. He,Z., Amo, K., DaCosta, A., Wijmans, J., & Baker, R. (2009) Membrane separation of nitrogen from natural gas: A case study from membrane synthesis to commercial deployment. *Journal of Membrane Science*, 346(2), 270-279.
6) Yang, D., Wang, A., Wang, J., & Wang, S. (2009) Parametric Study of the Membrane Process for Carbon Dioxide Removal from Natural Gas. *Industrial & Engineering Chemistry Research,* 48(19), 9013-9022.

7) Wankat, P.C. (2009) Separations: A Short History and a Cloudy Crystal Ball. *Chemical Engineering Education*, 43(4),286-295

8) Cohen, K. (1951) The Theory of Isotope Separation as Applied to Large-Scale production of U^{235}. 1st ed, ed. G.M. Murphy, New York: McGraw-Hill.

9) Pratt, H.R.C. (1967), Countercurrent Separation Processes. New York: Elsevier Publishing Co.

10) Benedict, M., Pigford, T.H., & Levi, H.W. (1981) Nuclear Chemical Engineering. 2nd ed., New York: McGraw-Hill.

11) Agrawal, R. (1997) A simplified method for the synthesis of gas separation membrane cascades with limited numbers of compressors. *Chemical Engineering Science*, 52(6), 1029-1044.

12) Xu, J. & Agrawal, R. (1996) Gas separation membrane cascades .1. One-compressor cascades with minimal exergy losses due to mixing. *Journal of Membrane Science*, 112(2), 115-128.

13) Agrawal, R. & Xu, J. (1996) Gas separation membrane cascades .2. Two-compressor cascades. *Journal of Membrane Science*, 112(2), 129-146.

14) Agrawal, R. & Xu, J. (1996) Gas-separation membrane cascades utilizing limited numbers of compressors. *AIChE Journal*, 42(8), 2141-2154.

15) Agrawal, R. (1996) Membrane Cascade Schemes for Multicomponent Gas Separation. *Industrial & Engineering Chemistry Research*, 35(10), 3607-3617.

16) Naylor, R. & Backer, P. (1955) Enrichment calculations in gaseous diffusion: Large separation factor. *AIChE Journal*, 1(1), 95-99.

17) Pathare, R. (2010) *Design and optimization of binary membrane-based separations*. Dissertation, Purdue University. Ann Arbor: ProQuest/UMI, (Publication No. AAT 3444742)

18) Pathare, R. & Agrawal, R. (2010) *Design of membrane cascades for gas separation*. Journal of Membrane Science, 364(1-2), 263-277.

19) Wolf, D., Borowitz, W., Gabor, A., & Shraga, Y. (1976) A General Method for the Calculation of an Ideal Cascade with Asymmetric Separation Units. *Industrial & Engineering Chemistry Fundamentals*, 15(1), 15-19.

20) Gottschlich, D.E., Roberts, D., Wijmans, J., Bell, C., & Baker, R. (1989) Economic comparison of several membrane configurations for H2/N2 separation. *Gas Separation & Purification,* 3(4), 170-179.

21) Herbst, R.S. and McCandless, F.P. (1994) No-Mix and Ideal Separation Cascades. *Separation Science and Technology*, 29(17), 2215-2226.

22) Olander, D.R. (1976) Design of ideal cascades of gas centrifuges with variable separation factors. *Nucl. Sci. Eng*. 60(4), 421-434.

23) Takashima, Y. (1965) Ideal cascade for asymmetric isotope separation. *Bull. Tokyo Inst. Technol*; 69, 21-37.

24) Yamamoto, I. & Kanagawa, A. (1978) Separative Power of Ideal Cascade with Variable Separation Factors. *Journal of Nuclear Science and Technology*, 15(6), 462.

25) Bernardo, P., Drioli, E., & Golemme, G. (2009) Membrane Gas Separation: A Review/State of the Art. *Industrial & Engineering Chemistry Research*, 48(10), 4638-4663.

26) Koros, W. J., & Mahajan, R. (2000). Pushing the limits on possibilities for large scale gas separation: which strategies? *Journal of Membrane Science*, 175(2), 181-196.

27) Tawarmalani, M., & Sahinidis, N. V. (2002). *Convexification and global optimization in continuous and mixed-integer nonlinear programming: theory, algorithms, software, and applications* (Vol. 65). Springer.

28) Sahinidis, N. V. (2003). Global optimization and constraint satisfaction: The branch-and-reduce approach. In *Global Optimization and Constraint Satisfaction* (pp. 1-16). Springer Berlin Heidelberg.

29) Underwood, A. J. V. (1948). FRACTIONAL DISTILLATION OF MULTICOMPONENT MIXTURES. *Chemical Engineering Progress*, 4(8).

30) Doherty, M. F., & Malone, M. F. *Conceptual design of distillation systems*, 2001. McGrawHill, New York..

31) Lockhart, F. J. (1947). Multi-column distillation of natural gasoline. *Petrol. Refiner*, *26*, 104.

32) Thompson, R. W., & King, C. J. (1972). Systematic synthesis of separation schemes. *AIChE Journal*, *18*(5), 941-948.

33) Sargent, R. W. H., & Gaminibandara, K. (1976). Optimum design of plate distillation columns. *Optimization in action*, 267-314.

34) Agrawal, R. (1996). Synthesis of distillation column configurations for a multicomponent separation. *Industrial & engineering chemistry research*, *35*(4), 1059-1071.

35) Fidkowski, Z. T. (2006). Distillation configurations and their energy requirements. *AIChE journal*, *52*(6), 2098-2106.

36) Rong, B. G., Kraslawski, A., & Turunen, I. (2003). Synthesis of functionally distinct thermally coupled configurations for quaternary distillations. *Industrial & engineering chemistry research*, *42*(6), 1204-1214.

37) Giridhar, A., & Agrawal, R. (2010). Synthesis of distillation configurations: I. Characteristics of a good search space. *Computers & chemical engineering*, *34*(1), 73-83.

38) Petlyuk, F. B., Platonov, V. M., & SLAVINSK. DM. (1965). Thermodynamically optimal method for separating multicomponent mixtures. *International Chemical Engineering*, *5*(3), 555.

39) Agrawal, R., & Fidkowski, Z. T. (1998). Are thermally coupled distillation columns always thermodynamically more efficient for ternary distillations? *Industrial & engineering chemistry research*, *37*(8), 3444-3454.

40) Shenvi, A. A., Shah, V. H., Zeller, J. A., & Agrawal, R. (2012). A synthesis method for multicomponent distillation sequences with fewer columns. *AIChE Journal*, *58*(8), 2479-2494.

41) Giridhar, A., & Agrawal, R. (2010). Synthesis of distillation configurations. II: A search formulation for basic configurations. *Computers & chemical engineering*, *34*(1), 84-95.

42) Shah, V. H., & Agrawal, R. (2010). A matrix method for multicomponent distillation sequences. *AIChE journal*, *56*(7), 1759-1775.

43) Fidkowski, Z. T., & Agrawal, R. (2001). Multicomponent thermally coupled systems of distillation columns at minimum reflux. *AIChE journal*, *47*(12), 2713-2724.

44) Fidkowski, Z., & Krolikowski, L. (1986). Thermally coupled system of distillation columns: optimization procedure. *AIChE journal*, *32*(4), 537-546.

45) Nikolaides, I. P., & Malone, M. F. (1988). Approximate design and optimization of a thermally coupled distillation with prefractionation. *Industrial & engineering chemistry research*, *27*(5), 811-818.

46) Halvorsen, I. J., & Skogestad, S. (2003). Minimum energy consumption in multicomponent distillation. 3. More than three products and generalized Petlyuk arrangements. *Industrial & Engineering Chemistry Research*, *42*(3), 616-629.

47) Halvorsen, I. J., & Skogestad, S. (2003). Minimum energy consumption in multicomponent distillation. 2. Three-product Petlyuk arrangements. *Industrial & engineering chemistry research*, *42*(3), 605-615.

48) Halvorsen, I. J., & Skogestad, S. (2003). Minimum energy consumption in multicomponent distillation. 3. More than three products and generalized Petlyuk arrangements. *Industrial & Engineering Chemistry Research*, *42*(3), 616-629.

49) Stichlmair, J. (1988). Distillation and rectification. *Ullmann's Encyclopedia of Industrial Chemistry*.

50) Levy, S. G., & Doherty, M. F. (1986, November). A design procedure for distillation columns with non-sharp splits. In *AIChE National Meeting, Miami Beach, November* (Vol. 2, No. 7).

51) Fidkowski, Z. T., Doherty, M. F., & Malone, M. F. (1993). Feasibility of separations for distillation of nonideal ternary mixtures. *AIChE journal*, *39*(8), 1303-1321.

52) Fidkowski, Z., & Królikowski, L. (1990). Energy requirements of nonconventional distillation systems. *AIChE journal*, *36*(8), 1275-1278.

53) Nallasivam, U., Shah, V. H., Shenvi, A. A., Tawarmalani, M., & Agrawal, R. (2013). Global optimization of multicomponent distillation configurations: 1. Need for a reliable global optimization algorithm. *AIChE Journal*, *59*(3), 971-981.

54) Caballero, J. A., & Grossmann, I. E. (2001). Generalized disjunctive programming model for the optimal synthesis of thermally linked distillation columns. *Industrial & Engineering Chemistry Research*, *40*(10), 2260-2274.

55) Caballero, J. A., & Grossmann, I. E. (2004). Design of distillation sequences: from conventional to fully thermally coupled distillation systems. *Computers & chemical engineering*, *28*(11), 2307-2329.

56) Türkay, M., & Grossmann, I. E. (1996). Logic-based MINLP algorithms for the optimal synthesis of process networks. *Computers & Chemical Engineering*,*20*(8), 959-978.

57) Caballero, J.A., & Grossmann, I.E. (2006). Structural Considerations and Modeling in the Synthesis of Heat-Integrated-Thermally Coupled Distillation Sequences. *Industrial and Engineering Chemistry Research*, 45(25):8454-8474.

58) Rod, V., & Marek, J. (1959). Separation sequences in multicomponent rectification. *Collection of Czechoslovak Chemical Communications*, *24*(10), 3240-3248.

59) Nallasivam, U., Shah, V.H., Shenvi, A.A., Huff, J., Tawarmalani, M., & Agrawal, R. (2014) Global optimization of multicomponent distillation configurations: 2. Enumeration based global minimization algorithm. *AIChE Journal*, submitted 9/2014.

60) Ferris, M.C., Jain, R., & Dirske, S. (2011) GDXMRW: Interfacing GAMS and MATLAB. http://research.cs.wisc.edu/math-prog/matlab.html

61) Yeomans, H., & Grossmann, I.E. (1999). Nonlinear disjunctive programming models for the synthesis of heat integrated distillation sequences. *Computers and Chemical Engineering*, 23 (9), 1135–1151.

62) Caballero, J.A., & Grossmann, I.E. (2013). Synthesis of Complex Thermally Coupled Distillation Systems Including Divided Wall Columns. *AIChE Journal*, 59(4), 1139-1159.

63) Fenske, M. (1932). Fractionation of straight-run Pennsylvania gasoline. *Industrial & Engineering Chemistry*, 24(5), 482-485.

64) Grossmann, I.E. (2013). Optimal Separation Sequences based on Thermally Coupled Distillation. http://newton.cheme.cmu.edu/interfaces/thermaldis/main.html.

65) Turton,R., Bailie, R. C., Whiting, W. B., & Shaeiwitz, J. A. (1998). *Analysis, synthesis, and design of chemical processes*. New York: McGraw-Hill.

66) Stilchmair, J. G., & Fair, J. R. (1998) *Distillation: principles and practice*. Wiley-Liss.

67) Itoh, J., Niida, K., Shiroko, K., & Umeda, T. (1980). Analysis of the available energy in a distillation system. *Int Chem Eng*, 20, 379-385.

68) Kaiser, V., & Gourlia, J. P. (1985). The ideal-column concept: applying exergy to distillation. *Chemical engineering, 92*(17), 45-53.

69) Taprap, R., & Ishida, M. (1996). Graphic exergy analysis of processes in distillation column by energy-utilization diagrams. *AIChE journal, 42*(6), 1633-1641.

70) Agrawal, R., & Woodward, D. W. (1991). Efficient cryogenic nitrogen generators: an exergy analysis. *Gas separation & purification, 5*(3), 139-150.

71) Agrawal, R., & Herron, D. M. (1997). Optimal thermodynamic feed conditions for distillation of ideal binary mixtures. *AIChE journal, 43*(11), 2984-2996.

72) Agrawal, R., & Herron, D. M. (1998). Intermediate reboiler and condenser arrangement for binary distillation columns. *AIChE journal, 44*(6), 1316-1324.

73) Agrawal, R., & Herron, D. M. (1998). Efficient use of an intermediate reboiler or condenser in a binary distillation. *AIChE journal, 44*(6), 1303-1315.

74) Kim, J. K., & Wankat, P. C. (2004). Quaternary distillation systems with less than N-1 columns. *Industrial & engineering chemistry research, 43*(14), 3838-3846.

75) Agrawal, R., & Yee, T. F. (1994). Heat pumps for thermally linked distillation columns: An exercise for argon production from air. *Industrial & engineering chemistry research*, 33(11), 2717-2730.

76) Madenoor Ramapriya, G., Tawarmalani, M., & Agrawal, R. (2014). Thermal coupling links to liquid-only transfer streams: A path for new dividing wall columns. *AIChE Journal, 60*(8), 2949-2961.

VITA

VITA

Joshua Lee Huff was born in Ponca City, Oklahoma, US on December 6, 1989. He graduated with a Bachelor of Science degree in Chemical Engineering from Texas A&M University in December 2009. He started his graduate studies at Purdue University in January 2010, joining the separations group under Prof. Rakesh Agrawal. He will graduate with a Ph.D. in Chemical Engineering from Purdue University in December 2014 and will begin a career as an Operations Research Engineer for Marathon Petroleum Corporation. He also received an M.S. in Chemical Engineering from Purdue University in May 2014.